

EXPRESSION AND CHARACTERIZATION OF A MATRIX
METALLOPROTEINASE (STROMELYSIN) USING A
RETROVIRAL GENE TRANSFER SYSTEM

by

Linda M. Bindewald Lund

A DISSERTATION

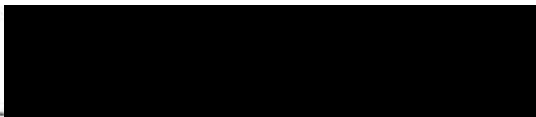
Presented to the Department of Biochemistry
and Molecular Biology,
and the Oregon Health Sciences University
School of Medicine
in partial fulfillment of
the requirements for the degree of

Doctor of Philosophy

January 1992

APPROVE 

(Professor in Charge of Thesis)



(Chairman, Graduate Council)

TABLE OF CONTENTS

	Page
I. Introduction	
A. Glaucoma	1
B. Evidence of a Role for the Trabecular Meshwork in Glaucoma	3
C. Extracellular Matrix and Its Turnover	5
D. Proteolytic Enzymes and the Trabecular Meshwork	7
E. The Matrix Metalloproteinases	9
F. Tissue Inhibitors of Metalloproteinases	20
G. Purpose for Using Ping-Pong Amplification of Stromelysin cDNA	23
H. Retrovirus Structure and Life Cycle	24
I. Friend Disease and Spleen Focus-Forming Virus	28
J. Expression Vector pSFF	30
K. Ping-Pong Amplification Expression System	32
II. Materials and Methods	
A. Cell Cultures	38
B. Stromelysin cDNA	38

C.	DNA Sequencing	39
D.	Construction of pSFF-SLN Retroviral Expression Vector	41
E.	Transfection	46
F.	Infection of Trabecular Meshwork Cells	47
G.	Radioimmunoassay	48
H.	Screening Transfected Cocultures	49
I.	Polymerase Chain Reaction with Multiple Primers	50
J.	Northern Blotting	51
K.	Immunohistochemistry	53
L.	Western Blots	54
M.	Zymograms	55
N.	Deglycosylation of Stromelysin	56
O.	SDS-PAGE to Estimate the Concentration of Stromelysin	57
P.	Activation of Prostromelysin	58
III.	Results	
A.	Sequencing pBS-SLN	60
B.	Subcloning of SLN-cDNA into pSFF	60
C.	"Ping-Pong" Amplification and Expression of Stromelysin	65

D.	SFF-GH Control Cultures	74
E.	Northern Blot	76
F.	Immunohistochemistry	82
G.	Western Blots of Coculture Media	102
H.	Substrate Gel Electrophoresis of Coculture Media	105
I.	Digestion of Stromelysin with Endoglycosidase D	108
J.	Estimation of Stromelysin Concentration in SFF-SLN Conditioned Media	109
K.	Activation of Prostromelysin	116
L.	PCR Assay for Stromelysin Inhibitor	127
M.	Infection of Trabecular Meshwork Cells	128
IV. Discussion		
A.	The Need for an Human Stromelysin Expression System	147
B.	Results of Stromelysin Expression Using Ping-Pong Amplification	148
	1. Preprostromelysin processing and post-translational modification	149
	2. Prostromelysin secretion	150
C.	Functional Activity of Stromelysin	151
	1. Reduction of cys disulfide does not inhibit enzymatic activity	151

2.	Activation of latent stromelysin	151
a.	Trypsin activation	152
b.	APMA activation	153
D.	SFF-SLN Clonal Cell Lines	154
1.	Northern blot shows increased level of expression of retroviral RNA	154
2.	PCR shows stromelysin mRNA is present in SFF-SLN clonal cell lines	155
3.	Estimation of prostromelysin concentration	156
4.	Clonal cell lines are unstable with high stromelysin production	156
E.	Cell-Matrix Destabilization -- A Possible Feedback Loop?	157
F.	Establishment of Cell Lines Infected with SFF-SLN	158
G.	Implications for the Study of Glaucoma	159
V.	Summary	161
VI.	References	163

LIST OF FIGURES

<u>Figures</u>	<u>Page</u>
Figure 1. Anatomical structure of the eye.	2
Figure 2. Human trabecular meshwork's extracellular matrices.	4
Figure 3. Domain structure of matrix metalloproteinases.	11
Figure 4. Regions of conservation across members of metalloproteinase family.	14
Figure 5. The cysteine switch.	16
Figure 6. Mechanism of proteolysis.	18
Figure 7. Life cycle of the retrovirus.	26
Figure 8. Construction of the pSFF expression vector.	31
Figure 9. Interference to multiple retroviral infections.	34
Figure 10. Schematic diagram of ping-pong amplification.	36
Figure 11. Stromelysin cDNA coding sequence.	40
Figure 12. Restriction digests of pBS-SLN and pSFF.	42
Figure 13. pSFF coding and noncoding regions.	44
Figure 14. Sequencing data from pBS-SLN.	61
Figure 15. Selection of pSFF-SLN clone following ligation.	63
Figure 16. Restriction digests of pSFF-SLN to check	

orientation.	66
Figure 17. Schematic diagram of restriction sites.	68
Figure 18. Screening pSFF-SLN transfected cocultures for SLN mRNA.	70
Figure 19. Producing clonal cell lines expressing SFF-SLN mRNA.	72
Figure 20. SFF-GH coculture radioimmunoassay.	75
Figure 21. Schematic diagram of growth hormone introns and exons.	77
Figure 22. Screening of SFF-GH cocultures using PCR.	78
Figure 23. Ethidium bromide stained formaldehyde gel of SFF-SLN coculture RNA.	80
Figure 24. Autoradiograph of Northern blot probed with ³² P-SLN cDNA.	83
Figure 25. Schematic diagram of retroviral RNAs made from the SFF-SLN provirus.	85
Figure 26. Immunohistochemistry of nonconfluent SFF-SLN clonal cell line.	87
Figure 27. Immunohistochemistry of nonconfluent SFF-GH clonal cell line.	89
Figure 28. Immunohistochemistry of confluent SFF-SLN clonal cell line.	91
Figure 29. Immunohistochemistry of confluent SFF-GH clonal cell line.	93

Figure 30.	Immunohistochemistry without membrane permeabilizing detergent of SFF-SLN clonal cell line.	96
Figure 31.	Immunohistochemistry with membrane permeabilizing detergent of SFF-SLN clonal cell line.	98
Figure 32.	Immunohistochemistry with membrane permeabilizing detergent of SFF-GH clonal cell line.	100
Figure 33.	Western blot of conditioned medium.	103
Figure 34.	Zymogram of conditioned medium.	106
Figure 35.	Endoglycosidase treatment of SFF-SLN conditioned medium.	110
Figure 36.	Coomassie blue SDS-PAGE gel of SFF-SLN clonal conditioned medium (used for estimation of concentration of SLN).	112
Figure 37.	Western blot of SDS-PAGE gel of SFF-SLN clonal conditioned medium (used for estimation of concentration of SLN).	114
Figure 38.	Estimation of concentration of prostromelysin produced by clonal cell line.	117
Figure 39.	Western blot of SFF-SLN clonal conditioned medium following trypsin activation.	118
Figure 40.	Zymogram of SFF-SLN clonal conditioned medium following trypsin activation.	121
Figure 41.	Western blot of SFF-SLN clonal conditioned medium following activation by APMA.	123
Figure 42.	Zymogram of SFF-SLN clonal conditioned medium following activation by APMA.	125

Figure 43.	PCR of clonal RNA from cultures at 15% and 30% confluency.	129
Figure 44.	PCR of clonal RNA from cultures at 50% and 100% confluency.	131
Figure 45.	Growth hormone radioimmunoassay of conditioned medium from TM cells infected with SFF-GH.	134
Figure 46.	PCR of RNA from TM cells infected with SFF-GH.	135
Figure 47.	Phorbol-ester stimulation of SLN mRNA in bovine TM culture.	138
Figure 48.	Immunohistochemistry of bovine TM culture.	140
Figure 49.	Immunohistochemistry of nonconfluent porcine TM culture.	142
Figure 50.	Immunohistochemistry of confluent porcine TM culture.	145

ACKNOWLEDGEMENTS

I feel very fortunate in having not only obtained a degree, but also in having met and worked with some wonderful people along the way. Their support and encouragement has been probably as valuable as the shared protocols.

I would like to thank Dr. Ted Acott for his advising and the encouragement he never failed to offer in the midst of this project. The lab was a fun place to work and the environment one of helpfulness. I would also like to thank the people with whom I've worked while in the Acott lab: Dan Carr, Mary Wirtz, Lisa Parshley, Preston Alexander, John Bradley, Ky Nyguen, Aurelie Fisk and all the others.

My thesis advisory committee has been excellent in their helpful comments, suggestions and directions. They are: Dr. Jim Hare, Dr. Bob Burgeson, Dr. Eric Barklis and Dr. Felix Eckenstein.

I will always be extremely grateful to Dr. David Kabat for his generosity and support in allowing me to work with the retroviral expression system. Sue Kozak provided the protocols I used and all her help and support was greatly appreciated.

My good friend, Gail Horenstein, has earned my undying gratitude for all her encouragement and beer. I hope I can repay you by the time you finish your thesis!

And last, but perhaps most importantly of all, I would like to thank my husband, Dick (at least I think we're still married), for all those things he did throughout the course of my graduate school work, including but certainly not limited to: eating hot dogs for days, cooking his own hot dogs, paying the bills, having enough foresight to get a good job so he could pay the bills, and bringing me flowers.

ABSTRACT

Stromelysin (SLN), a member of the matrix metalloproteinase (MMP) family of secreted zinc-proteinases, is of primary importance in initiating extracellular matrix (ECM) turnover. Important substrates include proteoglycans, laminin and fibro-nectin. We have hypothesized that SLN plays a major role in the etiology of the blinding eye disease, glaucoma. In glaucoma, the trabecular meshwork (TM) becomes "clogged", putatively due to a defect in matrix turnover. By selectively over-expressing SLN in the TM, we hope to design an *in vitro* model for the study of glaucoma.

We have subcloned a SLN cDNA into a retroviral gene transfer vector (pSFF) and transfected two murine fibroblast packaging cell lines, which are grown in coculture. The two strains of virion produced by the cocultures are capable of cross-infecting one another (i.e. "Ping-Pong" amplification) resulting in high level infection and an enhanced production of virally-encoded SLN. While the mRNA for SLN had been cloned and sequenced, it had not been expressed and characterized. Before it could be used for enzymatic expression studies, therefore, it was necessary to show proper processing and functional activity of the SLN cDNA encoded protein.

We have shown that this expression system produces a retroviral mRNA

which contains recombinant SLN. Appropriate RNA processing occurs with both a growth hormone control gene and the SFF-SLN gene product. This mRNA produces a preproSLN, which is post-translationally modified in the golgi and secreted as a latent proenzyme. The retrovirally expressed proSLN exhibits characteristic molecular weights on SDS-PAGE gels and zymograms. Anti-SLN peptide antibodies recognize proSLN, both immunohistochemically and on Western blots. The latent propeptide undergoes activation by both trypsin and organomercurials to yield mature, fully active SLN.

We have used the retroviral amplification system to produce clonal cell lines which are stably producing as much as 30 μ g of proSLN per 10^6 cells per 24 hours (approximately 6 mg/L of medium), a significant increase over traditional sources of proSLN. This constitutive over-expression of SLN has provided a system where we have begun to examine how MMPs, their inhibitors, ECM molecules and ECM receptors may be regulated and expressed in accordance with feedback received from the cell's surface. In initial studies, we find an absence of direct feedback from SLN over-production on TIMP-1 and TIMP-2 mRNA levels in pre- and post-confluent clonal cell lines.

In addition, the use of infective virions produced by the murine fibroblast coculture system has allowed the infection of cultured TM cells and stable over-

expression of SLN. This allows examination of the role of ECM turnover in glaucoma through the use of in vitro flow systems designed for TM cell cultures and explant systems.

I. INTRODUCTION

A. Glaucoma

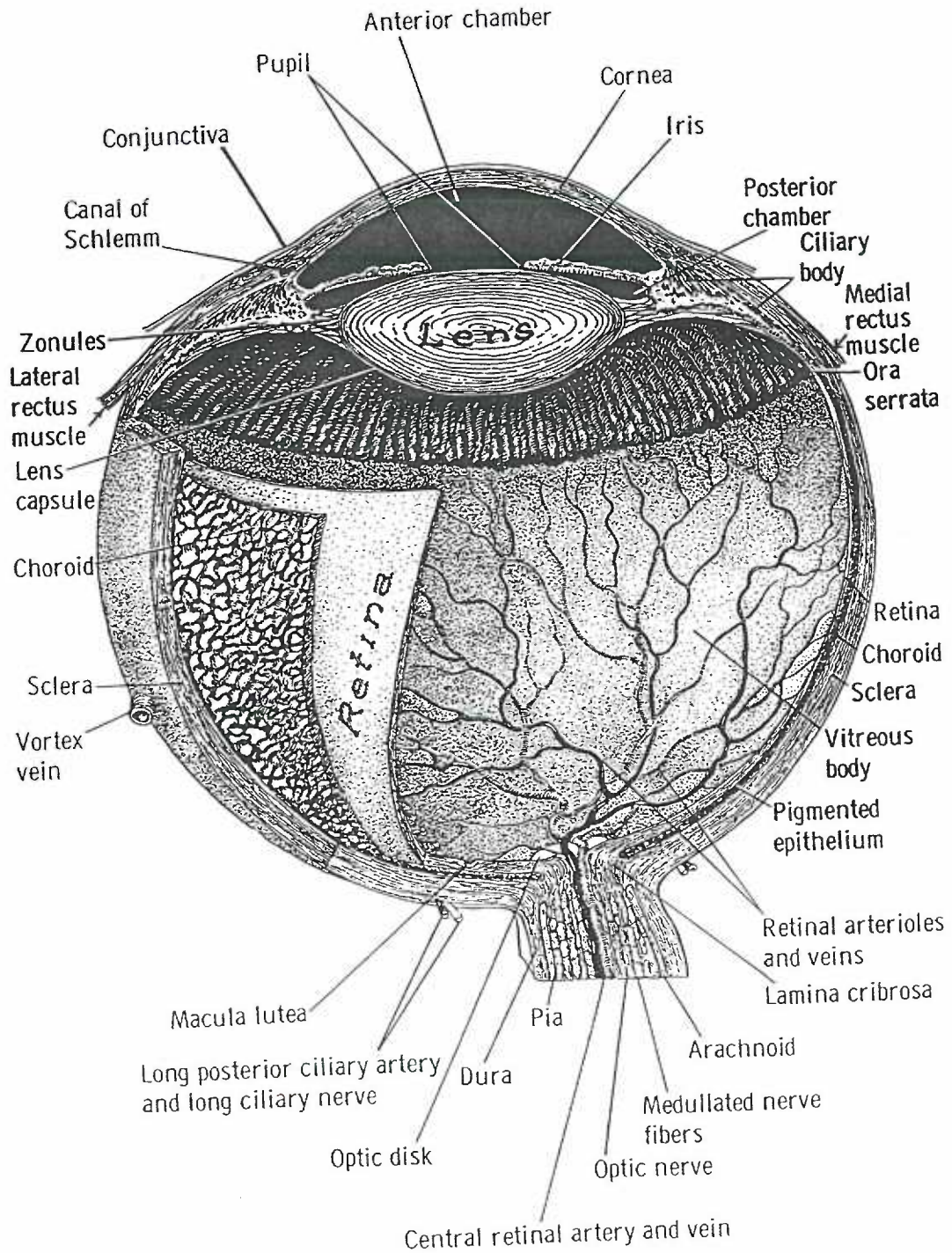
Primary open angle glaucoma (POAG) is a major blinding disease and the incidence increases dramatically with aging. Approximately 2% of Americans have glaucoma at age 40, while approximately 10% of the population have glaucoma by age 80.

Glaucoma is caused by an increase in intraocular pressure, which results when the outflow pathway for the drainage of aqueous humor from the anterior chamber of the eye becomes clogged. The increased intraocular pressure causes irreparable damage to the nerves which carry visual information from the retina to their brain targets, subsequently producing loss of vision.

Aqueous humor is made by the ciliary body (Fig. 1) and flows into the anterior chamber of the eye where it bathes the lens, iris and cornea. It exits the eye by flowing through a porous resistance filter called the trabecular meshwork (TM) and into Schlemm's canal where it enters the venous drainage system, carrying with it cellular debris and metabolites.

In glaucoma, the resistance to aqueous outflow through the TM increases, while the ciliary body continues to make aqueous humor at a constant rate,

Figure 1. Anatomical Structure of the Eye.
 (from: Daniel Vaughan, et al., *General Ophthalmology*,
 Chapter 1, First Edition, Lange Medical Publications, 1968.)



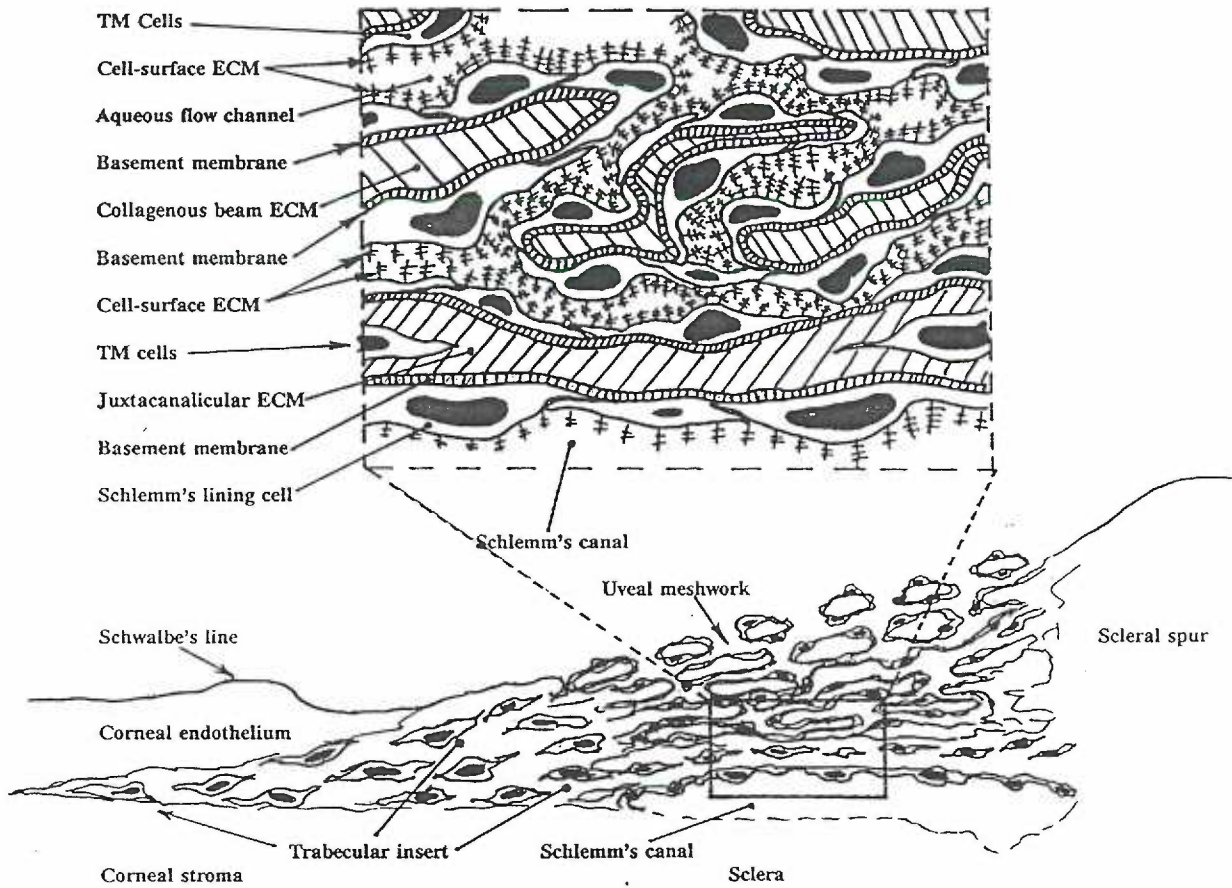
resulting in increased intraocular pressure. The molecular mechanism for trabecular obstruction has not been established.

B. Evidence of a Role for the Trabecular Meshwork in Glaucoma

The TM is composed of collagenous beams, laminin, fibronectin, and proteoglycans, which are made and maintained by the TM cells (Fig. 2). The aqueous outflow pathway consists of a series of channels through the meshwork's extracellular matrix (ECM). This ECM is particularly high in proteoglycans (PG) and their glycosaminoglycan (GAG) side-chains, which are synthesized and turned over by TM cells. The physical site of resistance to aqueous outflow appears to be in the deep corneoscleral and/or juxtacanalicular regions of the meshwork. The highly negatively-charged GAG side-chains of the PGs in the meshwork are a possible site for "clogging" by proteinaceous debris being carried away in the aqueous humor (1, 2).

In studies conducted in the early 1950's, the TM was perfused with hyaluronidase, a GAG degrading enzyme, resulting in a two-fold increase in outflow through the TM (3). From this work, it has been inferred, but not proven, that glaucoma results from an obstruction of the TM outflow pathway due to a change in the GAG side-chains of proteoglycans in the meshwork.

Figure 2. HUMAN TRABECULAR MESHWORK'S EXTRACELLULAR MATRICIES



The aim and focus of this thesis has been the establishment of an in vitro system, which will allow precise manipulation of extracellular matrix turnover. The application of this system to explants in tissue culture could provide a model for the study of the etiology of glaucoma. By manipulating the turnover of PGs, we will be able to evaluate changes in trabecular outflow and possible clinical treatments for glaucoma.

C. Extracellular Matrix and Its Turnover

Extracellular matrix (ECM), found within tissues and surrounding cells, can be very dynamic; under normal conditions a delicate balance exists between ECM synthesis and degradation. The major constituents of ECM are collagens, proteoglycans, fibronectin and laminin (4, 5).

Under normal conditions of homeostasis, ECM is turned over by proteolytic enzymes at a rate to balance its synthesis by the cells responsible for maintenance of the ECM. Two normally occurring biological processes where the balance between synthesis and degradation is altered, are angiogenesis (6) and wound/healing (7). In angiogenesis, proteolytic enzymes are released by capillary endothelial cells resulting in proteolysis of the underlying basement membrane. This allows migration of endothelial cells into the vessel wall stroma to establish

new capillaries (8). In the wound/healing paradigm, mitogens and growth factors cause increased synthesis and release of proteolytic enzymes, followed by tissue remodeling, cell migration and division in the wound site. When the regulation of the balance between ECM synthesis and degradation is altered, pathological states have been shown to result. These included rheumatoid arthritis, where the cartilage plate in joints is degraded (9), and tumor cell metastasis, where proteolytic enzymes are released resulting in proteolysis of healthy tissue allowing tumor cell invasion.

The complex ECM that makes up the trabecular meshwork is synthesized and turned over by the TM cells. The failure of the TM cells to maintain this filter is thought to cause glaucoma. TM cells use proteolytic enzymes to disrupt and engulf proteinaceous debris as it filters out of the aqueous humor flowing from the anterior chamber of the eye through the TM and into Schlemm's Canal. With the process of aging, several possible events could explain the TM cell's decreased ability to maintain the meshwork filter, including an age-related decline in cell number (10, 11) and/or reduced production of needed proteolytic enzymes.

TM cells synthesize six PG core proteins (12, 13, 14) and five associated GAG side-chains (15, 16, 17, 18, 19, 20, 21). Trabecular GAG biosynthesis and turnover normally occurs at a rapid rate with a half-life for the GAGs of

approximately 1.5 days compared to greater than 7 to 10 days in cornea or sclera (15, 22). If this turnover were slowed, the buildup of proteinaceous debris through the flow channels draining the anterior chamber of the eye could lead to an increase in intraocular pressure such as that which occurs with glaucoma.

D. Proteolytic Enzymes and the Trabecular Meshwork

Several different kinds of proteolytic enzymes are capable of degrading ECM components (23). They include serine proteases, such as plasminogen activators, elastase, and trypsin, which can degrade structural glycoproteins and cysteine proteases such as cathepsin B which can degrade denatured collagen. The largest and most important family of proteases involved in tissue maintenance, remodeling and wound/healing are the matrix metalloproteinases (MMPs), so named for their purported zinc-binding active site (136) and requirement of calcium for activity (9, 25).

Considering the comparatively rapid turnover of PGs and ECM in the meshwork and the endocytic/phagocytic function of the TM cells, the role played by proteinases in this tissue became a point of interest for the Acott lab. The serine proteinase, tissue plasminogen activator (tPA), has been identified in the TM (26, 27). The primary function of tPA has been shown to be the activation

of plasminogen, which is involved in dissolving fibrin clots, however, tPA has been shown to have some activity against certain ECM components (28). In cultures of TM cells, the ratio of secreted tPA to its inhibitor, tPA-I, has been shown to be relatively low (26). This has been interpreted to mean that tPA is present in this tissue more as a safeguard against a capillary disruption and the resultant damage that would be caused by intraocular blood clotting (26).

Since the MMPs and their inhibitors have been characterized in a variety of tissues (23, 29) and physiological circumstances (5, 6, 7, 8), they were investigated as being responsible for ECM turnover by the TM cells (128). In particular, one member of the matrix metalloproteinase family, stromelysin (SLN) (originally named "proteoglycanase") was of interest because of its role in the turnover of proteoglycans (9). If a slowed rate of proteoglycan turnover were responsible for glaucoma, then by manipulating the levels of SLN present in the meshwork, we should be able to manipulate flow rates.

A common clinical treatment for the amelioration of glaucoma uses a laser to make a series of 50 micron burns in the TM. This laser treatment has been shown to induce trabecular cell division followed by a change in the profile of GAGs being synthesized in the region (31). Upon closer inspection, it was shown that a rapid increase in mRNA levels of both MMPs and their inhibitors occurs

(32, 33) after laser treatment followed by an increase in the levels of these proteins to be found extracellularly (32, 33, 34). Using immunohistochemical and in situ hybridization techniques (34), increases in SLN can be localized to the TM areas adjacent to Schlemm's canal. This suggests that the relief in intraocular pressure, which is experienced after laser treatment, is mediated by increased ECM turnover due to the elevated SLN released in response to wounding of the TM.

E. The Matrix Metalloproteinases

The MMPs include three major subgroups, originally named for their substrate specificity. MMP-1 or interstitial collagenase initiates the degradation of native types I, II and III collagens by cleaving all three alpha chains of the triple helical structure (23) at a specific Gly-Ile or Gly-Leu bond (35, 36, 37). MMP-2 or Type IV Collagenase degrades denatured fibrillar collagens (gelatins) (38) and Type IV (39, 40), V (39, 40), VII (41) and XI (42) collagens, laminin and fibronectin. MMP-3 or SLN, degrades a wide variety of globular proteins (43) but most particularly, such basement membrane components as Type IV collagen, laminin, fibronectin and proteoglycans. It also cleaves at a Gly-Leu or Gly-Ile bonds, and others (9). Since proteoglycans have been implicated in glaucoma, SLN is the most likely candidate for a role in this disease.

Structurally, the different MMPs are closely related, for instance, with rabbit SLN sharing 51% sequence homology with rabbit interstitial collagenase (44). Interstitial collagenase is the best characterized of the MMP family. Much of the information about SLN is inferred from its structural and sequence similarity with interstitial collagenase. The active forms of the MMPs are made up of as many as five domains (45, 46). The amino terminal (putative active site) domain, zinc-binding domain, hemopexin-like domain, fibronectin-like domain and collagen-like domain (Fig. 3). The smallest MMP family member, Pump-1 (47), consists of two domains, the amino terminal and zinc-binding domains (48, 49).

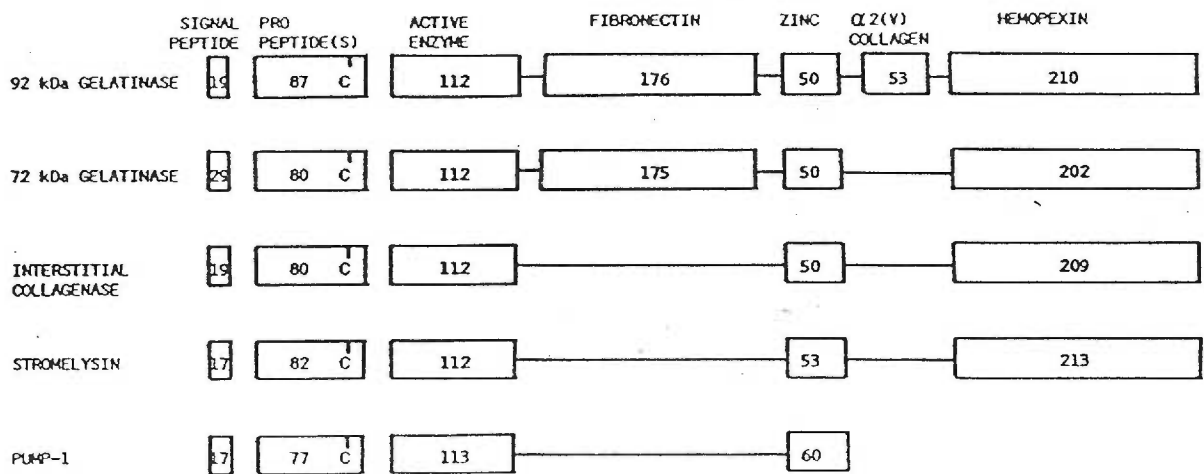
The zinc binding domain is highly conserved across all members of the MMP family and is encoded by a separate exon in each of the genes (50, 44). The zinc atom is proposed to be chelated to three amino acid residues including His²¹⁶ in the active site and to a fourth amino acid, an unpaired cys⁹⁰, in the propeptide amino terminal domain for SLN (51). This domain and the process of activation of SLN will be discussed in additional detail (see below).

A "hemopexin-like" carboxy-terminal domain has been described for at least two members of the MMP family, interstitial collagenase and SLN, and is thought to confer substrate specificity (52). Collagenase and SLN can undergo an autolytic cleavage, which removes this domain and gives a lower molecular weight form (21

Figure 3. Domain Structure of Matrix Metalloproteinases.

The number of amino acid residues is shown within each domain. Where domains are deleted, the connection of remaining domains is indicated by a single line. C indicates the approximate position of the cysteine involved in the activation of the latent "pro" form of the metalloproteinase to the active form.

(from: F. Woessner, "Matrix Metalloproteinases and Their Inhibitors in Connective Tissue Remodeling", The Faseb Journal, Vol 5, Page 2145, 1991.)



kD for SLN) of the active enzyme on an SDS-PAGE gel (45).

Type IV collagenase has been shown to be synthesized from at least two genes to produce a 72 kD and 92 kD protease. Both contain a fibronectin-like domain (53, 54) which probably functions in substrate recognition and binding. The two genes are differentially regulated at the level of transcription (141).

The last identified domain is in the 92 kD Type IV Collagenase which contains a collagen-like domain that serves an unknown function (53).

SLN and other MMPs are encoded and synthesized in the prepropeptide form (55). The signal peptide functions to route the nascent protein into the rough endoplasmic reticulum/golgi organelles. On SDS-PAGE gels, SLN has been shown to have a major 57 kD nonglycosylated form and minor 60 kD glycosylated form (55).

The latent form of the proteolytic peptides contain a "pro" peptide amino terminal sequence. The MMPs become activated by cleavage of this sequence following a variety of treatments (55). The "pro" form of SLN is approximately 57 kD on an SDS-PAGE gel (55) and when cleaved to its mature, active form is approximately 45 kD.

The MMPs are secretory proteins, but details of their release from cells are unknown. There appears to be a continuous low level of secretion, but it is not

known whether this is by way of membrane bound vesicles or some other mechanisms (55). Since SLN and other members of the MMP family are copurified by binding to a heparin sepharose column (56), and since heparin sulfate is present in abundance on the surface of cells as heparin sulfate proteoglycan, we also speculated that binding of SLN to the extracellular surface of the cell could be a means of localizing it to the cell's surface.

Sequence comparisons of MMP family members reveal two areas that are highly conserved. The first region is in the propeptide (Fig. 4). Its single unpaired cys residue is thought to be one of four amino acid ligands for the zinc atom of the active site. This "cysteine switch" maintains the latent state and this contact is broken when the enzyme becomes active.

The second highly conserved region is the putative zinc-binding region (Fig. 4). This region was identified based on its similarity to the zinc-binding region of the bacterial metalloproteinase, thermolysin. Thermolysin has been crystallized and studies using X-ray crystallography have shown a zinc atom is bound to two His and one Glu residue with a water molecule completing a tetrahedral coordination. A highly conserved region within interstitial collagenase and SLN contains an amino acid sequence of HExGH, which, based on similarity with the HExxH motif found in all identified metalloproteinases (57), is generally believed

Figure 4. Two regions of matrix metalloproteinases have been found to be highly conserved across all members of the family. The first region is located within the "pro" peptide sequence and referred to as the "cysteine switch". The second region of high sequence homology is in the enzymatic active site's zinc binding region.

(from: F. Woessner, "Matrix Metalloproteinases and Their Inhibitors in Connective Tissue Remodeling", The FASEB Journal, Vol 5, Page 2145, 1991.)

MMP-#	Source and enzyme	Cysteine switch region	Putative zinc binding region
MMP-1	Human fibroblast collagenase	68-MKQPRCGVPDVA	193-LHRVAA . HELGHS LGL SHST
MMP-1	Rabbit fibroblast collagenase	68-MKQPRCGVPDVA	193-LYRVAA . HELGHS LGL SHST
MMP-2	Human 72-kDa gelatinase	69-MRKPRCGNPDVA	364-LFLVAA . HEFGHAMGLEHSQ
MMP-3	Human stromelysin	70-MRKPRCGVPDVG	196-LFLVAA . HEIGHSLGLFHSA
MMP-3	Rabbit stromelysin	72- I RKPRCGVPDVG	197-LFLVAA . HELGHS LGL FHSA
MMP-3	Rat transin	68-MHKPRCGVPDVG	194-LFLVAA . HELGHS LGL FHSA
MMP-7	Human pump-1	65-MQKPRCGVPDVA	190- . FLYAATHELGHSLGMGHSS
MMP-8	Human neutrophil collagenase	66-MKKPRCGVPDSG	191-LFLVAA . HEFGHSLGLAHSS
MMP-9	Human 92-kDa gelatinase	75-MRTPRCGVPDLG	376-LFLVAA . HEFGHALGLDHSN
MMP-10	Human stromelysin-2	69-MRKPRCGVPDVG	195-LFLVAA . HELGHS LGL FHSA
MMP-10	Rat transin-2	70-MHKPRCGVPDVG	196-LFLVAA . HELGHS LGL SHSN

*Residues numbers from N-end of proenzyme, omitting signal peptide. Identities shown in boldface.

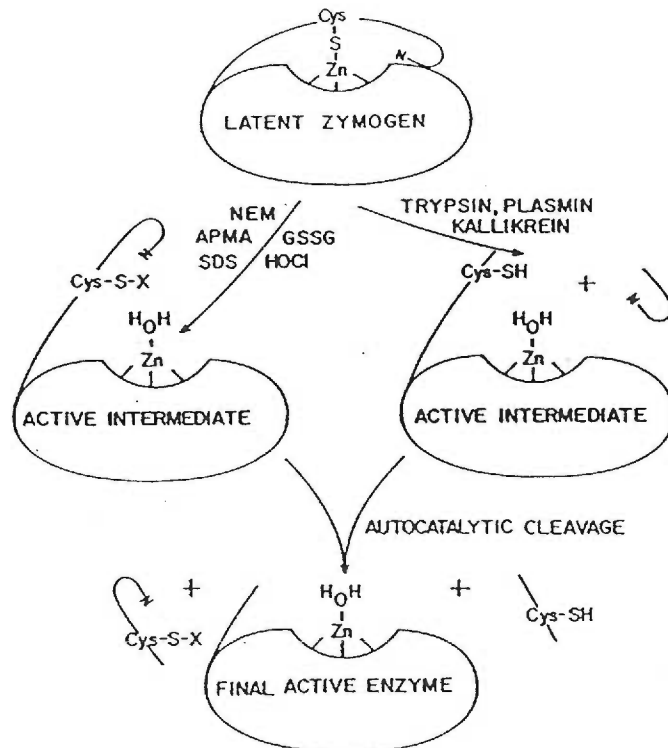
to form part of the zinc-binding site (51, 45). However, no X-ray structure for the MMPs is available to confirm this. Mutational studies of transin (ie. the rat homolog of SLN) have shown that point mutations of either His residues or the Glu residue result in functionally inactive enzyme (52).

The structural role played by zinc in protein conformation, such as in alcohol dehydrogenase, has been well described. Four coordination bonds with cys residues (tetradentate structure) (58) are formed and are essential to maintenance of the protein's structural integrity. The catalytic zinc of the MMPs is highly unusual in that it forms four coordination bonds with amino acids when the enzyme is in its latent propeptide form. In its catalytically active form, the cys of the cysteine switch propeptide, is removed (45) and replaced by a water molecule (tridentate structure). Even conservative point mutations in the cysteine switch result in the secretion of fully active transin (51, 52).

The first step in activation is to dissociate the cys residue from the zinc atom by changing the protein conformation, reducing the cys-S to cys-SH or proteolytic cleavage of the propeptide at any of several sites (45) (Fig. 5). Trypsin cleaves after Arg³⁷ in the propeptide sequence (63). With APMA activation, the second step is a cleavage in the propeptide at Val⁶⁹ for SLN (63) which occurs by an unknown mechanism. In experiments done with procollagenase, this activation

Figure 5. Schematic diagram of the cysteine switch mechanism for the activation of metalloproteinases. In the latent enzyme, zinc is coordinated to four amino acid residues in a tetradentate structure that is changed to one which is coordinated to three residues (tridentate). The cysteine that is removed is replaced by a water molecule. Structural perturbants can unfold the propeptide structure from the active site or proteolytic enzymes which cleave the propeptide. These intermediate forms undergo a second autolytic cleavage to the fully active form.

(from: F. Woessner, "Matrix Metalloproteinases and Their Inhibitors in Connective Tissue Remodeling", The FASEB Journal, Vol 5, Page 2145, 1991.)



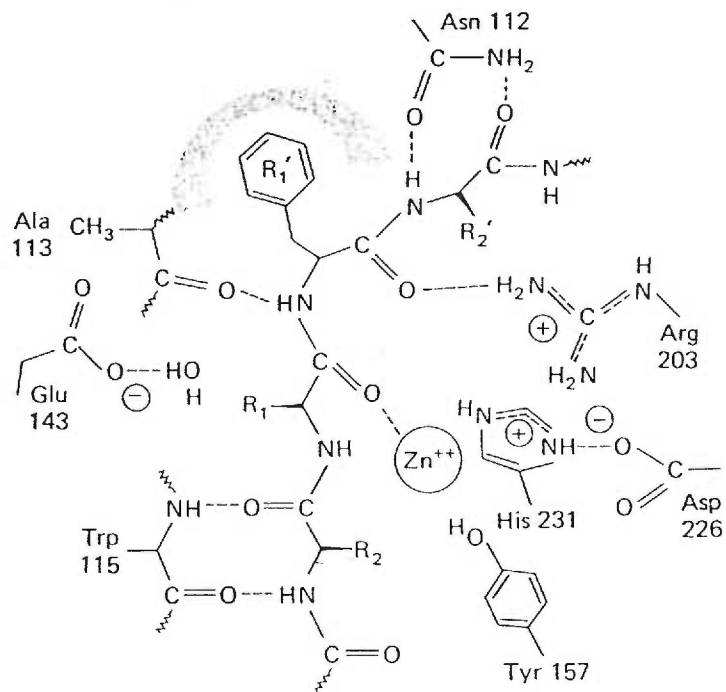
could be prevented by the presence of β -mercaptoethanol (25).

Okada et al. (61), using SLN purified from human rheumatoid synovial fibroblasts, showed the initial activation step with APMA probably involves a conformational perturbation. High salt, which stabilizes the conformation of proteins by increased ionic bonds, decreased the rate of activation of proSLN by organomercurials. The increased salt concentration, however, did not change the activity of already activated SLN.

The intermediate form of SLN created by trypsin and APMA is followed by a second cleavage between His⁸² and Phe⁸³, resulting in fully activated SLN at 45 kD (25, 61). The second cleavage is proposed to be an intermolecular event (63), because SLN substrates slow the conversion, suggesting competitive inhibition. Since the intermediate state resulting from trypsin and APMA activation is due to cleavage at different locations in the propeptide, these products electrophorese to 53 kD and 50 kD, respectively (63).

The mechanism of proteolysis by matrix metalloproteases is not known in detail, but inferences can be drawn from x-ray crystallography (143) of thermolysin, a bacterial metalloprotease. Upon binding its substrate, the carbonyl oxygen of the scissile peptide bond interacts with the Zn⁺² ion and replaces the water molecule of the active site (Fig. 6). An intermediate has been described for

Figure 6. Schematic drawing of the binding of thermolysin to a substrate. The peptide bond to be hydrolyzed is that between residues P_1 and P_1' . (From: "Proteins: Structure and Molecular Principles, T. E. Creighton, 1984).



thermolysin and one of its substrates, where a mixed anhydride is formed between the substrate and a Glu residue in the active site. The following structure is formed and the leaving amino group ("X") is proposed to be protonated by the His²³¹:



The latent form of the enzyme can be activated by protease treatment (25), conformational perturbants such as sodium dodecyl sulfate (59), organomercurials such as 4-aminophenylmercuric acetate (APMA) (60), other proteolytic enzymes, such as trypsin, chymotrypsin, plasma kallikrein, plasmin and thermolysin (61), as well as by spontaneous autoactivation (62).

To date, a second and third SLN gene have been identified and named SLN-2 (47) and SLN-3 (57). Sequence data shows SLN-2 to have 78% sequence similarity (64) with SLN. The rat homolog for SLN, transin, has been extensively studied by several labs (47, 51, 52, 65, 66, 67, 68, 69). It was originally discovered in a tumor cell line as a 1.9 Kb mRNA that was induced in response to exposure to growth factors (65, 66), tumor promoters such as phorbol-ester, 12-O-tetradecanoyl-phorbol-13-acetate (TPA) (67) and to oncogene activation (65). Transcriptional activation of the transin/SLN gene has been suggested to involve a c-fos/c-jun heterodimer intermediary in the case of at least one growth factor

(68). Working with the transin gene, Nicholson et al. have shown negative regulation of transcription to be mediated through an AP-1 binding site (69).

The cDNA sequence for SLN was determined by the Goldberg lab (55) using the deduced amino acid sequence from the amino terminal portion of the 45 kD form of SLN to make a degenerate 17mer oligonucleotide probe. A cDNA library made from human fibroblasts was screened and the largest clone sequenced. The clone was found to have 75% sequence homology with rat transin and 55% sequence homology with human collagenase. This sequence was identified as human SLN based on these homologies, but expression studies were not done to show an enzymatically active peptide would be produced from this sequence. We received this clone from the Goldberg lab and have conducted expression studies with it to show that a functionally active proteolytic enzyme can be made by eukaryotic cells. This includes the expected antigenic reactivity, golgi/RER processing, glycosylated and nonglycosylated forms, and treatment with organomercurials and trypsin to produce the intermediate activated form and fully activated mature form of SLN.

F. Tissue Inhibitors of Metalloproteinases

Herron et al. (70) observed that, while rabbit brain capillary endothelial cells

(RBCE) could be induced to secrete both procollagenase and prostromelysin by the phorbol ester, TPA, no enzyme activity could be measured in RBCE-conditioned medium even after activation of the proenzymes by trypsin or organomercurials. Enzymatic activity could be found, however, after conditioned medium had been analyzed by gel filtration or SDS electrophoresis (71). They subsequently show that metalloproteinase inhibitors of 30 kD (major band) and lesser amounts of a 22 and 19 kD inhibitor could be identified in the conditioned medium. These inhibitors were named tissue inhibitors of metalloproteinases or TIMPs.

The rate of ECM turnover is determined by the net activity of secreted proteases, which can be controlled at three levels: (1) rate of production of latent enzymes, (2) activation of latent enzymes by proteolytic processing and (3) production of specific inhibitors. To date at least two TIMP genes with differing glycosylation patterns have been identified, TIMP-1 (72) and TIMP-2 (73, 74). TIMP-1 has been shown to bind and inhibit interstitial collagenase (71), stromelysin (71) and Type IV collagenase (74). TIMP-1 binds the activated form of SLN in a 1:1 molar ratio (75) and forms a tight binding complex with an affinity constant of 3.8×10^{-10} M. No complex forms between TIMP-1 and the "pro" form of SLN (137). Experimentally, TIMP-SLN complexes have been shown to dissociate with 10 mM EDTA at 37° C and pH 3 (75). The zinc

chelator, 1,10-phenanthroline, was also shown to be capable of dissociating the complex, probably by way of conformational changes that result from the removal of the zinc atom. To date, no evidence has been presented that MMP and TIMP complexes are able to dissociate *in vivo*.

The balance achieved between the secretion and activation of proteolytic enzymes versus inhibitors will determine whether there is a net deposition of ECM occurring or a net degradation. During development, TIMP is expressed at low levels during embryogenesis, but transcripts increase in tissues undergoing ECM deposition such as sites of osteogenesis (77, 78). Over-expression of proteolytic enzymes is used by metastatic tumor cells to invade tissue, but a lack of TIMP can also result in the same phenomenon. In an experiment by Khokha et al., transfected Swiss-3T3 cells constitutively expressing TIMP-1 antisense RNA become invasive and tumorigenic (79). MMP and TIMP expression *in vivo* is coordinated and controlled by diverse stimuli including growth factors (80, 81, 82, 83), tumor promoting phorbol esters (84, 85, 86, 87, 88), hormones (89) and steroids (90).

Responsiveness of the TIMP-1 gene to such things as phorbol-esters and growth factors has been shown to be due to the promoter and enhancer element which contains a serum responsive element (SRE) and a phorbol-ester responsive

element (TRE) that binds an AP-1 heterodimer (91). This induction is similar to that of SLN and suggests a coordinate expression of proteolytic enzyme with its inhibitor as a means of preventing runaway proteolysis. TIMP-2, which is a separate gene product from TIMP-1, shares 41 % sequence homology with TIMP-1 and has been shown to bind interstitial collagenase (73, 74) and the active 72 kD Type IV collagenase (46). It has a molecular weight of 21.6 kD estimated from the amino acid sequence. Whether TIMP-2 binds to SLN is unknown. The TIMP-2 gene is under different regulation than the TIMP-1 gene. It shows no change in mRNA levels with TPA and, therefore, appears to be independently regulated from TIMP-1 (92).

Laser treated trabecular meshwork cells have also been shown to produce TIMP-1 in a coordinated fashion with SLN (32, 33) by Western blot analysis of conditioned media from laser treated TM explants.

G. Purpose For Using Ping-Pong Amplification of Stromelysin cDNA

By the subcloning and subsequent expression of SLN in a retroviral expression vector, four things will be gained: (1) the provirus is stably and permanently incorporated into the host cell's genomic DNA, thereby creating permanent cell lines which can be used for ongoing studies of SLN and ECM

turnover; (2) retroviruses use the host cell's transcriptional/translational processing machinery, which allows for such eukaryotic functions as "start" and "stop" codons, glycosylation of the nascent peptide and utilization of the cell's secretory pathway by the enzyme, as opposed to prokaryotic expression systems; (3) high level constitutive expression of SLN through the Ping-pong amplification system, devised by the Kabat lab, allows the characterization of the recombinant SLN to show its synthesis, processing as a secretory protein and enzymatic activity; and (4) the ability to infect other cell lines using the virions produced in the Ping-pong expression system allows the establishment of TM cultures constitutively expressing SLN.

With a tissue culture system for stably producing high amounts of SLN, it was hoped that purification of relatively large amounts of the enzyme would be possible. The creation of cell lines which are producing SLN would also allow the pursuit of studies examining how the over-expression of SLN in the trabecular meshwork could change the flow dynamics of aqueous humor through the tissue.

H. Retrovirus Structure and Life Cycle

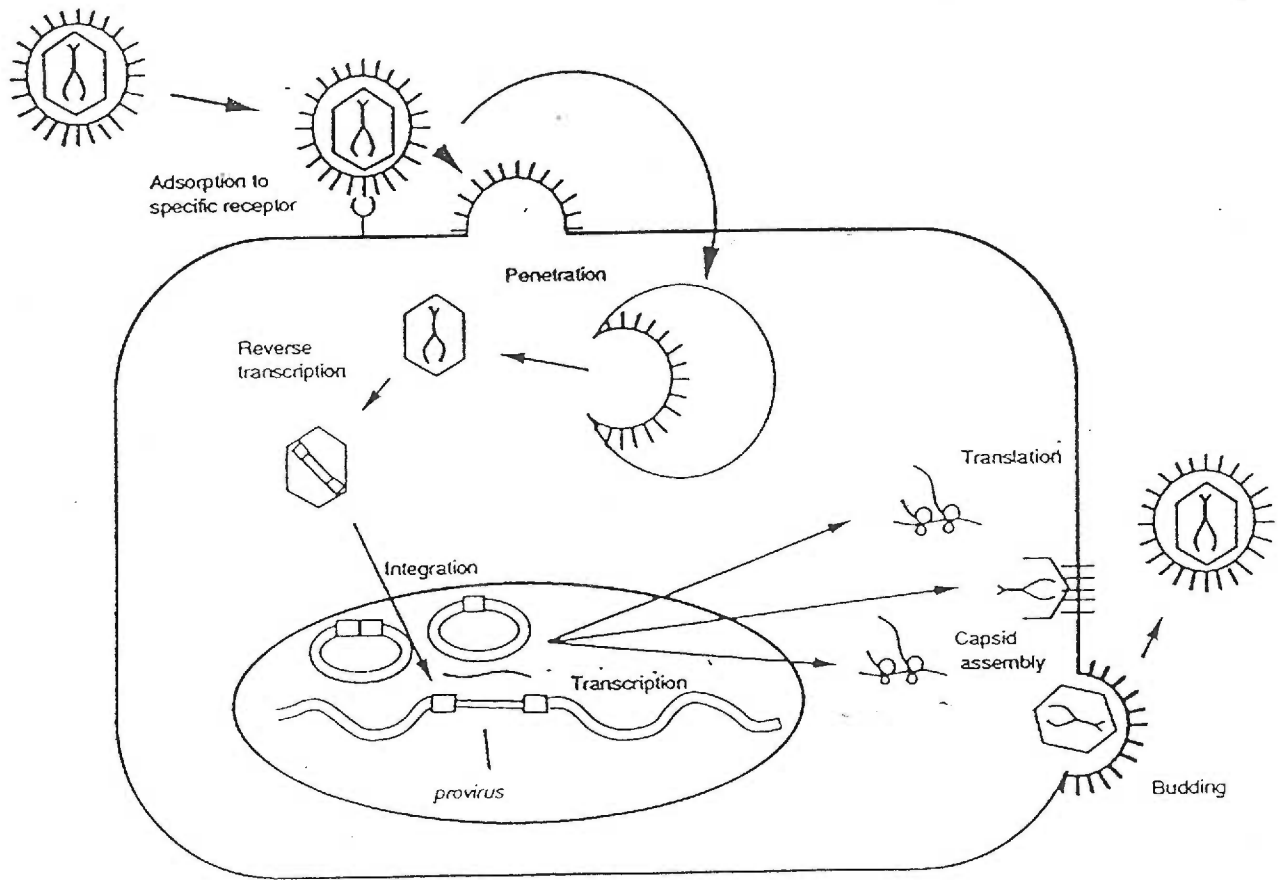
Retroviruses are characterized by the presence of the enzyme reverse transcriptase in the virions and use an RNA genomic template to produce a DNA

copy (93, 94), hence, the designation "retro" or backward. Many, but not all, of the known retroviruses carry in their genomes an oncogene capable of inducing sarcomas, leukemias, lymphomas and mammary carcinomas.

The extracellular virion contains two identical single-stranded copies of viral genomic RNA in a nucleocapsid core of viral proteins and enveloped by a membrane (derived from the previous host cell). This membrane is enriched in a viral glycoprotein (93) which is encoded by the viral env (for "envelope") gene. The nucleocapsid core is made up of proteins synthesized from the viral gag (for "group-specific antigen") gene. The pol (for "polymerase") gene encodes an integrase and reverse transcriptase with RNase-H (94) activity. The retroviral genomic RNA strongly resembles cellular mRNA in that it is capped at the 5' end and polyadenylated at the 3' end.

The retrovirus gains entry to a cell (Fig. 7) by binding of a specific cell surface protein with the retrovirally encoded envelope protein (95) which is expressed on the virion's surface; entry is through an unknown mechanism. Two suggested possibilities are receptor-mediated endocytosis (93) and fusion between the cell's membrane and the virion membrane (94). The cell surface receptor for one retrovirus, Murine leukemia virus, has recently been shown to be a basic amino acid transporter (96, 97).

Figure 7. Life Cycle of the Retrovirus.
(from: John M. Coffin, *Virology*, Chapter 51, Second Edition, ed. B. N. Fields, Raven Press, 1990.)



Once the virion core has penetrated the cell, the reverse transcriptase copies the genomic RNA into an intermediary minus-strand DNA with degradation of the RNA template by the RNase-H activity of the transcriptase. Plus-strand DNA synthesis then gives a double stranded intermediary (98). The DNA moves to the nucleus, where it can be found, transiently, as covalently-closed circular DNA. It then integrates into the host cell genomic DNA to form the provirus (94). Integration sites within the host chromosome appear to be in random locations (99, 100) that are unrelated to each other. However, the viral mode of integration is highly specific, occurring in the same place in the viral sequence (101, 102, 94).

Viral integration into the host cell DNA occurs most efficiently when the host cell's are dividing (103, 104, 105, 106). The efficiency of infection has been found to be 10-fold lower in G_0 - G_1 enriched, nondividing T-lymphocyte populations than S, G_2 and M phase cell populations (103). Stationary rat embryonic fibroblasts infected with an amphotropic retroviral vector containing neomycin resistance had a 100-fold lower infection rate than replicating fibroblasts (104). The block to formation of the provirus appears to occur following entry of the virus into the cell, but before formation of unintegrated viral DNA from the RNA genomic template (103, 104).

The retroviral integration sites are found in the noncoding "long terminal

repeats" (LTR) regions of the retroviral genome (diagrammed in Fig. 25). The coding and noncoding regions of the provirus contain several interesting features (102, 94, 93). LTRs have been found flanking the coding sequences on both the 5' and 3' ends and have been shown to be identical. The LTR contains enhancers and promoters in the U3 region. "R" is a region of terminal repeats and contains the 5' cap site and 3' polyadenylation signal. The primer binding site is 18 nucleotides long and binds a tRNA, which is used to initiate reverse transcription of minus-strand DNA. The "Psi site" is a packaging recognition signal on the 5' end of the retroviral genomic RNA used for the selective incorporation of viral RNA into assembling virions.

Three coding regions are generally described for most retroviruses. The gag region yields a polyprotein that can be cleaved to produce three to five capsid proteins. The gene contains a translational "stop" codon but an occasional read-through results in the reverse transcriptase encoded by the pol gene being made. The translational product of the env gene region, the viral envelope protein, is made from a subgenomic RNA, which results when the full-length genome is spliced at the 5' "splice donor" and 3' "splice acceptor" sites.

I. Friend Disease and Spleen Focus-Forming Virus

Spleen focus-forming virus (SFFV) was identified as the oncogenic component of Friend disease, a murine leukemia (107). It is replication defective with gene defects in its gag, pol and env genes. When murine erythroblasts carrying a helper virus, Friend Murine leukemia virus (F-MuLV), are infected with SFFV the resulting leukemia appears to arise in a two step process. First, the SFFV env protein, GP-55, acts as an erythroblast mitogen causing an erythroblastosis but producing cells which have only a limited self-renewal capacity. The proliferating cells continue to release viruses packaged by the F-MuLV and the continued infection of new erythroblasts results in a polycythemia. The proliferative capacity of these dividing cells is limited and they differentiate or die.

Two to three weeks later, in the second phase of the disease, infected cells can be detected, which have become immortalized by rare proviral integrations and rearrangements in the 5' region of the Spi-1 gene. This results in the high level expression of Spi-1, a homolog of the transcriptional activator PU.1 (108). When Spi-1 is inappropriately activated in erythroid cells, cell division (109, 110, 111) and an immortalized erythroid clonal cell population results.

An enhancer element has been identified in SFFV, which has a 42 base pair direct repeat (112).

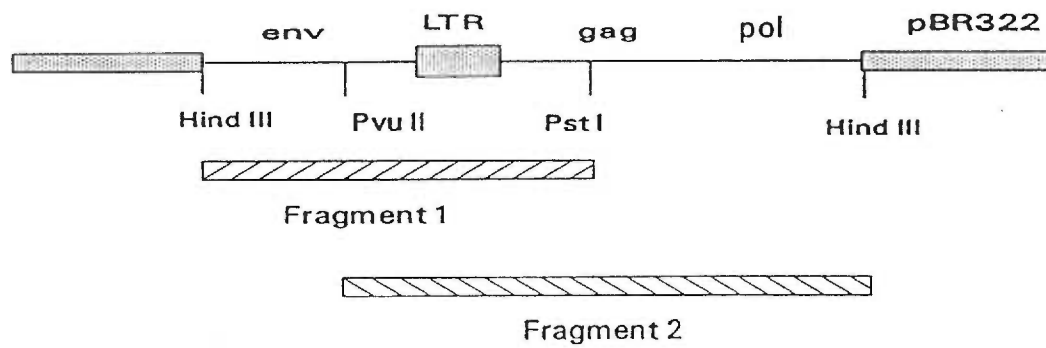
An anemia-producing form of Friend disease, designated SFFV_A, has also been described. It appears to be encoded in the 3' region of the SFFV env gene and results in a proliferation of erythroblasts followed by an ineffective erythropoiesis which results in the anemic state (107).

J. Expression Vector pSFF

To construct the pSFF expression vector, a clone of the Lilly-Steeves polycythemia strain of SFFV was cloned in pBR322 (113) (Fig. 8). The resultant vector was digested with Pst I and Hind III to produce fragment 1, which contains the env and LTR regions; fragment 1 was then subcloned into pSP65. A second fragment of Pvu II-Hind III digested pBR322 vector and containing the LTR, gag and pol regions was subcloned into pSP64. A unique Xmn I site in both pSP65 and pSP64 used in conjunction with the Hind III site, allowed the two resulting fragments to be ligated together to form a plasmid containing the entire SFFV proviral genome (95). This plasmid construct was further modified to make the expression plasmid, pSFF, by deletions in the pol and env gene regions. The addition of a multiple cloning site in the env gene was accomplished through the use of linkers allowing other DNAs to be subcloned into the expression vector (114).

Figure 8. Construction of the pSFF Expression Vector.

Fragment 2, containing the LTR, gag and pol regions, was removed with restriction enzymes Pvu II and Hind III. It was ligated with Hind III/Pst I digested Fragment I, containing env and the LTR, using their common Hind III restriction site.



(In the following discussions of this system, "pSFF-SLN" or "pSFF-GH" will be used to designate the plasmid expression vector, which contains the spleen-focus forming virus and the inserted human stromelysin cDNA or human growth hormone gene. When discussing the cell cultures produced following transfection with this plasmid vector and virions made by these cells, "SFF-SLN" or "SFF-GH" will be used to designate the proviral form of the vector or its RNA.)

K. Ping-Pong Amplification Expression System

Typically, a cell will be infected only once by a particular retrovirus, which stably inserts itself at the long terminal repeats (LTR's) into the host cell's genome, apparently at random (101, 100, 99). The host cell's transcriptional and translational machinery is then utilized to produce RNA and proteins encoded by the gag, pol and env genes. Proteins from these three gene products are required for the assembly of infectious virions. Defects in these gene products result in "replication-defective" retroviruses, such as SFFV (114). Infectious virions of the murine Type-C variety (93) bud out from the cell's surface and are released, in this case, into the media (Fig. 7).

To infect a cell, the virion uses the env proteins on its surface to bind and interact with cell surface receptors. An infected cell will express some of the

retroviral env protein on its surface, where it appears to interact with these cellular receptors and prevent further infection of that cell by more virions using the same type of receptors (94). This process is called "interference" and typically limits multiplicity of infection to one viral copy per cell (Fig. 9).

Murine Type-C retroviruses are classified according to the host-range of their env proteins (94). Ecotropic viruses are capable of infecting only murine cells. Amphotropic viruses infect murine cells and most other species. Xenotropic viruses infect other species, but not murine cells.

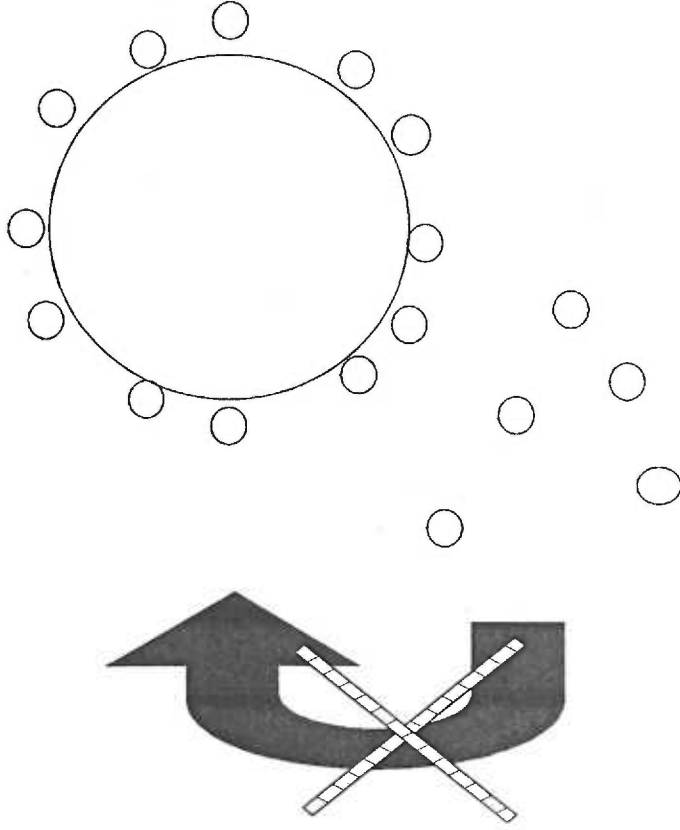
The Ping-pong amplification system, developed by the Kabat lab (114, 115), provides a means of circumventing the interference that results from expression of the env protein on the cell surface, thus allowing multiple infections of cells. With the increased multiplicity of infection the amount of retrovirally encoded protein made as a percentage of total cellular protein rises and has been found to be as high as 4-6% of total cellular protein synthesis (115).

To achieve this amplified retroviral infection, two murine packaging cell lines are grown in coculture. These two packaging lines, Psi-2 (116) and PA-12 (117) cells, are capable of packaging the genomic RNA of other retroviruses into virions, but their own packaging signal is defective. Psi-2 cells, of the ecotropic host-range, and PA-12 cells, of the amphotropic host-range, each release virions

Figure 9. Interference prevents multiple infections of same host.

PA-12

Amphotropic cells



capable of infecting the other cell line (Fig. 10), but not themselves. Since they will be packaging SFF-SLN as their genomic material, which contains a defective and truncated env protein into which SLN has been inserted, the cell surface receptors will not be blocked by interference, hence, the occurrence of multiple infections of any particular cell.

The process of multiple viral infections is begun by transfection of Psi-2 and PA-12 cocultures utilizing a calcium phosphate precipitate of the pSFF-SLN expression vector. Once inside the cell, some of the plasmid vectors will make their way to the nucleus and incorporate into the host cell's genomic DNA as the proviral form using the retroviral LTRs (94). Following incorporation, SFF-SLN RNA is made using the host cell's transcriptional machinery, and has two fates: one pool of RNA can be processed into functional proteins, the second is packaged into infectious virions which are released. Once integrated into the host's genomic DNA, the provirus is stable and will be inherited by daughter cells in future cellular divisions (94), thus creating cell lines which are capable of permanently expressing a particular gene.

By the creation of permanent cell lines which stably over-express SLN, we hoped to be able to produce high enough levels to characterize this previously unexpressed cDNA in both the intracellular and media-borne forms. These cell

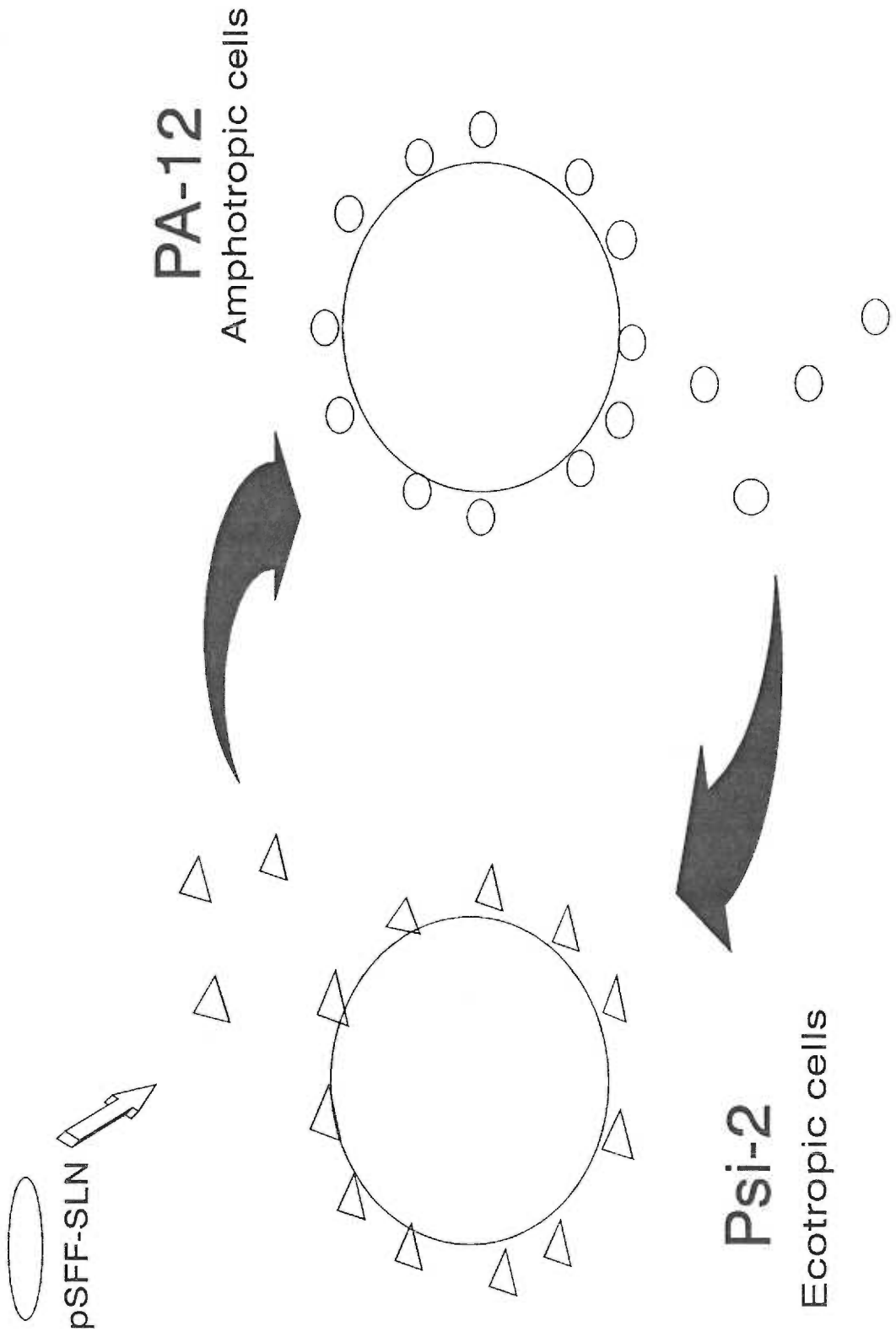


Figure 10. Ping-pong amplification following transfection of pSFF-SLN

lines could also provide a means of studying cellular response to constitutive synthesis and secretion of SLN. And thirdly, infectious virions harvested from the cocultures could be used to establish TM cell cultures synthesizing SLN, for the purpose of establishing working models of ECM turnover and its role in glaucoma.

II. MATERIALS AND METHODS

A. Cell Cultures

Psi-2 (116) and PA-12 (117), murine fibroblast packaging cell lines were grown in T25 flasks (Costar) using 5 mls Dulbecco modified Eagle medium (DMEM) supplemented with 10% fetal bovine serum (FBS) at 37° C and 5% CO₂.

Bovine and porcine trabecular meshwork cells were grown in T25 flasks with 5 mls DMEM supplemented with 5% Nu-Serum (Collaborative Research, Inc.) at 37° C and 5% CO₂ (118, 15). Cultures were used at passage number 5.

B. Stromelysin cDNA

The human stromelysin cDNA (SLN-cDNA) used was provided in the plasmid vector pBS (pBS-SLN) by the G. Goldberg lab (55).

E. coli DK-1 cells were transformed with 100 ng of pBS-SLN and grown overnight on luria-agar plates in the presence of 50 µg/ml ampicillin according to the methods of Maniatis et al. (119). Two colonies were selected and grown overnight in 100 ml liquid luria broth cultures. Total cellular nucleic acids were extracted from the cells using NaOH-SDS (120). Ethidium bromide and cesium chloride were added to a final concentration of 1.7 mg/ml and 10.4 M,

respectively, put in 10 ml "Ultraclear" centrifuge tubes (Beckman) and low density (4.5 M) cesium chloride was carefully layered on top. The tubes were centrifuged overnight in a Beckman L755 Ultracentrifuge, T80 rotor at 50,000 rpm and 20° C (119). The supercoiled plasmid DNA band was removed by a 16-gauge needle puncture and ethidium bromide was extracted from the DNA using isopropanol saturated with 5 M NaCl (119). The concentration and purity of recovered DNA was determined using A260/A280 spectrophotometric readings. Plasmid DNA was brought to 1 mg/ml final concentration, digested with several restriction enzymes and subjected to agarose gel electrophoresis to verify restriction sites and purity.

C. DNA Sequencing

To ensure the 5' region of the pBS-SLN construct, which encodes the "pre-pro-" portion of the enzyme (Fig. 11), was intact, the plasmid was sequenced using the "Sequenase" Chain Termination Sequencing kit (U. S. Biochemical Corp.). A universal primer (-40 primer) which binds to pBS (5' to the insertion site of SLN) was used to start the sequencing reaction. Two μg of pBS-SLN were heated to 65° C and cooled slowly to allow primer annealing. The deoxynucleosides, dCTP, dGTP, dTTP and $\alpha\text{-}^{35}\text{S}\text{-dATP}$, are incorporated in 4 reaction tubes by "Sequenase" (DNA polymerase) using the DNA template.

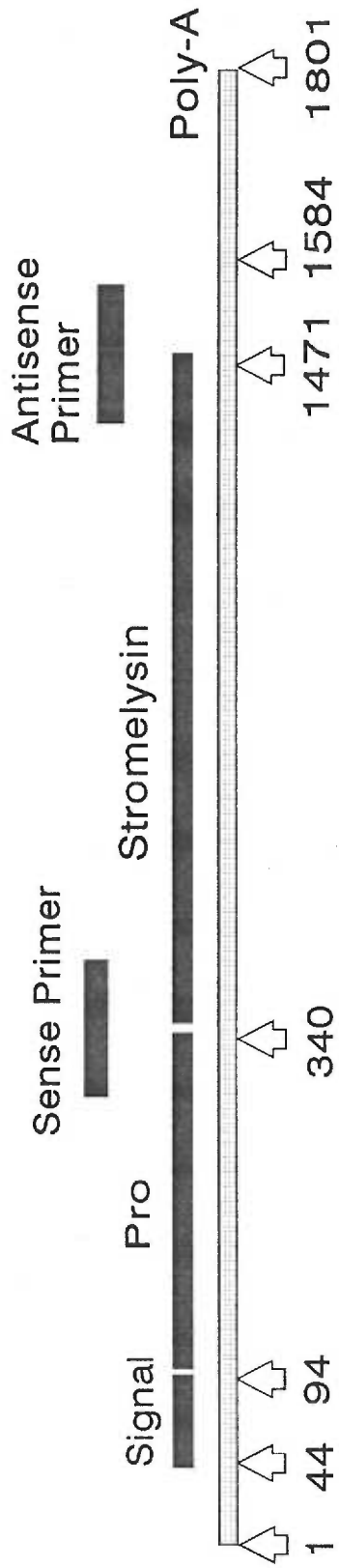


Figure 11. SLN coding regions and cDNA.

Reactions are randomly terminated when a dideoxynucleotide (one ddNTP used per reaction tube) is incorporated by the enzyme into the template, resulting in chains of different lengths. When electrophoresed on a 6% denaturing polyacrylamide gel (8.3 M urea, 1 M Tris-Borate, 20 mM EDTA, pH 8.3 gel buffer) a different pattern of DNA fragments for each reaction vial is seen. When read next to one another this provides the sequence of the DNA. The gel was run for 2 hours at 1300 V, washed in 10% acetic acid, 12% methanol, 1% glycerol, dried for 1 hr. at 80° C under vacuum and autoradiographed overnight with X-OMAT AR5 film (Kodak Labs).

D. Construction of pSFF-SLN Retroviral Expression Vector

For the purpose of ligating SLN-cDNA into the pSFF expression vector, 1 μ g of pBS-SLN was digested with the restriction enzyme Bam HI (BRL Labs, Inc.) (cuts at 5' end of SLN-cDNA) and electrophoresed on a 1% agarose gel. This resulted in a linear DNA at 4.5 Kb (Fig. 12). Xho I (BRL Labs, Inc.) was used to cut at the 3' end and results in two bands, one at 3.0 Kb (pBS backbone) and one at 1.6 Kb (SLN-cDNA). pSFF was also digested with Bam HI and Xho I cleaving at the 5' and 3' ends, respectively, of a multiple cloning site located in the env gene region (Fig. 13). A linear band is observed at approximately 9.2 Kb

Figure 12. Restriction Digests of pBS-SLN and pSFF.

- Lane 1: pBS-SLN digested with Bam HI results in a linear plasmid at 4.5 Kb when electrophoresed on a 1% agarose gel.
- Lane 2: pSFF digested with Bam HI results in a linear plasmid at 9.2 Kb.
- Lane 3: Molecular weight standards (Hind III digest of lambda DNA) Bands at 23.1, 9.4, 6.6, 4.4, 2.3, 2.0, 0.6 Kb.
- Lane 4: pBS-SLN digested with Xho I and Bam HI results in a pBS band at 3.0 Kb and SLN at 1.6 KB. The SLN insert was used for ligation into the pSFF expression vector.
- Lane 5: pSFF digested with Xho I and Bam HI results in a linear plasmid at 9.2 Kb. (The fragment between the two restriction sites is too small to noticeably change the size of pSFF on a gel.)

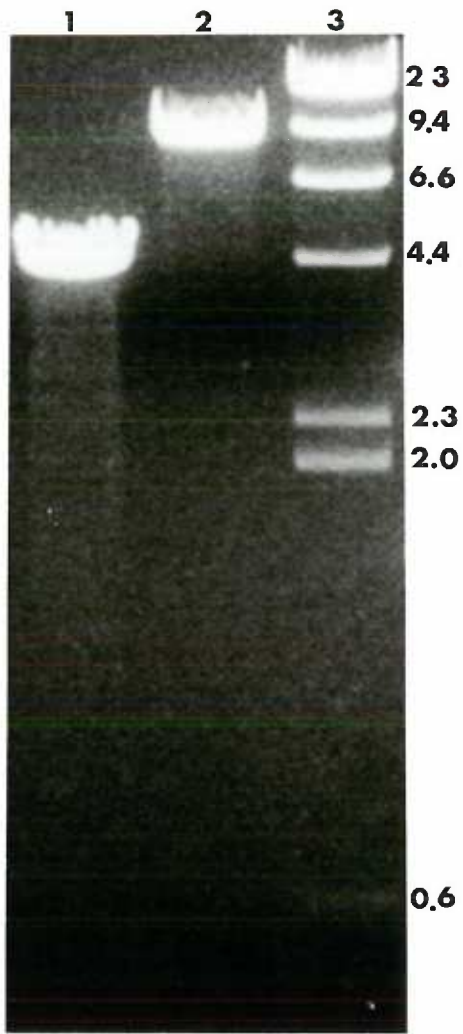
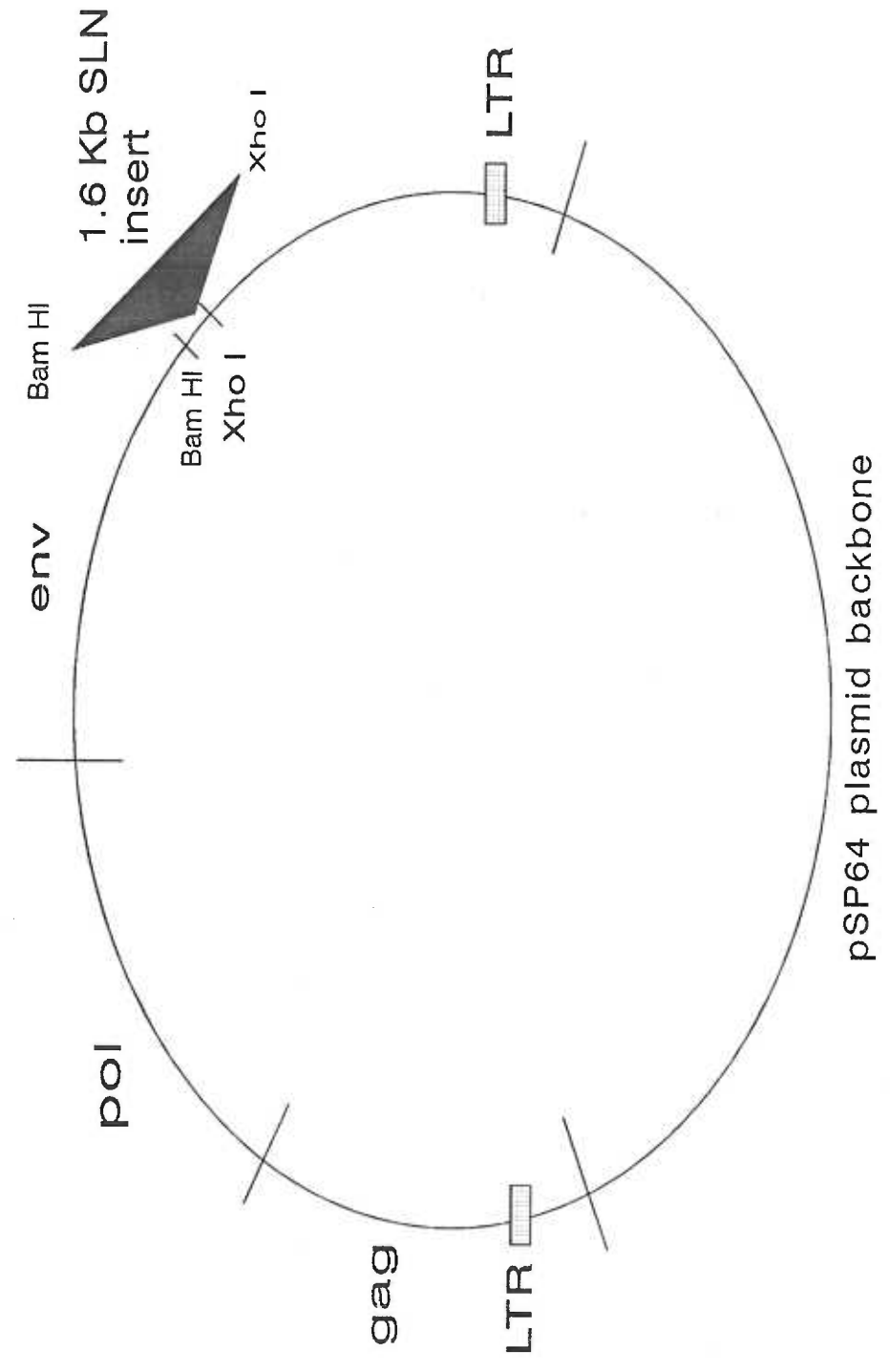


Figure 13. Structure of the pSFF-SLN vector. SLN cDNA was inserted into the expression site of the pSFF retroviral vector.



following agarose gel electrophoresis (Fig. 12).

A preparative electrophoretic gel (1% agarose, TAE buffer) was run to separate the two digested plasmids (119) and the appropriate bands were excised from the gel. The DNA was eluted from the gel slices using the microfuge spin technique of Heery et al. (121). Briefly, a 0.65 ml microfuge tube is punctured at the bottom with a needle, plugged with glass wool, siliconized and autoclaved. The gel slice is placed in the tube and the tube is placed inside a 1.5 ml microfuge tube and centrifuged for 10 min. at 12,000 X G. The DNA elutes from the gel slice with the gel buffer and collects in the bottom microfuge tube.

SLN-cDNA was ligated into pSFF using T4-DNA Ligase (BRL, Inc.) overnight at 14° C. DK-1 E. coli cells were made competent using CaCl₂ (119), frozen at -70° C, and thawed before using for transformation. To transform, an estimated 16 ng of plasmid DNA from the ligation was added to 100 μ l of DK-1 cells, heat shocked for 5 min. at 37°, spread on luria-agar plates containing 100 μ g/ml ampicillin and grown overnight at 37° C (119).

Several of the colonies growing on the plates were selected and grown up in overnight luria broth liquid cultures and the plasmid DNA was isolated using a mini-prep protocol (119). Plasmid DNA from the mini-preps was digested with Xho I and Bam HI, and electrophoresed on a 1% agarose gel. Of the colonies

which yielded bands of the expected sizes (i.e. 9.2 Kb for pSFF and 1.6 Kb for SLN), two were selected for further analysis by restriction digestion, grown up and the plasmid DNA purified using cesium chloride and ultracentrifugation as previously described.

E. Transfection

To make cocultures for transfecting, Psi-2 and PA-12 packaging cell lines were trypsinized, counted with a hemocytometer and seeded 1:1 in T25 flasks at a final cell density of 500,000 cells per flask. Cocultures were grown for 48 hours in 5 mls DMEM before transfecting.

DNA for transfection was precipitated as a calcium phosphate aggregate (51) by mixing 10 μ g plasmid DNA with 0.5 ml of 250 mM CaCl_2 and adding 0.5 ml phosphate buffer (50 mM HEPES, 250 mM NaCl, 1 mM NaH_2PO_4 , pH 7.1) dropwise, with mixing, to the solution. Medium was aspirated from flasks, 1 ml of DNA aggregate was added per flask and flasks were incubated at room temperature for 20 minutes. Three mls of transfection medium (DMEM, 10 mM HEPES, 10% FBS, 0.12% NaH_2CO_2 , pH 7.1) was added, flasks were tightly capped and incubated for 4 hours at 37° C. The cells were glycerol shocked by aspirating off the medium, rinsing with phosphate buffered saline (10X solution:

10 mM NaH₂PO₄, 1.3 M NaCl, 30 mM KCl, 0.3 M Hepes, 0.1 M glucose) and incubating with 10% glycerol in phosphate buffered saline at room temperature for 2 minutes. The glycerol solution was removed, growth medium added back to the cells and they were grown for several days before passaging (122, 123, 124).

Mock transfected control cells went through the process of transfection, however, did not receive any retroviral vector. Retroviral control transfected cells received pSFF which contained the human growth hormone gene (pSFF-GH) (114).

To establish clonal cell lines of retroviral infected cells, cocultures were trypsinized as for passaging, the cells were counted with a hemocytometer and then diluted to a final concentration of 30 cells per 20 ml of media. The diluted cells were then plated into a 96-well tissue culture plate (Falcon, Inc.) at 0.2 ml media per well and incubated for ten days. At the end of that time, wells with colonies growing in them (typically 10-20 wells per plate) were trypsinized, reseeded into 24 well tissue culture plates (Falcon, Inc.), incubated for 1-2 days, and then passaged into T25 flasks.

F. Infection of Trabecular Meshwork Cells

Medium was collected from transfected pSFF-SLN, pSFF-GH and mock

transfected cocultures, aliquoted and stored frozen at -20° C. To infect bovine and porcine trabecular meshwork cells, TM cultures were passaged and seeded into new flasks at 200,000 cells per flask with 3 mls of fresh DMEM and a 1 ml aliquot of thawed coculture medium (from SFF-GH, SFF-SLN or mock control cocultures). The next day, an additional aliquot of the respective coculture medium was added to the appropriate flasks. Cultures were passaged and the process repeated a second time on day 4. At the end of approximately one week, cultures were assayed for gene expression using polymerase chain reaction, radioimmunoassay or immunohistochemistry. PCR was carried out using SLN sense and antisense primers as described below (Point H). RIA was performed on 100 μ l from a total volume of 2.5 or 5 mls of conditioned media, which was harvested at 24 or 48 hours. Immunohistochemistry is detailed below (Point K).

G. Radioimmunoassay

Cell culture medium was tested (100 μ l of conditioned medium used from 2.5 or 5 ml total volume, after a 24 or 48 hour exposure) for the presence of human growth hormone using Quantitope Radioimmunoassay kit (Kallestad Diagnostics, Chaska, MN). Assay sensitivity was to 1.5 ng of GH/ml media.

H. Screening Transfected Cocultures

The polymerase chain reaction (PCR) was used to screen transfected murine cocultures for SFF-SLN positive cocultures. To obtain the cellular RNA, cells were trypsinized from flasks, counted with a hemocytometer, and nucleic acids from 1×10^5 cells were extracted using 4 M guanidinium isothiocyanate, 30 mM sodium acetate, and 1 mM β -mercaptoethanol (125). Protein was removed by extraction with an equal volume of phenol:chloroform:isoamyl alcohol (25:24:1) and the nucleic acids precipitated using 1.0 volume isopropyl alcohol at -20°C followed by centrifugation (119).

The SLN mRNA was reverse transcribed into cDNA using 200 Units Moloney murine leukemia virus reverse transcriptase (BRL, Inc.), 10mM dNTPs and 10 pM antisense primer. The primer was a 33mer (Operon Technologies, Inc.) which anneals to the stromelysin mRNA at +1443 base pairs (Fig. 11).

DNA amplification was conducted in a PCR thermal-cycler (Perkin-Elmer Cetus, Norwalk CT) using 1 Unit *Thermus aquaticus* DNA polymerase (Perkin-Elmer Cetus) and 50 pM of the 27mer stromelysin sense primer (Operon Technologies, Inc.) with homology to the 5' region 36 bp downstream from the AUG start site (Fig. 11). Thermal cycling (35 cycles) was conducted for 1 min. at 94°C to melt, 1 min. at 55°C to anneal and 2 min. at 72°C to extend. From

the reaction volume of 100 μ l, 10 μ l was used for an analytical 1% agarose gel. Hind III digested lambda DNA (New England Biolabs, Inc.) was run as a molecular weight standard, with bands at 23.1, 9.4, 6.6, 4.4, 2.3, 2.0, 0.6 and 0.1 Kb. A 1.4 Kb PCR product is made from this combination of stromelysin primers.

I. Polymerase Chain Reaction with Multiple Primers

To test for the presence of Tissue Inhibitors of Metalloproteinases (TIMP-1 and TIMP-2), RNA was extracted from 6.25×10^5 cells, as previously described, and resuspended, following alcohol precipitation, in 50 μ l diethylpyrocarbonate (DEP)-treated H₂O. Cells were harvested at 24, 48, 72 and 144 hours, representing 15%, 30%, 50% and 100% confluent cultures, respectively. For reverse transcription, RNA was aliquoted in five 10 μ l amounts with reagents and antisense primers added as described previously. Thermal cycling was conducted as described above using the appropriate sense primer.

Each of the five aliquots received primers to make one of the following cDNA's: stromelysin, growth hormone, TIMP-1, TIMP-2 or glyceraldehyde-3-phosphate dehydrogenase (G-3-PD), used as an internal standard. Primers to make all five cDNAs were approximately 25-33mers in size and made to unique

sequences within the gene of interest. The PCR products made using these primers were electrophoresed on a 1% agarose gel. Their sizes were: 0.40 Kb for TIMP-1, 0.44 Kb for TIMP-2, 0.3 Kb for G-3-PD, 0.4 Kb for growth hormone and 1.4 Kb for SLN.

J. Northern Blotting

RNA was extracted from two T-25 flasks using guanidium isothiocyanate by the method of Wilkinson (125) and pelleted from 5.7 M cesium chloride (spin for 16 hrs. at 55,000 rpm, 18° C in a Beckman TL-100 Tabletop Ultracentrifuge). Spectrophotometric readings at A260/A280 were used to determine nucleotide/protein concentrations of all RNA preps.

The purified, extracted RNA was run on a 15 X 15 cm 1% formaldehyde-agarose gel overnight at 25 Volts (0.2 M MOPS, 50 mM sodium acetate, 10 mM EDTA, 1.1 M formaldehyde running gel buffer). An RNA ladder (BRL, Inc.) was run as a size marker, with bands at 9.5, 7.5, 4.4, 2.4, and 1.4 Kb. Samples were electrophoresed in the presence of ethidium bromide to allow visualization of RNA. The RNA ladder and 18/28S rRNA bands were marked on the gel under ultraviolet light and the gel was photographed using a Polaroid camera and 667 film (Kodak).

The gel was blotted following the methods of Maniatis, et al. (119) for 3 hrs. with a Nytran membrane (Bio-Rad, Inc.). RNA was cross-linked to the blotting membrane with ultraviolet radiation using a Stratalinker (Stratagene, Inc.).

To probe the northern blot, pBS-SLN was digested with Bam HI and Xho I restriction enzymes (BRL Labs, Inc.), and the resultant DNA run on a 1% low-melt agarose (Sigma Labs) gel in TAE buffer. The band of interest (1.6 Kb for SLN) was excised and the DNA purified according to the methods of Qian & Wilkinson (126), where buffer is added to the gel slice, heated until boiling, spun in a microfuge for 5 min. and buffer (containing DNA) removed from the pellet. An estimated 25 ng of SLN cDNA was used for labeling with the "Prime-It" Random Primer Kit (Stratagene, Inc.) using 50 μ Ci of α -³²P-ATP (New England Nuclear). To remove unincorporated counts, the probe was spun for 4 min. over a "Biospin-30" chromatography column (Bio-Rad) and added to the hybridization buffer on the blot. The probe was labeled to a specific activity of 1.2×10^9 dpm/ μ g as determined by liquid scintillation counting. Probing was done overnight at 42° C, according to Maniatis et al. (119) and the blot washed, then autoradiographed with X-OMAT AR5 or OMC film (Kodak Labs) in film cassettes with intensifying screens (Kodak Labs).

K. Immunohistochemistry

Murine coculture cells to be stained were grown on 2-well microscope slides (Lab-Tek Chamber slides, Nunc Inc.) until reaching the desired state of confluency, then fixed with 4% paraformaldehyde for 1 hour. Cells were incubated overnight with an immunoaffinity purified anti-SLN polyclonal antibody produced in rabbits to a unique 15mer peptide sequence (amino acids 274 to 290) from human SLN (127, 128). Wells were washed with TTBS buffer (20 mM Tris, pH 7.5, 0.5 M NaCl, 0.1% v/v Tween-20, 0.02% NaN₃) and incubated for 1 hour with biotinylated goat anti-rabbit IgG₁ (Sigma Chemicals). After washing, wells were incubated for 45 min. with Extravidin horseradish peroxidase (Sigma Chemicals) then developed with 0.5 mg/ml diaminobenzidine dihydrochloride (Sigma Chemicals). Cultures were photographed at 40X (Nikon Optiphot) using Tekpan film (Kodak Labs).

Murine cocultures to be stained with and without detergent permeabilization of the plasma membrane were first incubated in 0.3% H₂O₂ to block endogenous peroxidase activity. To bind endogenous avidin and biotin sites, cultures were incubated with avidin and biotin reagents (Vector Labs, Inc.). Cultures were then incubated overnight with an immunoaffinity purified anti-SLN polyclonal antibody produced in chickens. Wells were washed with TTBS and incubated for 1 hour

with mouse anti-chicken IgG₁ (Sigma Chemicals) and processed as previously described for immunohistochemical staining with the rabbit polyclonal antibody. Cultures stained without detergent were washed and incubated in similar solutions, in the absence of Tween-20.

Bovine and porcine TM cells to be stained for immunohistochemistry were grown in 2-well microscope slides or T25 flasks, paraformaldehyde fixed and incubated overnight with chicken anti-SLN or immunoaffinity purified rabbit anti-SLN polyclonal antibody (127, 128). Bovine cultures were photographed at 40X magnification on an inverted microscope (Zeiss, Inc.) under phase contrast optics. Porcine cultures were photographed as described for murine cultures.

L. Western Blots

Cultures were washed with phosphate buffered saline and grown for 24 or 48 hours in the presence of DMEM supplemented with insulin, selenium and transferrin ("ITS", Sigma Chemicals) diluted 1:1000. Final concentrations in the media were 5 μ g/ml insulin, 5 μ g/ml transferrin and 5 ng/ml selenium. Media was harvested and stored at -20° C. For gels, samples were mixed with 0.1 volume of 10X gel loading buffer (4% sucrose, 10% SDS, 0.25 M Tris, 0.1% bromphenol blue) and 50 μ l final volume loaded per lane. Samples were run on

a standard 10% SDS-PAGE gel (with and without 100 mM dithiothreitol) with a 3% stacking gel according to the methods of Laemmli (129). The gel was blotted onto nitrocellulose for 1 hour at 100 V (blotting buffer: 20 mM tris, 150 mM glycine, pH 8.0, 20% methanol). Blots were stained for 15 min. with Ponceau S stain (Sigma Chemicals) to visualize major protein bands and then photographed. After destaining the blot, 3% non-fat milk was used as a blocking agent, then it was incubated with primary antibody (chicken anti-SLN IgY) overnight at 4° C with shaking. The blot was washed with TTBS (20 mM Tris, pH 7.5, 0.5 M NaCl, 0.1% v/v Tween-20, 0.02% NaN₃) incubated for 2 hours with rabbit anti-chicken IgG (Sigma Immunochemicals, Inc.) conjugated to alkaline phosphatase and developed with 0.33 mg/ml p-nitro blue tetrazolium chloride (Sigma Chemicals) and 1.65 mg/ml 5-bromo-4-chloro-3-indolyl phosphate (Sigma Chemicals). Molecular weight markers (BioRad, Inc.) were at 200, 116, 97, 66, 43, 31, 21 kD.

M. Zymograms

Zymograms are standard Laemmli (129) SDS-PAGE gels that are cast with an enzyme substrate in the gel. After running, the gels are incubated in buffer to activate the enzyme, which cleaves its substrate. The gel is stained with

Coomassie blue, coloring the gel blue because of the substrate, but bands of clearing appear where enzyme activity has degraded the substrate which then diffuses from the gel, resulting in an inverse staining pattern compared to typical PAGE gels (15).

Media samples were collected as described previously for Western Blots. Polyacrylamide gels (10%, 0.75 mm thick) were cast and a 3% stacking gel was added. After electrophoreses, gels were incubated in 2.5% Triton-X 100 for 45 min. to remove the sodium dodecyl sulfate. For stromelysin activity, casein is used as the substrate (0.15% w/v), 30 μ l media loaded per lane and gels electrophoresed for 4 hours at 7.5 mAmps constant current or overnight at 45 V constant voltage with cooling. Gels were incubated for 16 hours in activation buffer (0.15 M NaCl, 10 mM CaCl₂, 50 mM Tris, 1 μ M ZnSO₄, pH 8.0), Coomassie stained and dried. To inhibit stromelysin activity, 10 mM 1,10-phenanthroline (Sigma Chemicals, Inc.) was added to the activation buffer.

N. Deglycosylation of Stromelysin

To remove oligosaccharides from SLN, 200 μ l conditioned "ITS" media from SFF-SLN clonal cell lines was incubated with 5 μ l of 1 U/ml Endo- β -N-acetylglucosaminidase D (Boehringer-Mannheim, Inc.) in the presence of 1.5% v/v

Nonidet P-40 (LKB-Producter AB, Bromma, Sweden) and 100 mM DTT for two hours at 37° C. The media was electrophoresed on a 10% SDS-PAGE gel as previously described and blotted onto nitrocellulose. Immunopurified chicken anti-SLN peptide antibody was used to detect immunoreactive protein bands, as previously described. The blot was scanned using a Hoeffer Scientific GS-300 gel scanner in the vertical direction. The absorbance of the upper (glycosylated form) of SLN was divided by the absorbance of the lower (nonglycosylated form) of SLN to give a ratio.

O. SDS-PAGE to Estimate the Concentration of Stromelysin

Conditioned media from SFF-SLN cell line #G-11 and bovine serum albumin (BSA) (Sigma Chemicals) standards were electrophoresed as previously described using 10% polyacrylamide separating gels with a 3% stacking gel. The gels were either stained with Coomassie blue (Bio-Rad, Inc.) or Western blotted as previously described using a chicken anti-human immunoaffinity purified peptide antibody.

The Coomassie blue stained gels were dried onto BioGelWrap (BioDesign of New York) and the protein bands of interest were scanned in the horizontal and vertical directions using a GS-300 scanning densitometer (Hoefer Scientific).

P. Activation of proSLN to the Latent Form

One ml of 24-hour conditioned media from SFF-SLN clonal cell line #G-11 was used for studies showing the activation of SLN from the "pro" form to the latent form.

Media was incubated with 400 ng trypsin (Sigma Chemicals, Inc.) at 37° C. To stop the reaction, 100 μ l was removed from the incubation mix and 50 μ g of Soybean Trypsin Inhibitor (Sigma Chemicals) and 10 mM phenylmethylsulfonyl fluoride (Sigma Chemicals) were added. The samples were stored at -20° C until prior to electrophoresis.

To activate proSLN using 4-Aminophenylmercuric acetate (APMA) (Sigma Chemicals), a 100 mM stock of APMA was prepared in 0.1 N NaOH. Tris buffer (1 M, pH 7.5) was added to 1 ml of conditioned media to a final concentration of 1 mM. APMA was added to a final concentration of 5 mM and samples were incubated at 37° C. To stop the reaction, 100 μ l of sample was removed at various time points and frozen at -20° C until prior to electrophoresis.

To electrophorese, samples were thawed, 10 μ l of 10X gel loading buffer added and the sample vortexed. Samples were heated to 100° C for three minutes and 10 μ l per lane for zymograms and 50 μ l per lane for Western blots were electrophoresed, as previously described.

Coomassie stained zymograms were dried onto BioGelWrap (BioDesign of New York). Western blots were immunochemically stained as described above.

III. RESULTS

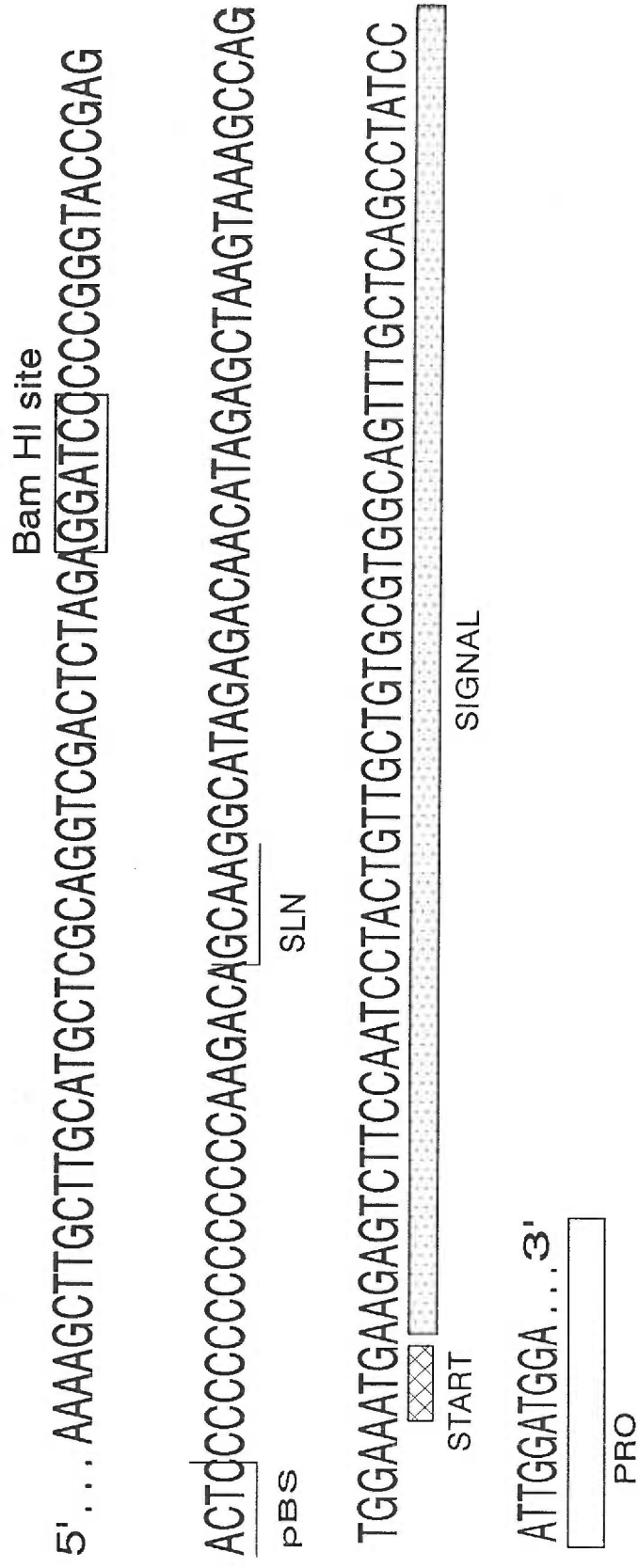
A. Sequencing pBS-SLN

Since SLN is a secretory protein (55), it was necessary to verify that the gene regions encoding such portions of the protein as the signal sequence were intact in the pBS-SLN vector to ensure proper eukaryotic processing and secretion of the nascent protein (Fig. 11). Using a primer which binds to the pBS plasmid upstream from the multiple cloning site into which the human SLN-cDNA had been inserted (i.e. "-40 primer"), it was possible to sequence about 150 base pairs into the SLN-cDNA region. The sequence obtained (data in Fig. 14), when compared to previously published SLN sequences (131), revealed an intact ATG translational start site, the complete signal peptide and a portion of the "pro" peptide sequence, which is present in the enzymatically inactive form of SLN (43).

B. Subcloning of SLN-cDNA into pSFF

To construct the pSFF-SLN retroviral expression vector, SLN-cDNA was cut from the pBS-SLN vector using two restriction enzymes, Bam HI at the 5' end and Xho I at the 3' end. These enzymes leave incompatible sticky ends, and therefore, the excised SLN-cDNA will only directionally ligate into its new vector.

Figure 14. Sequence of pBS-SLN



As the new retroviral expression vector will ultimately be used for the production of the SLN protein, the directional requirement ensures that a backward or nonsense expression will be avoided.

The Bam HI site, utilized for the 5' cut, is a restriction site in the pBS multiple cloning cartridge and a small portion of the plasmid remains attached to the 5' end of the SLN-cDNA (Fig. 14). The Xho I cut site is at +1,584 base pairs and cutting with both enzymes results in a SLN fragment of approximately 1,600 base pairs in length. The translational start and stop sites are at +44 and +1469, respectively, (Fig. 11) and remain with the excised fragment, while the polyadenylation site at +1801 is removed (a retroviral polyadenylation signal will be utilized following ligation of the insert into the pSFF expression vector).

The pSFF expression vector has been constructed so that the gag, pol and env genes are no longer capable of producing functional retroviral gene products (114, 95). There is contained within the env gene region a multiple cloning site with Bam HI and Xho I restriction sites (Fig. 13), which were digested and ligated to the similarly prepared SLN-cDNA.

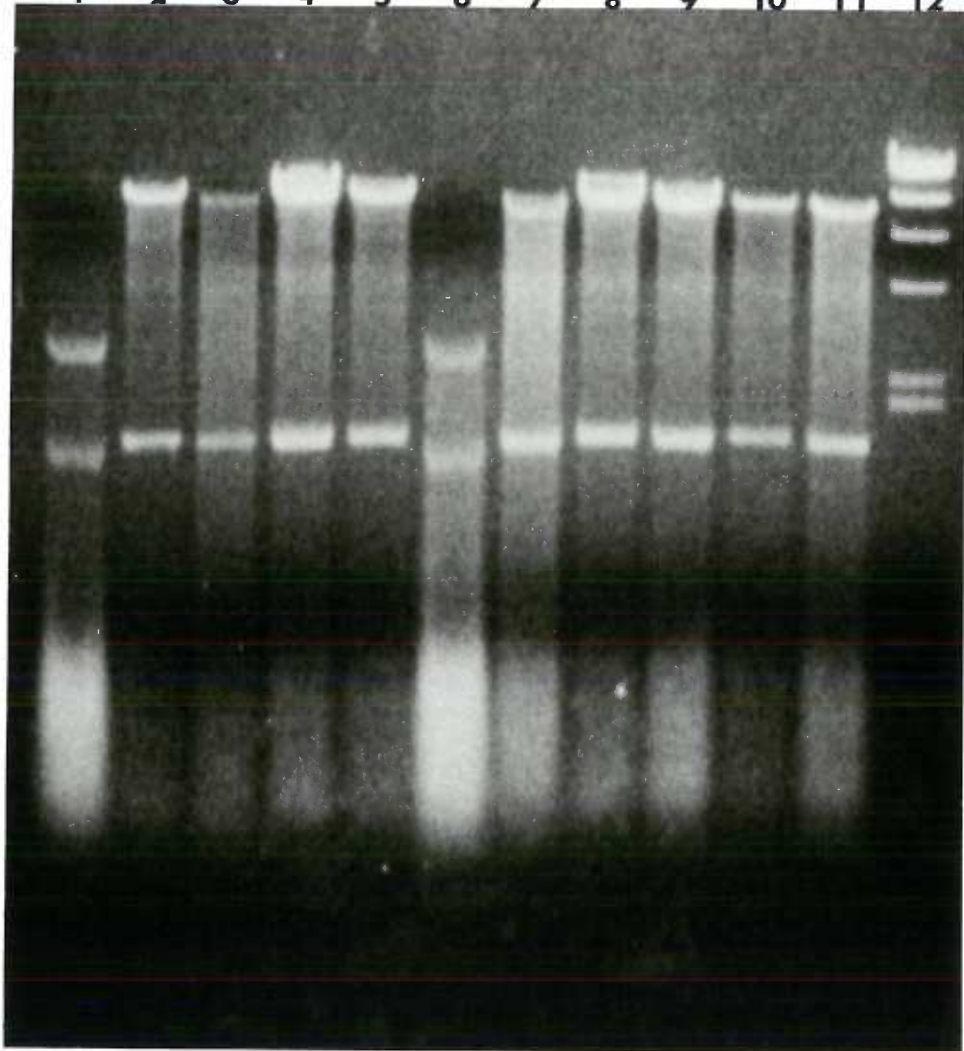
Following ligation of the excised SLN-cDNA into pSFF, DK-1 cells were transformed and of the resultant colonies, several were grown up for analysis. Two of these, clones #16 and #22, were selected for further analysis (Fig. 15).

Figure 15. Selection of pSFF-SLN clone following ligation.

Overnight cultures of colonies, resulting from transformation of the SLN insert ligated into pSFF, yielded plasmid DNA which, when digested with Bam HI and Xho I, gave two bands: pSFF at 9.2 Kb and SLN at 1.6 Kb.

- Lane 1,6: Band sizes at 3.0 and 1.6 Kb suggest these two constructs are pBS religated with SLN.
- Lane 2-5,7-11: pSFF-SLN clones. Clones #16 (lane 5) and #22 (lane 11) were selected for further characterization.
- Lane 12: Molecular weight standards: 23.1, 9.4, 6.6, 4.4, 2.3, 2.0, 0.6 Kb.

1 2 3 4 5 6 7 8 9 10 11 12



Both colonies were digested with several restriction enzymes, including Pvu II, Cla I, Hind III, Nco I, Xba I, and Eco RI, to verify the presence of expected restriction sites and to confirm proper 5' to 3' orientation of the SLN-cDNA into pSFF. For instance, Eco RI cuts one time (Fig. 16), 3' to the Xho I restriction site and should give a linear plasmid (verified in lane 2). Nco I cuts two times in pSFF and one time in SLN and results in three bands of 9, 1.6 and 0.7 Kb (lane 3). Cutting with both enzymes results in a small fragment at 0.3 Kb being cut from the 3' end of SLN (Fig. 17).

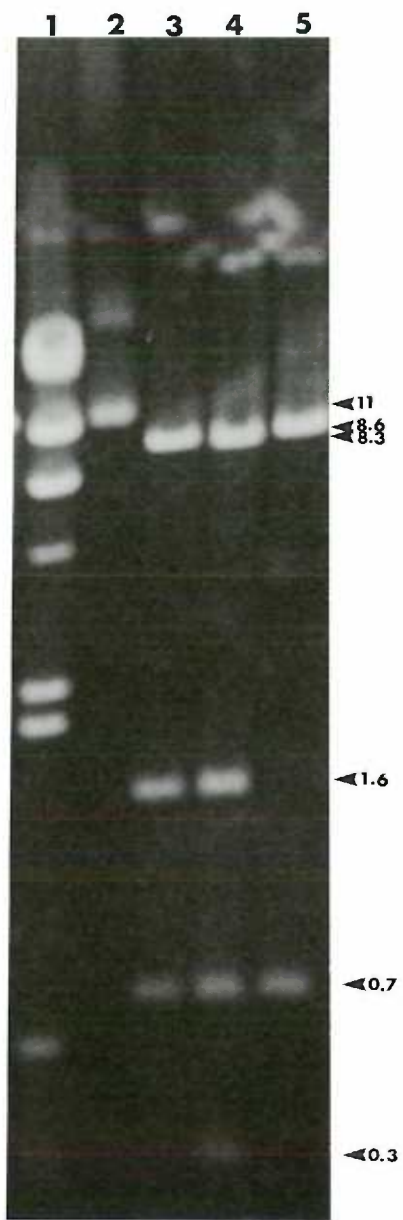
The various restriction digests (data not shown) confirmed the SLN-cDNA was ligated in the pSFF vector in the proper orientation, and 5' and 3' ends of both vector and insert appeared to remain intact after the restriction digests and ligation process.

C. "Ping-Pong" Amplification and Expression of SLN

Cocultures were seeded into T25 flasks 48 hours prior to transfection. To transfect, vector DNA (pSFF-GH or pSFF-SLN) was added to the cocultures as a calcium phosphate precipitate. Mock transfected controls did not receive any vector DNA. After transfection, the cocultures were grown and maintained for several weeks to allow the infection process to continue (115). The infection

Figure 16. Restriction digests of pSFF-SLN construct to check orientation and presence of restriction sites following the ligation of SLN cDNA insert into the pSFF expression vector.

- Lane 1: Molecular weight standards: 23.1, 9.4, 6.6, 4.4, 2.3, 2.0, 0.6 Kb.
- Lane 2: pSFF-SLN (clone #16) digested with Eco RI results in a single band of linear plasmid at approximately 11 Kb.
- Lane 3: pSFF-SLN construct digested with Nco I produces bands of 8.6, 1.6, and 0.7 Kb.
- Lane 4: pSFF-SLN construct digested with Eco RI and Nco I results in four bands of 8.3, 1.6, 0.7 and 0.3 Kb. (See Fig. 17 for restriction sites in the plasmid and insert.)
- Lane 5: pSFF vector digested with Nco I gives two bands of approximately 8.7 and 0.7 Kb.



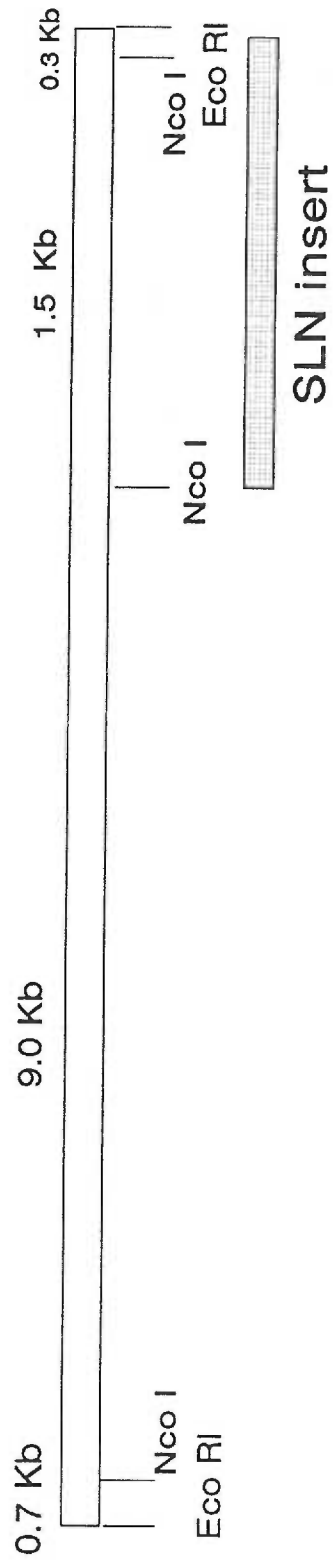


Figure 17. Nco I/Eco RI restriction sites in pSFF-SLN.

process was stopped, typically 3 weeks later, when high levels of SLN RNA could be detected by means of polymerase chain reaction assay (Fig. 18). When high level infections are achieved the process is stopped, because the continued insertion of retroviruses into the host cell's genome carries with it an increasing probability that a retrovirus will randomly insert in a necessary, functioning gene and either kill or transform the cell (115). It was observed that these infectious cocultures became more fragile and unstable, if the infection process were allowed to continue indefinitely.

To stop the cross-infection process, the cells were limit-dilution cloned in 96-well tissue culture plates (see Methods). Approximately 15 wells per plate contained single cells, which were grown up as clonal cell lines. These clonal cell lines consisted of cell populations which contained the same number and insertion pattern of retroviruses in their genomic DNA, having arisen from the same original precursor cell (115). Some of the clonal cell lines established expressed SLN at high levels (Fig. 19) and were used to characterize the production of SLN at both the RNA level and the protein level.

Cocultures and clonal cell lines producing SLN were kept below 75% confluency. The SFF-SLN cultures, as opposed to the SFF-GH or mock transfected control cultures, appeared to retain their cell-to-cell attachments,

Figure 18. Screening of pSFF-SLN transfected cocultures for SLN mRNA using PCR.

Lane 1-5, 7-11: Represent 10 different cocultures all of which produce a 1.4 Kb PCR (arrow) product using the SLN primers. (The doublet in lane 9 is of unknown origin.)

Lane 6: Molecular weight standards: 23.1, 9.4, 6.6, 4.4, 2.3, 2.0, 0.6 Kb.

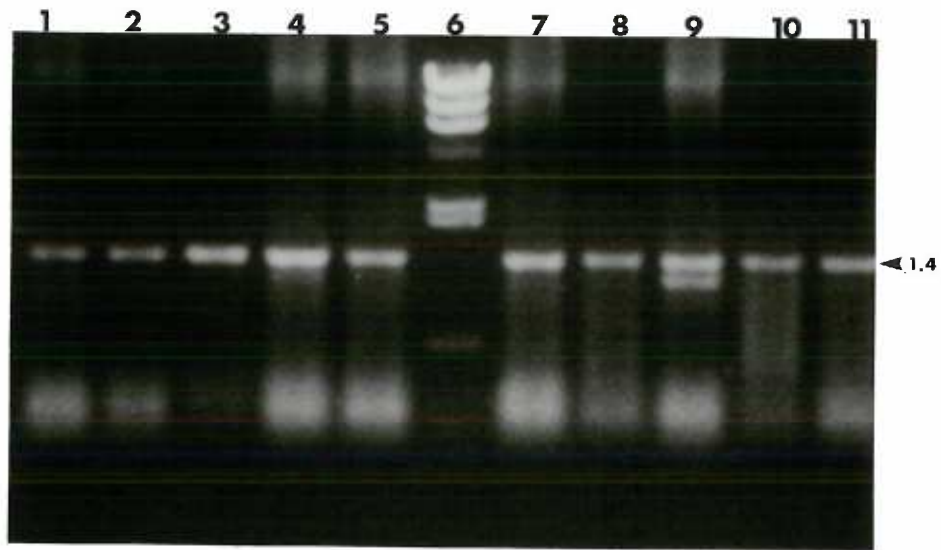
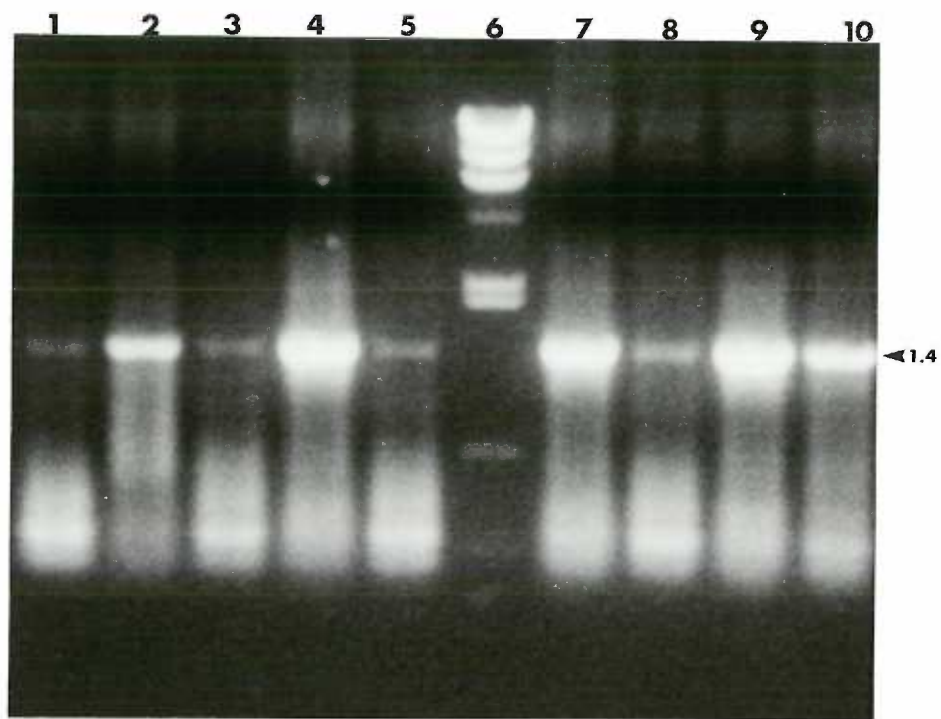


Figure 19. Producing clonal cell lines expressing SFF-SLN mRNA.

Cocultures F and G (lanes 7 and 8, Fig. 18) were selected to make clonal cell lines of SLN producing cells. Limiting dilution was used to clone cell populations, which were then screened for the presence of SLN mRNA using PCR.

Lane 1-5, 7-10: Each represent a cell line producing the SLN 1.4 Kb PCR product (arrow). Clones #G-7 (lane 4), #G-11 (lane 7), and #F-1 (lane 9) were used for further experiments to characterize the SFF-SLN protein product.

Lane 6: Molecular weight standards: 23.1, 9.4, 6.6, 4.4, 2.3, 2.0, 0.6 Kb.



as confluent cultures, but they were difficult to maintain and detached from the tissue culture flask as an intact sheet. This observation has not been quantitatively pursued, but could perhaps be approached by seeding multiple SFF-SLN and SFF-GH cultures, scoring the number of detached cultures at confluency and computing the areas of the cellular sheets that have floated free from the surface.

D. SFF-GH Control Cultures

In order to ensure that the expression of SLN was not being induced in the cultures studied in response to the presence of a retrovirus (133, 122), two kinds of control cocultures were utilized. One, was a mock transfected control (i.e. cocultures that went through the process of transfection, but did not receive any retroviral expression vector), and a second was transfected with pSFF-GH (114) which contains the human growth hormone gene. These cultures were treated as the SFF-SLN cultures in all assays.

To screen cultures and establish clonal lines of cells expressing high levels of GH a radioimmunoassay was utilized, which allowed the quantitation of the amount of GH protein made. While a wide range of GH production was found across different SFF-GH clonal lines, high producing clones were found which made as much as 96 ng/ml of GH (Fig. 20).

PCR sense and antisense primers were also made to unique human growth

Figure 20. Radioimmunoassay for human growth hormone expression by murine cocultures transfected with pSFF-GH, pSFF-SLN and mock transfected controls. Confluent T25 culture flasks received fresh DMEM which was allowed to condition for 24 hours then assayed.

Cell Line Assayed:	GH (ng/ml)
Mock transfected control	0
SFF-SLN, clone #3.1	0
SFF-SLN, clone #11.1	0
SFF-GH, clone #2.1	47.0
SFF-GH; clone #2.2	96.0
SFF-GH; clone #2.3	40.0
SFF-GH; clone #2.4	73.0
SFF-GH; clone #2.5	65.0
SFF-GH; clone #2.6	82.0
SFF-GH; clone #2.7	82.0

hormone gene sequences. The pSFF-GH expression vector contains the human GH gene (134, 114) which carries not only the exons but also the intervening sequences. The retroviral RNA expressed from pSFF-GH may undergo splicing to remove the cellular intron prior to packaging. Retroviruses which have captured cellular proto-oncogenes through recombination have been reported to have lost the intron regions through splicing (94). The PCR primers for GH were selected from two exon regions (Fig. 21) giving a 400 base pair PCR product (Fig. 22). Occasionally, a faint band of 700 base pair size would be faintly visible on an agarose gel following PCR (see Lane 1, Fig. 22). This band was only seen in clones which had very high levels of GH PCR product and it may have been either amplified GH genomic DNA or amplified GH RNA, suggesting that in some of the clones, the exons remained in the virus with passaging.

E. Northern Blot

Retroviral coculture RNA was isolated during the infection process, and when run on a formaldehyde gel in the presence of ethidium bromide (Fig. 23), shows 18S and 28S ribosomal RNA bands for all samples. The gel was then blotted onto nylon and probed with a human ³²P-SLN probe. The autoradiograph of the blot revealed two bands at 6.0 Kb and 3.3 Kb only in the lanes which

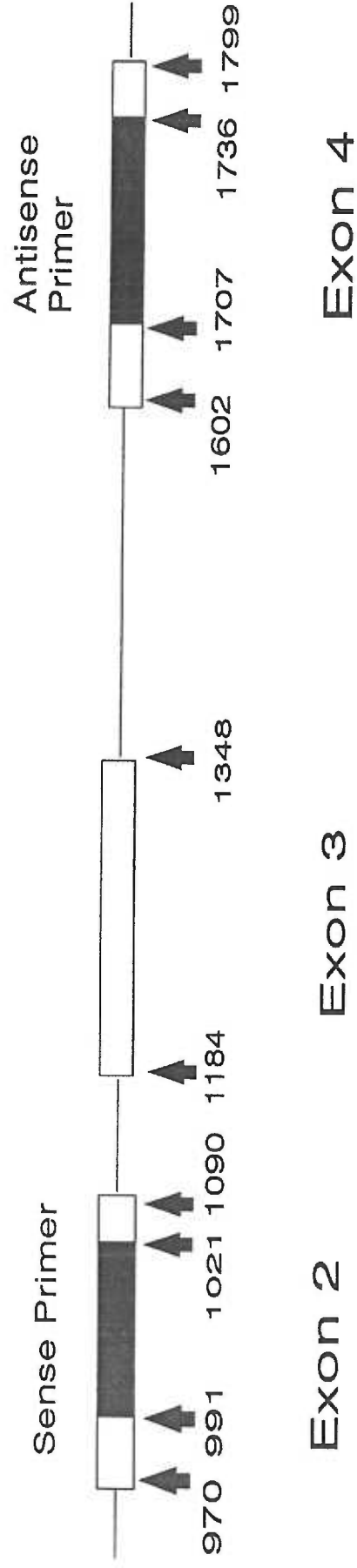


Figure 21. GH gene with introns and exons, showing the 700 or 400 bpr PCR product made.

Figure 22. Screening of pSFF-GH transfected cocultures using PCR and GH specific primers.

Transfected cocultures were screened for GH PCR product made from the GH primers. The major band at 400 base pairs (lower arrow) represents the GH mRNA which has been spliced to remove intervening sequences. A minor band is occasionally seen at 700 base pairs (upper arrow).

Lane 1-4,6,7: SFF-GH cocultures. The coculture represented by lane 6 was selected for limiting dilution to produce SFF-GH clonal cell lines.

Lane 5: Molecular weight standards: 23.1, 9.4, 6.6, 4.4, 2.3, 2.0, 0.6 Kb.

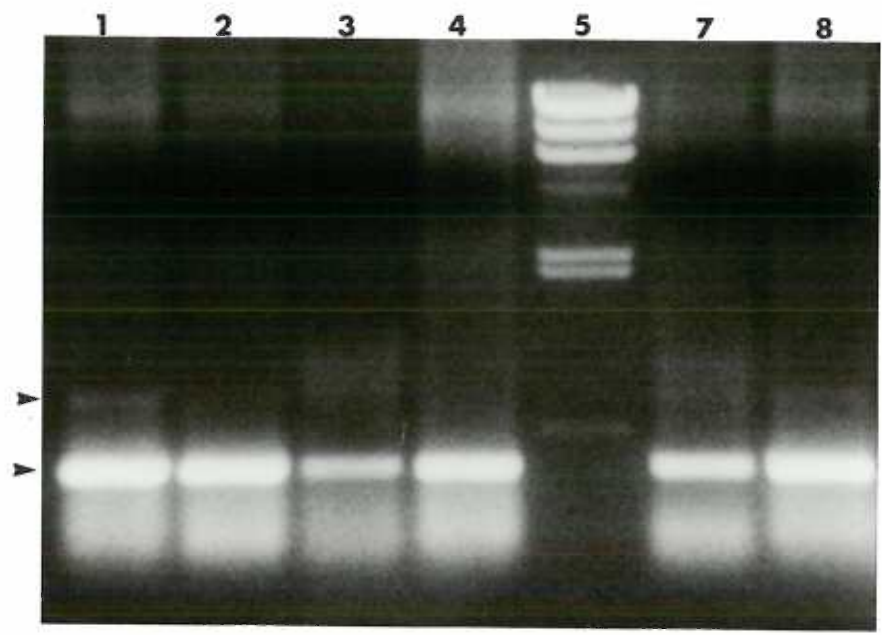


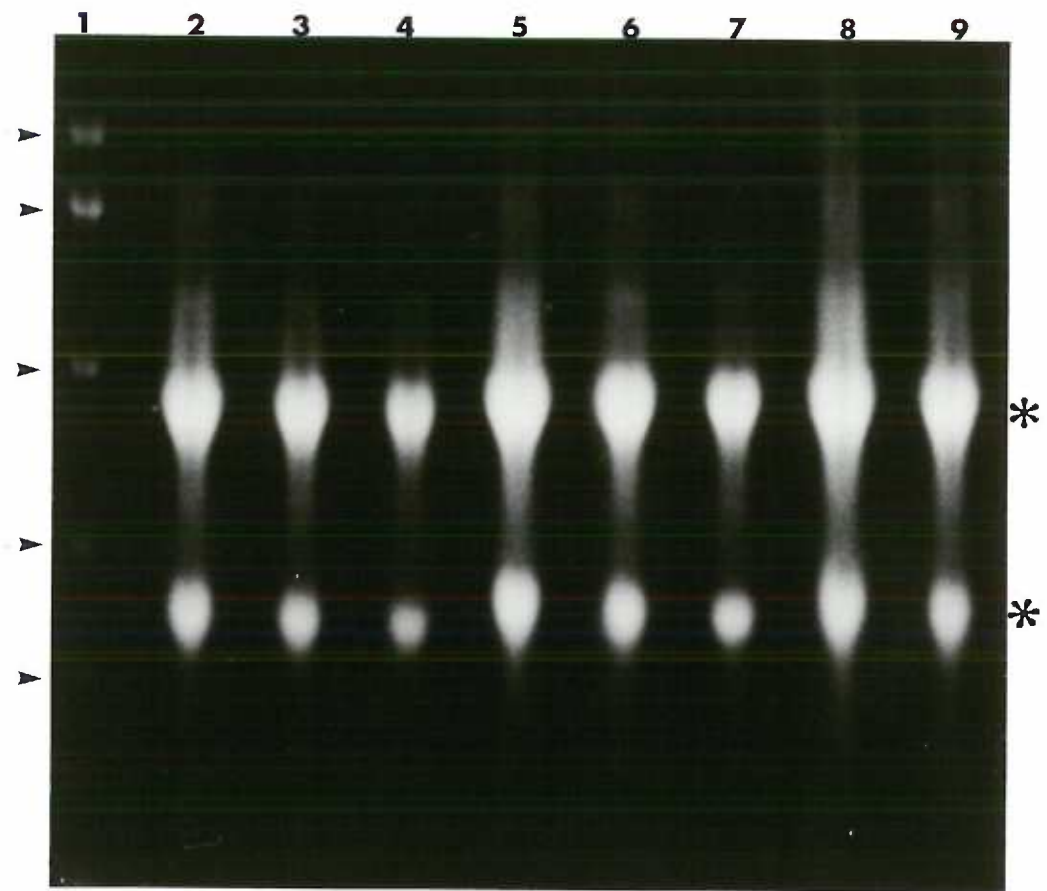
Figure 23. Ethidium bromide stained formaldehyde gel of SFF-SLN and SFF-GH coculture RNA which was later blotted and probed (see Figure 24). Asterisks at 4.0 and 1.8 are the 28S and 18S ribosomal RNA bands, respectively.

Lane 1: RNA molecular weight ladder with bands at 9.5, 7.5, 4.4, 2.4, and 1.4 Kb (arrows).

Lane 2,3,4: 10, 5, and 2.5 μ g RNA from SFF-SLN coculture #3.

Lane 5,6,7: 10, 5, and 2.5 μ g RNA from SFF-SLN coculture #9.

Lane 8,9: 10, and 5 μ g RNA from SFF-GH coculture #2.



contained RNA from cell lines transfected with pSFF-SLN (Fig. 24). The largest band, 6.0 Kb, is the appropriate length to contain the full length message made from the retroviral coding sequences. This band would contain the SLN insert in the env region and is packaged as genomic RNA. The 3.3 Kb band is the appropriate size for a spliced form of that full length message, which occurs when the message is cut at the "splice donor" and "splice acceptor" sites (Fig. 25) and truncated. This mechanism is the means by which the retrovirus achieves expression of the envelope encoded regions relative to the gag and pol gene products (94).

The endogenous murine SLN message, if present, should be found at 1.9 Kb (47). No detectable band was seen at that size, supporting the PCR observation that endogenous murine SLN is not expressed, or if so, at levels that were not detectable.

F. Immunohistochemistry

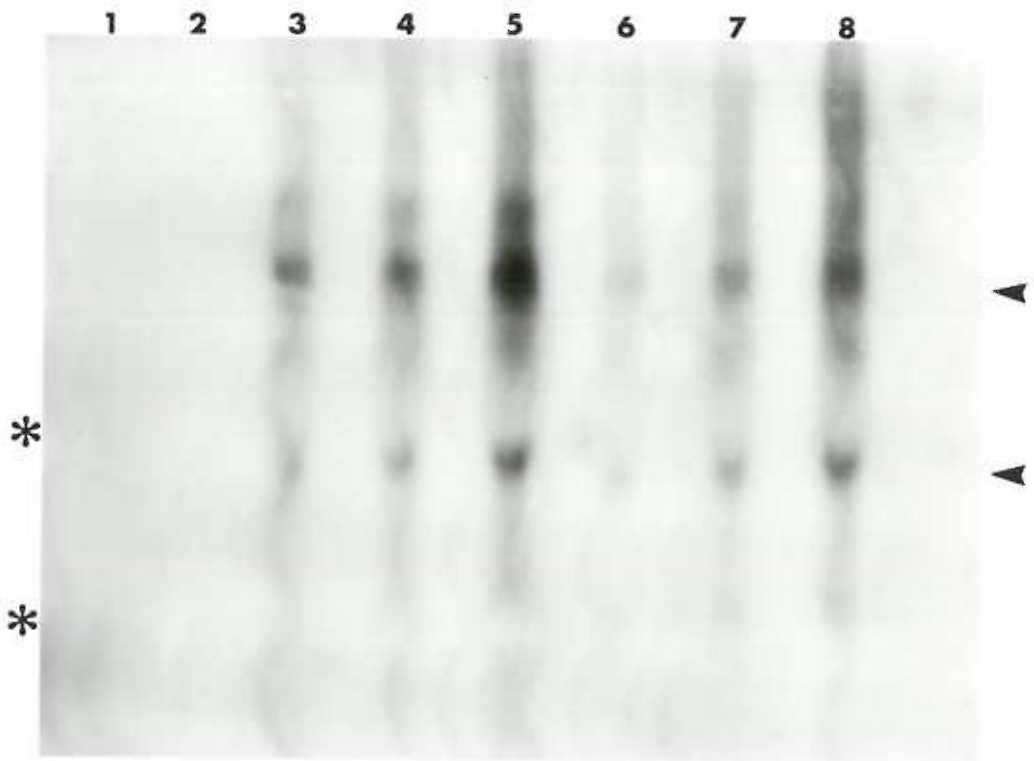
Murine clonal cultures expressing SFF-SLN and SFF-GH RNA were stained immunohistochemically for the presence of SLN using anti-human SLN peptide antibodies made against two unique regions of SLN. Both peptides were selected from the carboxy terminal half of the protein. Antibodies made against one

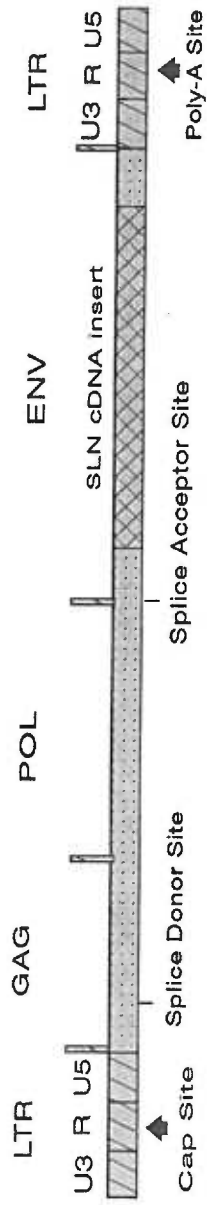
Figure 24. Autoradiograph of Northern blot probed with ^{32}P -SLN cDNA (same gel as pictured in Fig. 23). Asterisks denote position of 28S and 18S rRNA, as shown on the ethidium bromide stained gel.

Lane 1,2: 5, 10 μg RNA from SFF-GH coculture #2.

Lane 3,4,5: 2.5, 5, and 10 μg RNA from SFF-SLN coculture #9. Bands (arrows) are 6.0 and 3.3 Kb.

Lane 6,7,8: 2.5, 5, and 10 μg RNA from SFF-SLN coculture #3.





Proviral form of pSFF-SLN

Transcripts made:

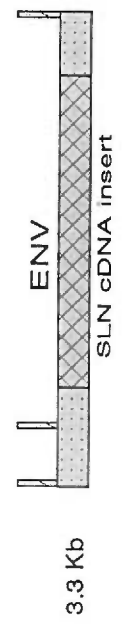
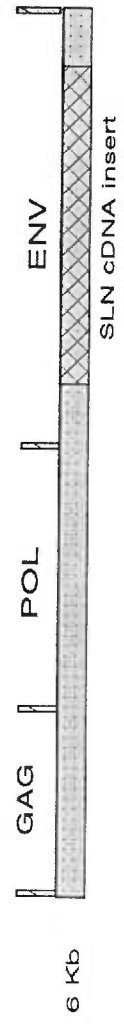


Figure 25. SFF-SLN and transcripts

peptide did not produce staining significantly above background, which may suggest its recognition sequence is no longer recognizable or available to the antibody following paraformaldehyde fixation of cells.

SFF-SLN clonal cultures stained with the rabbit anti-human SLN peptide antibody showed very heavy staining when compared to SFF-GH cultures. Cultures were stained in both the nonconfluent (Fig. 26 and 27) and confluent (Fig. 28 and 29) states. In the nonconfluent SFF-GH culture (Fig. 27), the nuclei of cells can be seen quite distinctively. An anti-SLN antibody would not be expected to stain the nuclei of cells. While it is not clear what the cause of this effect is, the level of contrast in the region of the nucleus for both the SFF-GH and the SFF-SLN cells appears to be similar while the staining in the cytoplasm appears to increase markedly for the SFF-SLN cultures.

Occasional SFF-GH cells in nonconfluent cultures could be found which were expressing detectable amounts of SLN. SLN is normally expressed by cells as they undergo cell division and these cells may have been in the process of division, since they also tended to be small, rounded up and visually consistent with the appearance of a dividing cell.

The pattern of staining over the surface of the cells and out into the cellular

Figure 26. Immunohistochemistry of nonconfluent SFF-SLN clonal cell line using a rabbit anti-human SLN polyclonal antibody.

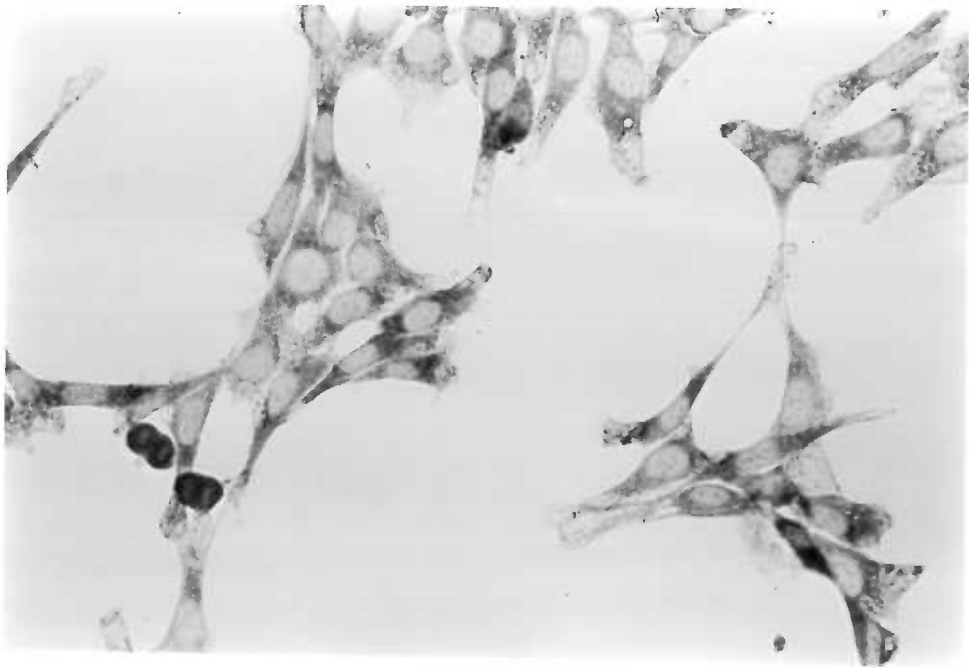


Figure 27. Immunohistochemistry of nonconfluent SFF-GH control clonal cell line using a rabbit anti-human SLN polyclonal antibody.



Figure 28. Immunohistochemistry of confluent SFF-SLN clonal cell line using a rabbit anti-human SLN polyclonal antibody.

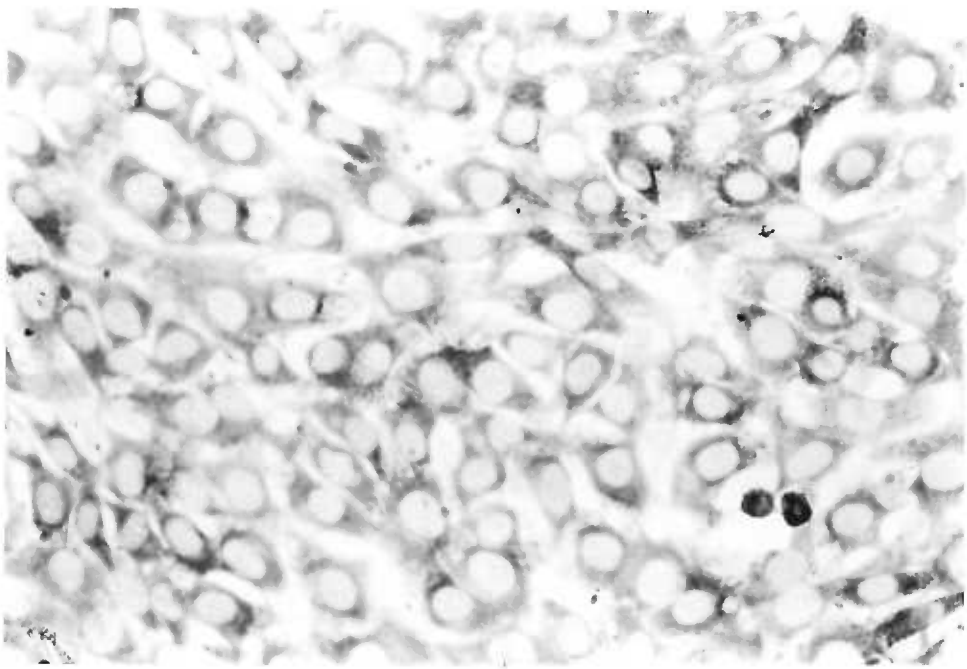


Figure 29. Immunohistochemistry of confluent SFF-GH control clonal cell line using a rabbit anti-human SLN polyclonal antibody.



processes (Fig. 26) suggested that a measurable amount of the secreted stromelysin remained associated with the cell surface. Cells normally synthesize and express a variety of proteoglycans containing heparin-sulfate moieties on their surface (18), which can bind SLN (56).

To better differentiate extracellular versus intracellular SLN, SFF-SLN (Fig. 30 and 31) and SFF-GH (Fig. 32) clonal cell lines were immunohistochemically stained using a chicken anti-human SLN peptide antibody in the presence and absence of membrane permeabilizing detergent and photographed for comparison. This chicken anti-SLN antibody, while made against the same SLN peptide as the rabbit peptide antibody used in Figures 26-29, never gave as intense a level of staining as the rabbit antibody. Clones stained without detergent present appeared to have a light staining across the surface of the cell body and processes (Fig. 30), but when compared to photographs of the SFF-GH control cultures, it was not possible to determine visually whether the SFF-SLN staining was above that of SFF-GH (Fig. 32). When cultures were stained with detergent present, a punctate, cytoplasmic pattern of staining, especially in the region surrounding the nucleus, was found (Fig. 31). This pattern is consistent with rough endoplasmic reticulum and golgi staining.

Figure 30. Immunohistochemistry without membrane permeabilizing detergent of confluent SFF-SLN clonal cell line using a chicken anti-human SLN polyclonal antibody.



Figure 31. Immunohistochemistry with membrane permeabilizing detergent of confluent SFF-SLN clonal cell line using a chicken anti-human SLN polyclonal antibody.

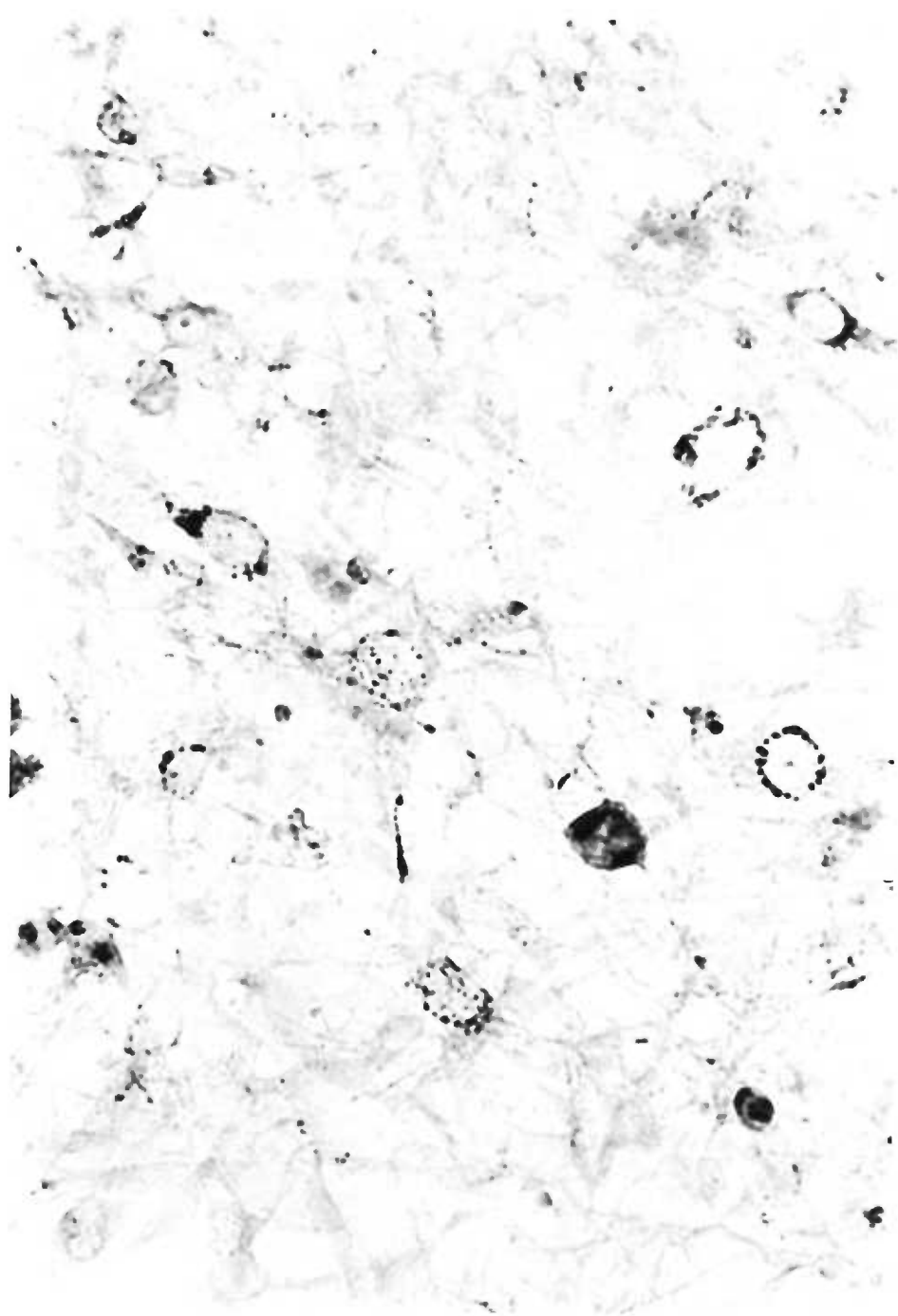
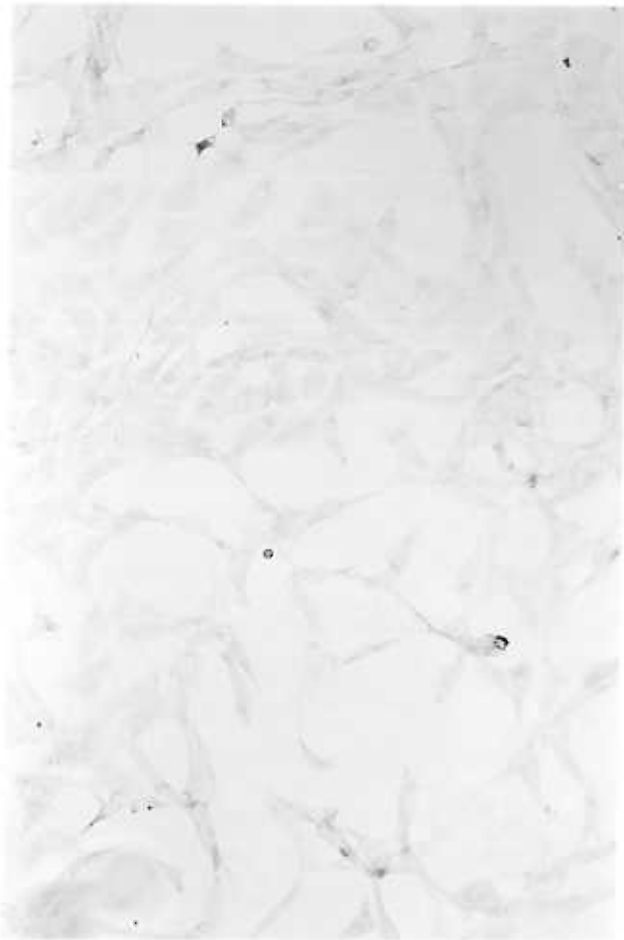


Figure 32. Immunohistochemistry with membrane permeabilizing detergent of confluent SFF-GH control clonal cell line using a chicken anti-human SLN polyclonal antibody.



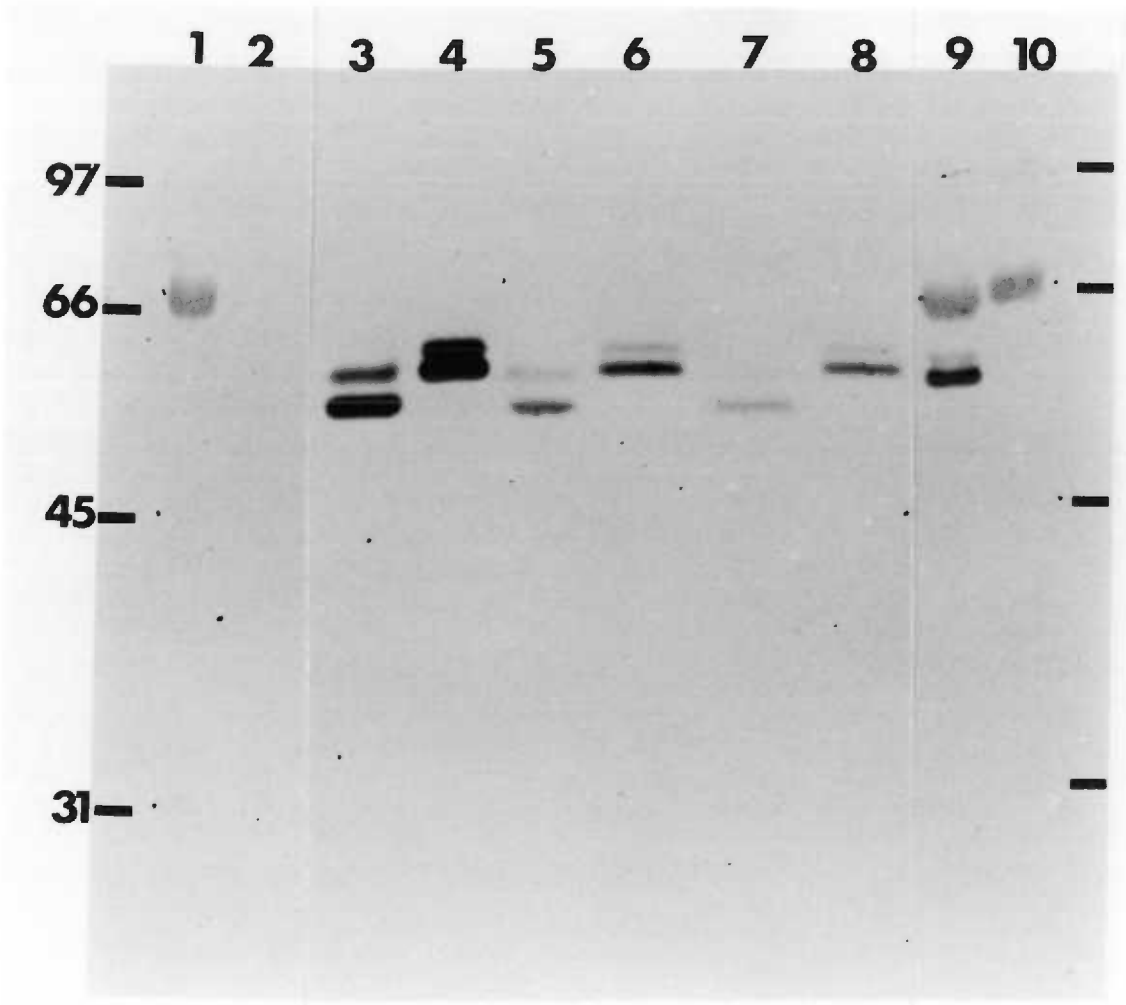
G. Western Blots of Coculture Media

When clonal cultures were grown and maintained in their usual growth conditions, DMEM media with 10% fetal bovine serum, the high percentage of serum proteins present interfered with any attempts to visualize the SFF-SLN protein product by polyacrylamide gels or Western blots. This was due in particular to a very dense bovine serum albumin band, which runs at a molecular weight close to the expected size of SLN (66 kD for BSA versus 57 and 60 kD for proSLN).

Three SFF-SLN clones maintained in the presence of serum-free DMEM supplemented with ITS (insulin, transferrin, selenium) contained no serum proteins. To run on the PAGE gels, 45 μ l of DMEM/ITS media conditioned for 24 or 48 hours (from 2.5 or 5 mls total volume) was loaded per lane. When the media was run on a polyacrylamide gel, blotted and immunohistochemically stained (Fig. 33), a doublet was found at approximately 57 and 60 kD. This is similar to what has been reported for proSLN (43). Western blots stained with Ponceau S showed the proSLN to be a major protein in the media. The three SFF-SLN clones were making different amounts of the SLN protein. This paralleled PCR data for the same clones, showing different levels of SLN mRNA present (data not shown). When media samples were reduced with 100 mM DTT

Figure 33. Western blot of conditioned medium from clonal cell lines.

- Lane 1,10: Molecular weight markers: 97, 66, 45, 31 kD.
- Lane 2: 50 μ l media from mock-transfected coculture controls.
- Lane 3: 50 μ l media from SFF-SLN clone (#S1W10-D).
- Lane 4: 50 μ l media plus 10 mM DTT from SFF-SLN clone (#S1W10-D).
- Lane 5: 50 μ l media from SFF-SLN clone (#S1W10-K).
- Lane 6: 50 μ l media plus 10 mM DTT from SFF-SLN clone (#S1W10-K).
- Lane 7: 50 μ l media from SFF-SLN clone (#S1W10-L).
- Lane 8: 50 μ l media plus 10 mM DTT from SFF-SLN clone (#S1W10-L).
- Lane 9: Positive control. 10 μ l conditioned media plus 10 mM DTT from trabecular cells stimulated with 1 μ M dexamethasone and 40 U/ml IL-1 α for 72 hrs. Media was concentrated 20-fold. SLN doublet is at 64 and 62 kD. (Band at 66 kD is BSA from the media which stains nonspecifically with anti-SLN antibody).



before electrophoresis, the doublet of antigenic reactivity was found to run at 60 and 62 kD. Two cysteines in a disulfide bond are reduced in SLN. Mock transfected control and SFF-GH media did not exhibit any detectable antigenic bands on Western blots.

H. Substrate Gel Electrophoresis of Coculture Media

Substrate gel electrophoreses using standard SDS-PAGE gels, which have been cast with an enzyme substrate, in this case casein, were used to determine whether a protein band has enzymatic activity. The gel is incubated in activation buffer following electrophoresis and then stained with Coomassie blue. Bands of clearing develop where SLN has proteolytically cleaved the substrate which then diffuses from the gel during the incubation process. DMEM/ITS media from SFF-SLN and SFF-GH clones were prepared as for Western blots discussed above, and 30 μ l per lane was electrophoresed. Two bands of activity were found in the SFF-SLN lanes at 57 and 60 kD (Fig. 34), consistent with the bands of antigenic activity found in the SFF-SLN samples on the Western blots. When samples were first reduced with 100 mM DTT, the doublet of enzymatic activity was found at 60 and 62 kD molecular weight, also consistent with the Western blot.

Incubating the zymogram in activation buffer with the addition of 1, 10-

Figure 34. Zymogram of conditioned medium from clonal cell lines. (Zymogram with lanes 6, 7, 8, 9 was activated in the presence of 10 mM 1,10-phenanthroline, a preferential zinc chelator.)

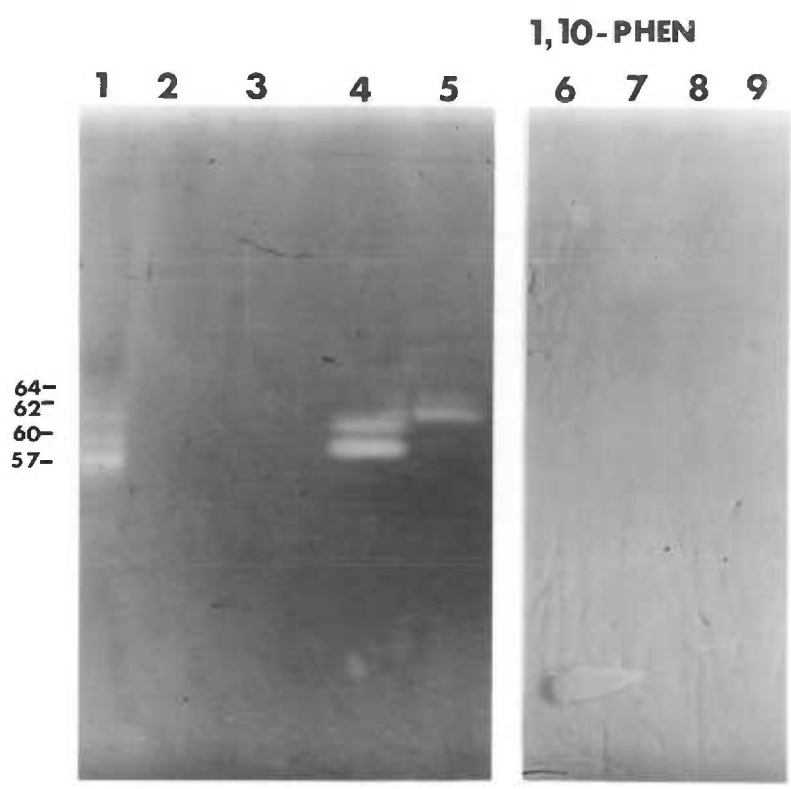
Lane 1: 5 mls of conditioned media from trabecular cells stimulated with 1 μ M dexamethasone and 40 Units/ml IL-1 α for 72 hours was concentrated 20 fold and 5 μ l loaded as a positive control. SLN is doublet at 62 and 60 kD. (64 and 57 kD bands are interstitial collagenase which is also stimulated by dexamethasone and has some activity on casein zymograms.)

Lane 2, 6: 20 μ l media (unconcentrated) from mock-transfected coculture controls.

Lane 3, 7: 20 μ l media from mock-transfected coculture controls, plus 10 mM DTT.

Lane 4, 8: 20 μ l media from SFF-SLN clone (#S1W10-D).

Lane 5, 9: 20 μ l media from SFF-SLN clone (#S1W10-D), plus 10 mM DTT .



phenanthroline, a zinc chelator and a known inhibitor of metalloproteinase enzymatic activity (9), resulted in the loss of activity of both the 57 and 60 kD bands and the 60 and 62 kD reduced bands (Fig. 34).

I. Digestion of Stromelysin with Endoglycosidase D

The polysacchride side-chains of SLN were determined by Wilhelm et al. (142) to be N-linked, by using [³H]-mannose to label fibroblast glycoproteins and immunoprecipitating proSLN. SDS-PAGE gels and Western blots revealed a protein doublet, of which the upper, minor band was also radiolabeled. They also digested their labeled proSLN with Endoglycosidase H, which cleaves high mannose polysaccharides, without success.

Therefore, Endoglycosidase D, which cleaves mature, low mannose polysaccharides at a (1-4) N-acetyl glucosamine linkage, was used to remove polysaccharide side-chains from proSLN. Following enzymatic digestion, the samples were subjected to SDS-PAGE electrophoresis under reducing conditions then Western blotted. There was no positive control used for Endoglycosidase activity. To analyze shifts from the reduced glycosylated 62 kD form to the nonglycosylated 60 kD form, the lanes were scanned with a densitometer. The absorbance for each glycosylated band was divided by the absorbance for each

nonglycosylated band. This ratio was plotted as a bar graph (Fig. 35) and shows a shift from the glycosylated to the nonglycosylated form.

While some digestion of polysaccharide side-chains occurred, there was a significant amount which remained in the immunoreactive, upper band of proSLN. Fully mature polysaccharide side-chains may also contain additional moieties, such as sialic acid residues, which can interfere with the ability of Endoglycosidase D to cleave the hybrid oligosaccharide. An alternative enzyme which may be useful would be N-Glycosidase F.

J. Estimation of Stromelysin Concentration in SFF-SLN

Conditioned Media

Conditioned media from SFF-SLN clone #G-11 was subjected to SDS-PAGE electrophoresis under nonreducing conditions in three concentrations, 50, 100 and 150 μ l. Following electrophoresis, the gel was stained with Coomassie blue (Fig. 36). The same samples were electrophoresed and Western blotted. The heavy 57 kD protein band in the Coomassie blue stained gel corresponded to the proSLN immunoreactive band of the Western blot, also at 57 kD (Fig. 37). The 57 kD immunoreactive band of the Western blot was also the major protein band visualized on the Ponceau S stain of the blot before immunochemical processing.

Figure 35. Western blot of conditioned medium from SFF-SLN clonal cell line (#S1W10-D) following treatment with Endoglycosidase D.

Lane 1, 3: 50 μ l conditioned media plus 10 mM DTT.

Lane 2, 4: 50 μ l conditioned media plus 10 mM DTT following digestion for 1 hour at 37° C with 25 μ U Endoglycosidase D.

Lane 5: Molecular weight standards.

Bar graph: Each lane was scanned by densitometry and the absorbance of the top band (glycosylated) was divided by the absorbance of the bottom band (nonglycosylated). The ratio for each pair of bands is plotted as a bar graph under their respective lanes.

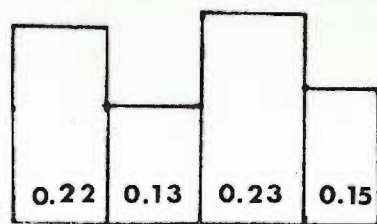
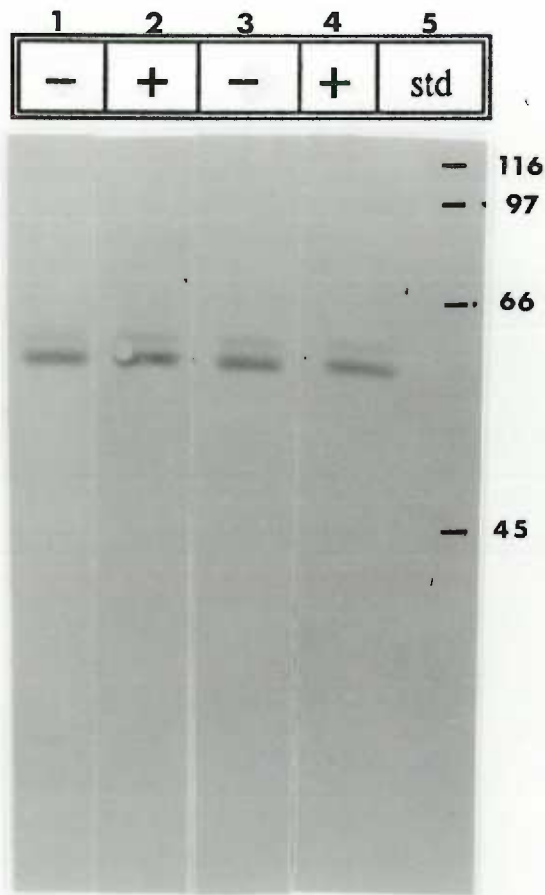


Figure 36. Coomassie blue SDS-PAGE gel of bovine serum albumin and SFF-SLN conditioned media. BSA standards were scanned with a densitometer and the absorbance versus concentration was plotted (Fig. 38). The concentration of the 57 kD SLN band (Lane 5) was estimated from the BSA standard curve.

- Lane 1: 50 ng BSA standard.
- Lane 2: 100 ng BSA standard.
- Lane 3: 200 ng BSA standard.
- Lane 4: 400 ng BSA standard.
- Lane 5: 50 μ l SFF-SLN conditioned media.
- Lane 6: 100 μ l SFF-SLN conditioned media.
- Lane 7: 150 μ l SFF-SLN conditioned media.

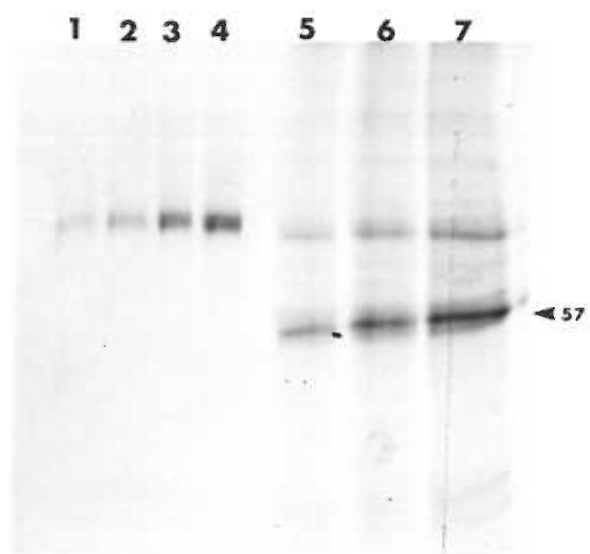
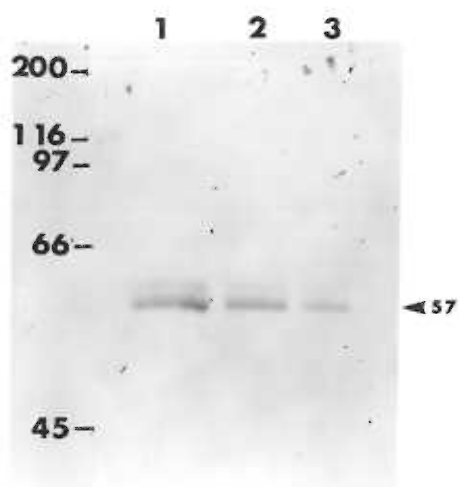


Figure 37. Western blot of SDS-PAGE gel of SFF-SLN conditioned media. The 57 kD band was both visualized on the Ponceau S staining of the nitrocellulose blot and immunochemically stained by the anti-SLN peptide antibody.

Lane 1: 150 μ l SFF-SLN conditioned media.
Lane 2: 100 μ l SFF-SLN conditioned media.
Lane 3: 50 μ l SFF-SLN conditioned media.



The Coomassie stained proSLN band was scanned with a densitometer in both the vertical and horizontal directions. BSA was also electrophoresed at 50, 100, 200 and 400 ng and similarly scanned as a reference.

The absorbance for 50, 100 and 150 μ l of proSLN in SFF-SLN conditioned media, when scanned vertically was 7,201, 12,518 and 18,848 Density Units, respectively. In the horizontal direction, the absorbance was 16,497, 31,392 and 53,036 Density Units. Since the horizontal and vertical absorbance for the 50 μ l SFF-SLN sample fell within the range of the values for the BSA standards, the concentration of proSLN could be estimated from plots of the band density vs. concentration for BSA (Fig. 38). From these plots, proSLN was estimated to be present at a concentration of 5-6 μ g/ml in 24 hour condition media.

K. Activation of proSLN to the Latent Form

Two methods were employed to activate proSLN. The first, trypsin digestion, was carried out by incubating 1 ml of SFF-SLN (Clone #G-11) conditioned media with 400 ng trypsin for various lengths of time.

When electroblotted and immunostained on a Western blot (Fig. 39), the proSLN doublet at 60/63 kD shifted first to the intermediate activation state at 54/57 kD and then was further processed over time to the 47/50 kD active form.

Figure 38. SDS-PAGE lanes were scanned and analyzed for Coomassie blue staining density. Bovine serum albumin was applied in the amounts indicated; undiluted conditioned media from SFF-SLN clone #G-11 was electrophoresed at 50, 100 and 150 μ l per lane. Similar proSLN concentrations were obtained by both methods.

Stromelysin production of high-producing clones was estimated at 5.5 μ g per milliliter of culture media.

Estimation of Stromelysin Production By Murine Coculture Clones

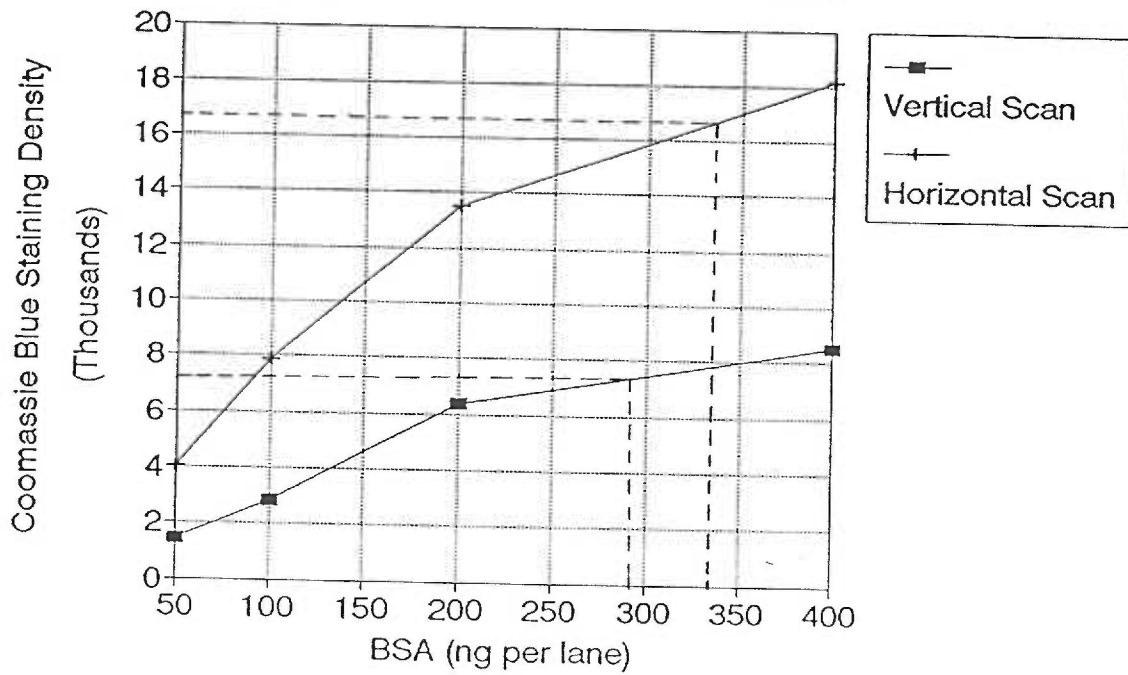


Figure 39. Western blot of conditioned medium from SFF-SLN clonal cell line (#G-11) following activation of proSLN with 400 ng/ml trypsin at 37° C.

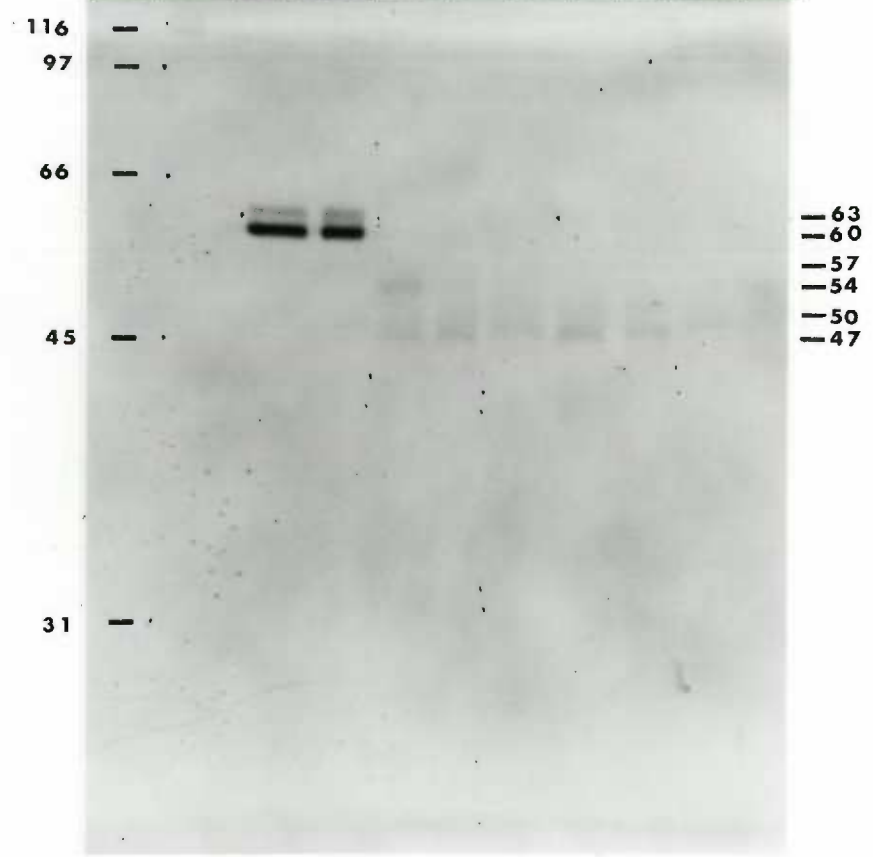
Lane 1: Molecular weight standards: 200, 116, 97, 66, 45, 31 kD.

Lane 2: 20 ng trypsin (control).

Lane 3: Control. 50 μ l untreated conditioned media.

Lane 4-11: Time course of activation by trypsin treatment. 50 μ l conditioned media at time 0 to 18 hr., as indicated.

std	try	con	0 min	20 min	30 min	1 hr	2 hr	3 hr	4.5 hr	18 hr
-----	-----	-----	-------	--------	--------	------	------	------	--------	-------



By 4.5 hours most of the immunoreactivity at all molecular weights has disappeared and by 18 hours is completely gone as the 45/50 kD active form is further processed by cleavage of the carboxy terminal domain to a 31 kD form. The anti-SLN antibody used for these Western blots does not detect the 31 kD form. The same samples, when electrophoresed on a zymogram (Fig. 40), show bands of enzymatic activity that correspond with the bands of immunoreactivity.

The second method used for activation of proSLN involved the use of an organomercurial, 4-aminophenylmercuric acetate (APMA). On a Western blot, the major bands of immunoreactivity occur at 60/62 kD, with the 62 kD form being the minor glycosylated form (Fig. 41). The next major immunoreactive band is at 52 kD, and is probably the intermediate activation state of the 60 kD nonglycosylated proSLN. The next identifiable band is at 47 kD and represents fully activated SLN. Since the glycosylated proSLN is present in greatly reduced quantities to begin with and as a glycoprotein will electrophorese as a more diffuse band, the intermediate activation state and the fully activated form of glycosylated SLN does not appear to be visibly detectable on the Western blot.

When these samples were electrophoresed on a zymogram (Fig. 42), the bands of enzymatic activity corresponded with the bands of immunoreactivity on the Western blot. The 52 kD band was enzymatically much more active than the

Figure 40. Zymogram of conditioned medium from SFF-SLN clonal cell line (#G-11) following activation of proSLN with 400 ng/ml trypsin at 37° C.

Lane 1: Molecular weight standards: 200, 116, 97, 66, 45
31 kD.

Lane 2: 4 ng trypsin (control).

Lane 3: Control. 10 μ l untreated conditioned media.

Lane 4-11: Time course of activation by trypsin treatment.
10 μ l conditioned media at time 0 to 18 hr.,
as indicated.

(Bands of enzymatic activity at 97 kD are probably the 92 kD Type IV Collagenase. These bands were not immunoreactive with the anti-SLN antibody.)

std	try	con	0 min	20 min	30 min	1 hr	2 hr	3 hr	4.5 hr	18 hr
-----	-----	-----	-------	--------	--------	------	------	------	--------	-------



-97
-62
-60
-57
-54
-50
-45

Figure 41. Western blot of conditioned medium from SFF-SLN clonal cell line (#G-11) following activation of proSLN with 5 mM APMA.

Lane 1: High molecular weight protein standards: 200, 116, 97, 66, 45, 31 kD.

Lane 2: 50 μ l untreated conditioned media.

Lane 3-8: Time course. 50 μ l conditioned media treated with APMA at time 10 min. to 18 hr., as indicated.

std	con	10 min	30 min	1 hr	2 hr	3 hr	18 hr
-----	-----	--------	--------	------	------	------	-------

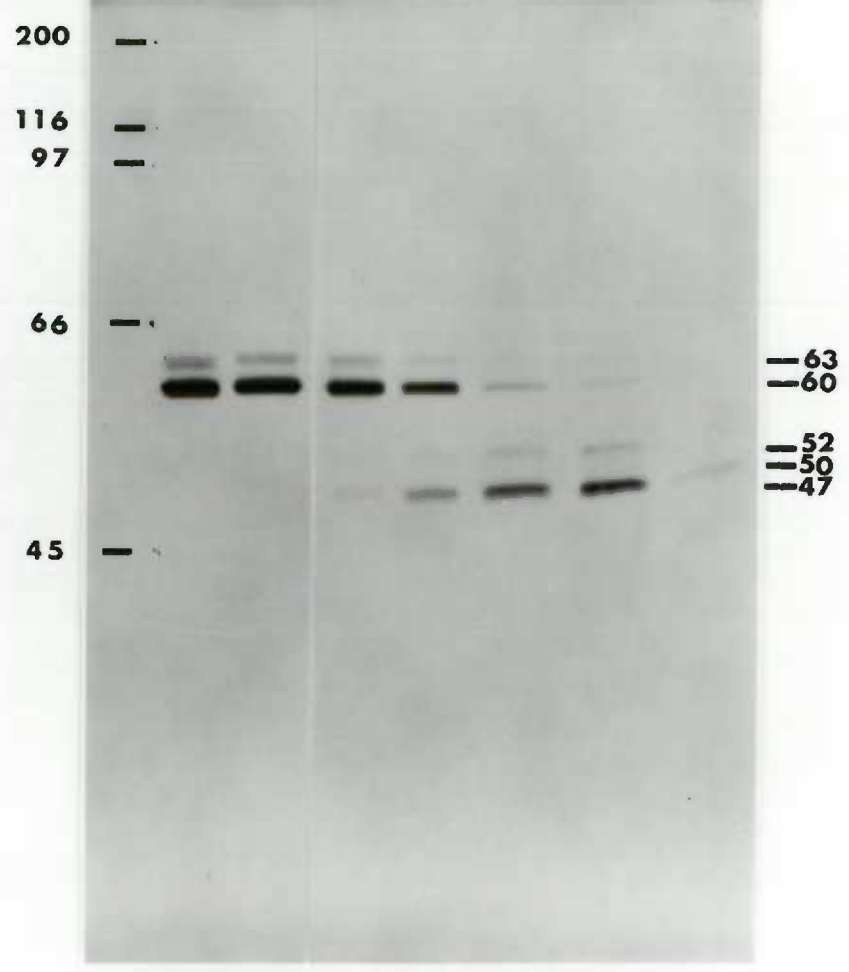


Figure 42. Zymogram of conditioned medium from SFF-SLN clonal cell line (#G-11) following activation of proSLN with 5 mM APMA.

Lane 1: 10 μ l untreated conditioned media.

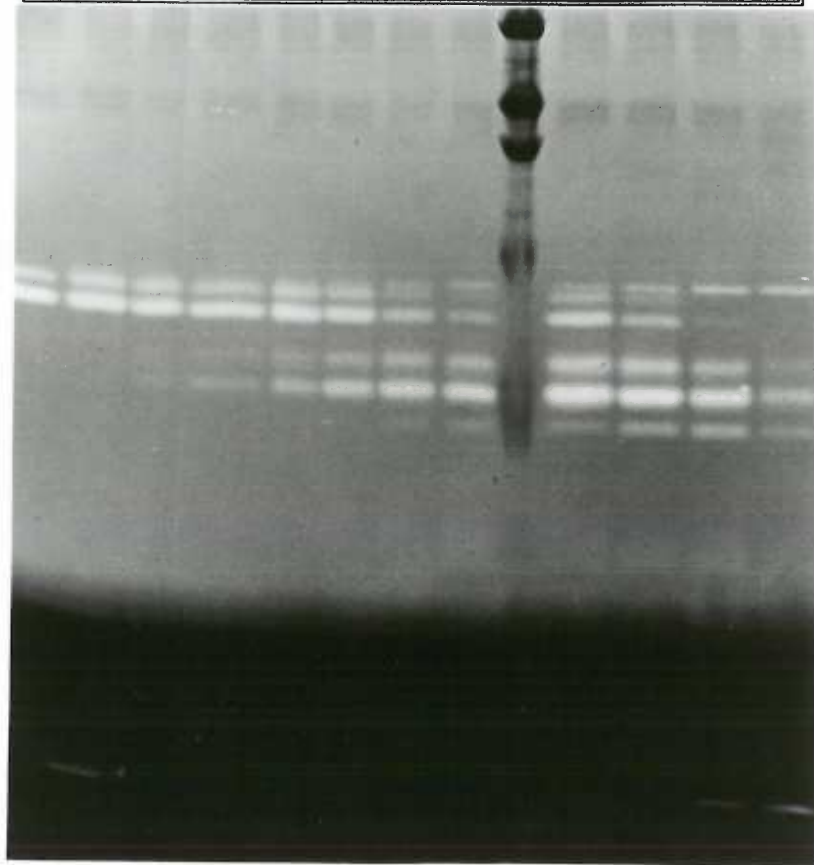
Lane 2-8: Time course #1. 10 μ l conditioned media treated with APMA at time 0 to 3 hr., as indicated.

(The band at 67 kD which appears over the time course is not immunoreactive with the SLN antibody and is probably the 72 kD Type IV Collagenase, which is also activated by APMA.)

Lane 9: High molecular weight protein standards: 200, 116, 97, 66, 45, 31 kD.

Lane 10-13: Time course #2. 10 μ l conditioned media treated with APMA for 2 to 20 hours.

con	0 min	10 min	20 min	30 min	1 hr	2 hr	3 hr	std	2 hr	3 hr	6 hr	20 hr
-----	-------	--------	--------	--------	------	------	------	-----	------	------	------	-------



-67
-62
-60
-53
-49
-45

protein concentration shown on the Western blot suggested it would be. Either the APMA intermediate activation state has more enzymatic activity than the fully activated 47 kD form, or the glycosylated form of the fully activated enzyme has run as a diffuse band that is overlapping the 52 kD intermediate activation form but is not discretely detectable on the Western blot.

L. PCR Assay for SLN Inhibitor

To examine whether the constitutive expression of SLN by SFF-SLN clonal cultures could be detected by the cell and used as a signal to increase production of SLN's inhibitors, TIMP-1 and TIMP-2, cultures were assayed using PCR to see whether these PCR products appeared to change. Three cultures were used: a mock transfected control cell line, a SFF-GH clone #5 and SFF-SLN clone #G-22.

Cells were harvested across time points for four days, which represented the cultures moving from approximately 15% confluency to 100% densely confluent cultures. The densely confluent, contact-inhibited culture represented the point where cellular homeostasis should be occurring. Each of the three cell lines were assayed for the presence of five RNAs: SLN, TIMP-1, TIMP-2, GH and G-3-PD, an enzyme from the glycolytic pathway selected to serve as a putative nonchanging internal standard. The agarose gels revealed bands for G-3-PD in all three cell

lines which remains at a stable level across all four time points. Likewise, a SLN band, which appears only in SFF-SLN clone #G-22 at each time point, is also stable, as is the GH band found in SFF-GH #5 extracted RNA. TIMP-2 was present and appeared to be constitutively expressed in all cell lines and across all states of confluency. TIMP-1, if present in any of the cell lines, appeared to be in very low levels and was not induced to any appreciable extent (Fig. 43, 44).

This assay is not quantitative as performed here. An RNA standard curve would demonstrate whether or not the bands seen for the various PCR products fall within the linear range of the curve and do not exceed the maximum levels of detection.

M. Infection of Trabecular Meshwork Cells

As a step in developing an in vitro culture system where the maintenance and turnover of extracellular matrix could be studied, the SFF-SLN retroviral expression vector was used to infect trabecular meshwork (TM) cells, which make and maintain the extracellular matrix of the TM (11, 12, 17, 18, 19, 20). Hypothetically, this is the primary lesion site in the eye disease, glaucoma. Since the PA-12 cell line produces amphotropic virions capable of infecting cells from other species, bovine and porcine TM cultures were grown and maintained in the

Figure 43. Clonal cell lines at 15% and 30% confluency. RNA was extracted from three cell lines: Mock-transfected control cocultures, SFF-GH clonal cell line and SFF-SLN clonal cell line. RNA from each cell line was assayed using the polymerase chain reaction with five primers: Glyceraldehyde-3-phosphate dehydrogenase (internal standard) (0.4 Kb), SLN (1.4 Kb), TIMP-2 (0.44 Kb), TIMP-1 (0.4 Kb) and Growth hormone (0.4 Kb).

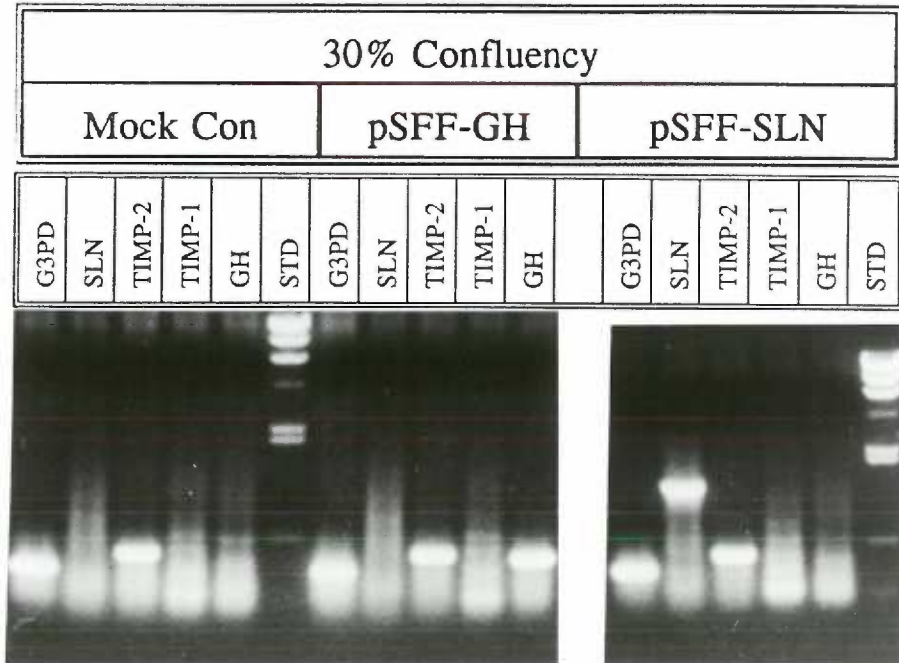
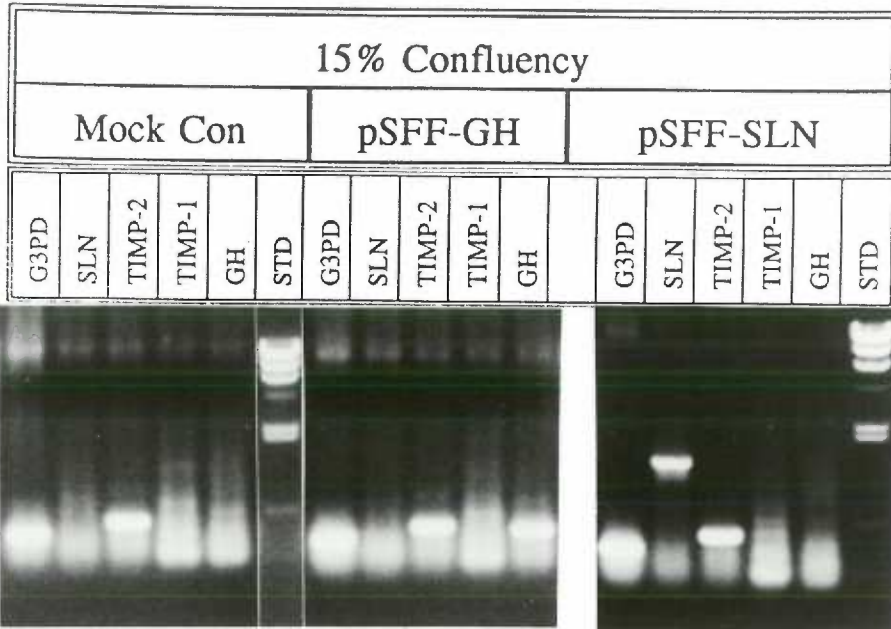
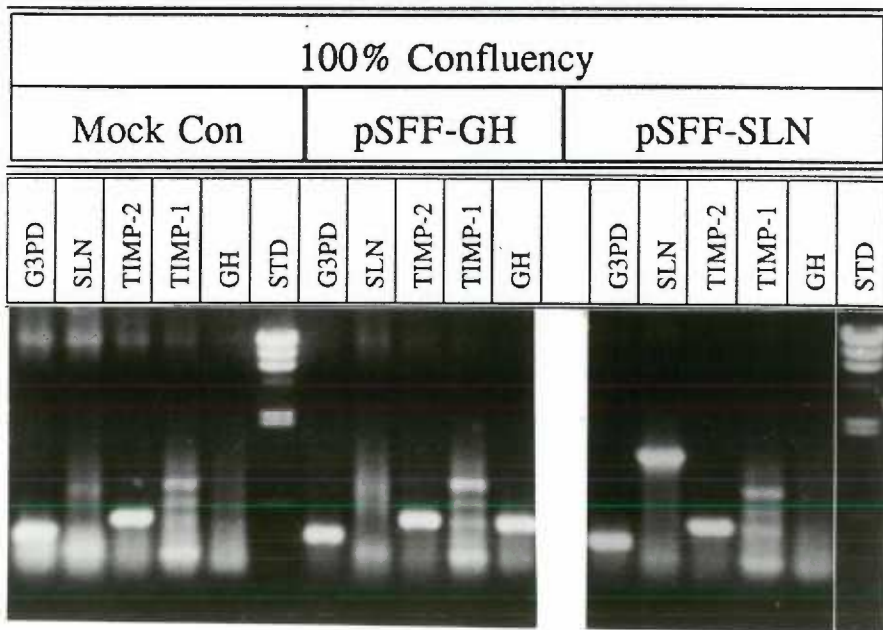
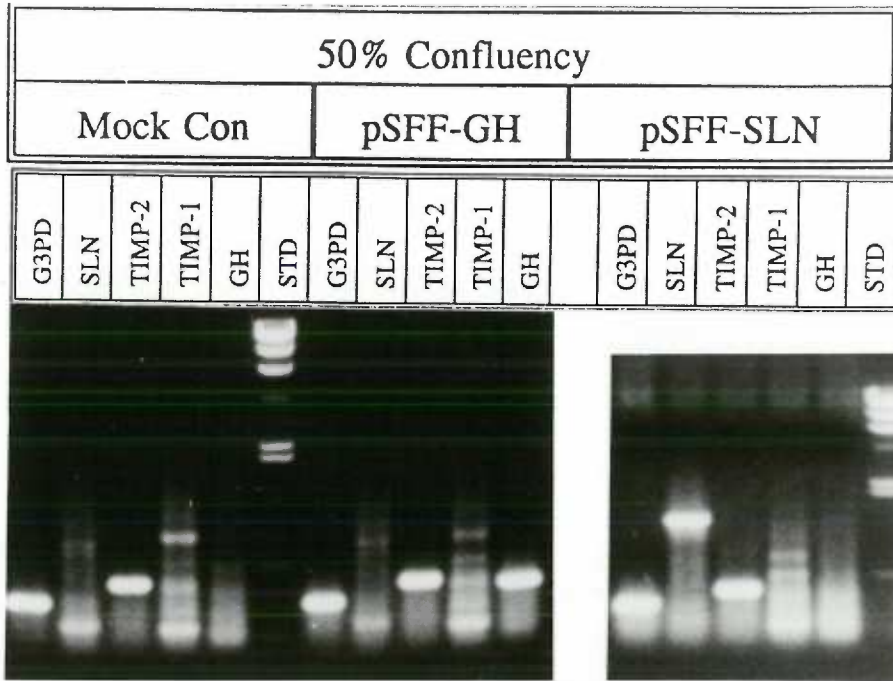


Figure 44. Clonal cell lines at 50% and 100% confluency. RNA was extracted from three cell lines: Mock-transfected control cocultures, SFF-GH clonal cell line and SFF-SLN clonal cell line. RNA from each cell line was assayed using the polymerase chain reaction with five primers: Glyceraldehyde-3-phosphate dehydrogenase (internal standard), SLN, TIMP-2, TIMP-1 and Growth hormone.



presence of conditioned media from SFF-SLN, SFF-GH and mock infected murine cocultures.

The TM cultures were kept at a low state of confluency to optimize the incorporation of virions into dividing cells (105, 106, 103). After approximately two weeks in culture with exposure to media-borne virions, the cells were assayed for the production of SLN and GH using PCR, radioimmunoassay and immunohistochemistry.

The radioimmunoassay conducted using media from both bovine and porcine TM cultures showed GH production in the range of 8.5 ng/ml (in 48 hours). This occurred only in the cultures infected with SFF-GH (Fig. 45). Amounts of GH detected in TM infected cultures were significantly lower than levels found in the murine fibroblast SFF-GH clonal cell lines, which had undergone the amplification process. These lower levels of GH production suggested that the rate of cellular infection by the PA-12 amphotropic viruses was low and might be increased by concentrating the coculture conditioned media used for the infection process.

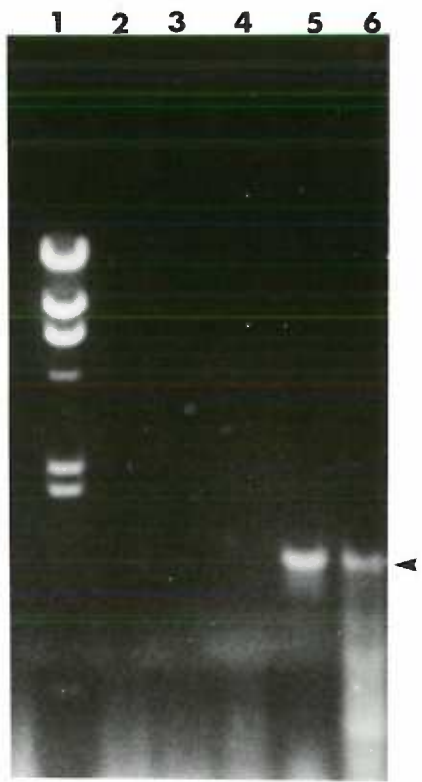
PCR analysis, using the SLN sense and antisense primers, was conducted with cellular RNA extracted from bovine TM cultures. This revealed that SLN mRNA was present only in cultures grown in the presence of SFF-SLN conditioned coculture media (Fig. 46). One TM culture (Lane 4) was exposed to

Figure 45. Radioimmunoassay for human growth hormone expression by bovine and porcine TM cultures grown in the presence of conditioned media taken from SFF-SLN, SFF-GH, and mock transfected murine cocultures. Growth hormone values are ng/ml of 24 or 48 hour medium conditioned by the TM cultures following infection.

Type of murine coculture transfection used to produce infective conditioned medium	Porcine TM cells GH (ng/ml)	Bovine TM cells GH (ng/ml)
mock transfected control (48 hr)	0	0
SFF-SLN (48 hr)	0	0
SFF-GH & SFF-SLN (48 hr)	5.2	ND
SFF-GH (24 hr)	ND	1.25
SFF-GH (48 hr)	8.5	2.2

Figure 46. Bovine TM cell expression of SLN mRNA. Total cellular RNA was extracted from bovine TM control cultures and TM cultures which had been infected with SFF-GH or SFF-SLN amphotrophic virions. PCR was used to assay for the presence of SLN mRNA.

- Lane 1: Molecular weight standards: 23.1, 9.4, 6.6, 4.4, 2.3, 2.0, 0.6 Kb.
- Lane 2: TM culture grown in the presence of murine mock-transfected control media.
- Lane 3: TM culture grown in the presence of conditioned media from a murine pSFF-GH transfected coculture.
- Lane 4: TM culture grown in the presence of conditioned media from a murine pSFF-SLN transfected coculture (a low SLN producing clone).
- Lane 5: TM culture grown in the presence of conditioned media from a murine pSFF-SLN transfected coculture (a high SLN producing clone).
- Lane 6: 0.1 pg pBS-SLN plasmid DNA (amplified as a PCR control).



conditioned media from a pSFF-SLN transfected coculture which had been shown, by PCR analysis, to have very low levels of SLN mRNA present. This conditioned media appears to have produced little or no detectable infection of the TM culture. Unstimulated TM control cultures were shown, by PCR analysis, to produce undetectable levels of SLN (Fig. 47). TM cells stimulated with the phorbol-ester, TPA, which acts through the AP-1 binding site in the promoter region of the SLN gene (68), were also shown to contain detectable SLN mRNA (Fig. 47), however, the RNA used for this assay was extracted from approximately five times as many cells as the experiment depicted in Fig. 46.

Immunohistochemistry of porcine TM cells (Fig. 49) showed 32% of the cultures staining positively for SLN (Table I). Bovine nonconfluent (Fig. 48) TM

Table I. The anti-SLN immunoreactive porcine TM cells were counted for SFF-GH and SFF-SLN infected cultures.

Type of TM Culture	Averaged Percent Immunostained*	S.E.M.
SFF-GH	3.62 %	0.79 %
SFF-SLN	32.4 %	2.01 %

* $p < 0.0001$, student's t-test

cultures grown in the presence of SFF-SLN conditioned media showed similar

Figure 47. Bovine TM cell expression of SLN mRNA when stimulated with the phorbol-ester, TPA.

- Lane 1: pBS-SLN plasmid DNA (0.1 pg) amplified as a PCR control.
- Lane 2: RNA extracted from 3.0×10^9 unstimulated TM cells and assayed for the presence of SLN mRNA.
- Lane 3: TPA stimulated TM cells (total RNA extracted from 3.0×10^9 cells).
- Lanes 4-6: RNA extracted from SFF-GH clonal cell lines was assayed using the SLN primers.
- Lane 7: RNA extracted from mock transfected control cell line was assayed using the SLN primers.
- Lane 8: Molecular weight standards: 23.1, 9.4, 6.6, 4.4, 2.3, 2.0, 0.6 Kb.

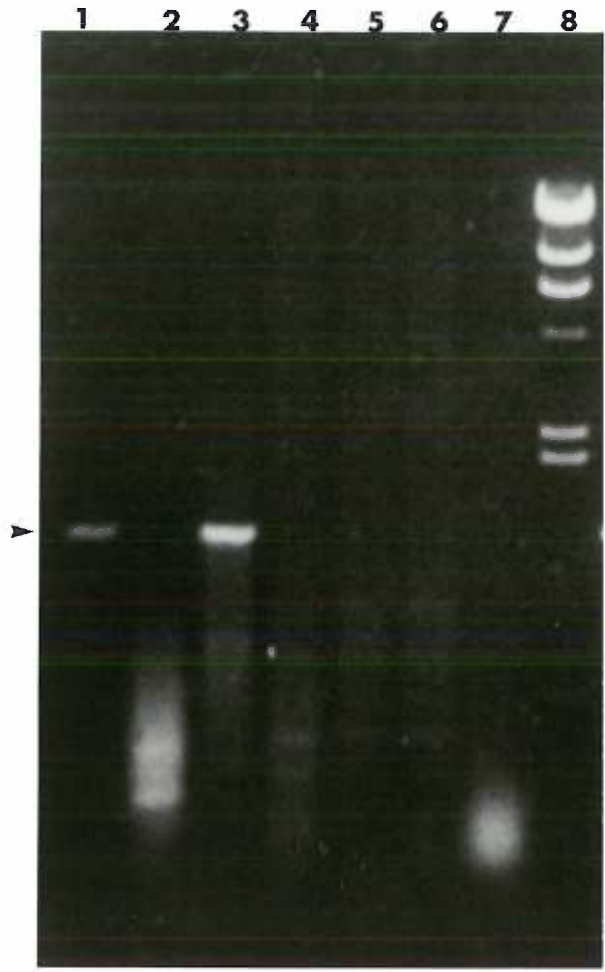


Figure 48. Bovine TM culture immunohistochemically stained with a rabbit anti-human SLN polyclonal peptide antibody. Culture was photographed on an inverted microscope using dark field illumination.

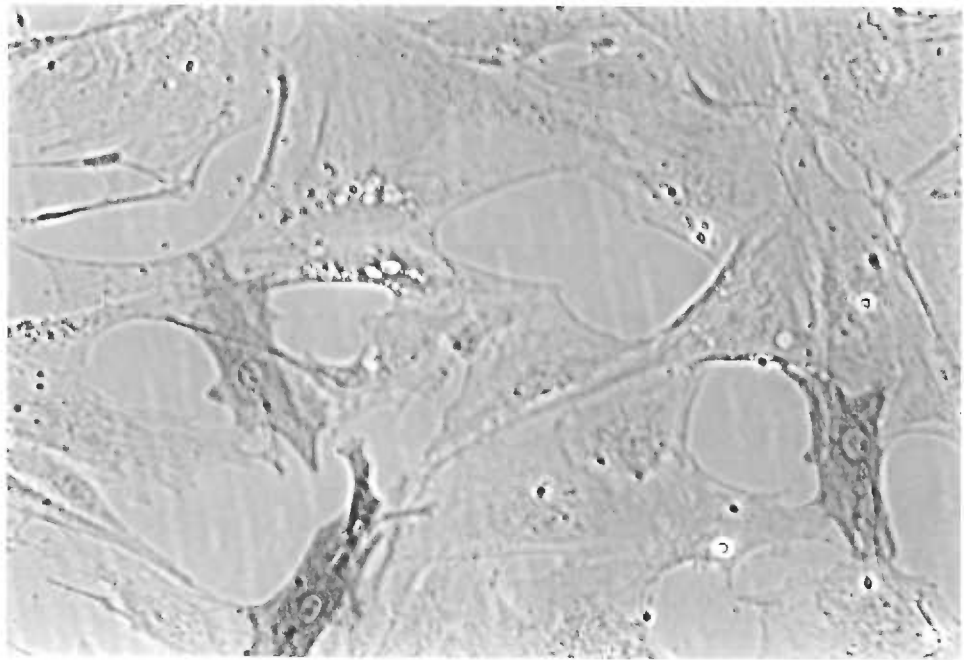


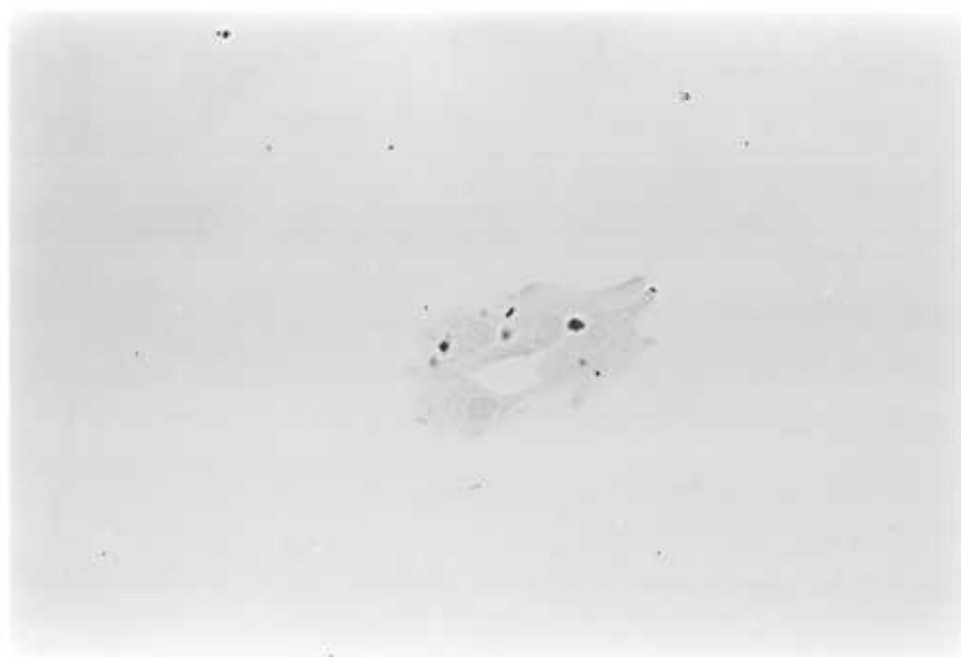
Figure 49. Porcine TM cultures immunohistochemically stained using a chicken anti-human SLN polyclonal peptide antibody. A nonconfluent culture showing approximately 10 cell bodies which were stained positively for the presence of SLN. Two illuminated nuclei (arrows) indicate cells which were not SLN-positive in the field.



numbers of SLN-positive cells. These results confirm the GH-RIA data that suggested the numbers of infected TM cells was significantly lower than the levels of infection and expression seen with the murine fibroblast clonal cell lines. This lower level of SLN-positive cells could either be attributed to a lower rate of viral infection achieved (as compared to the murine coculture amplification system) or due to decreased SFFV promoter efficiency in the trabecular cells.

The pattern of staining, when compared with the murine fibroblast SFF-SLN cultures, was not as intense nor punctate in appearance. It appears to be a more uniform cell surface staining. As with the SFF-GH cultures, the nuclei of some of the stained cells are distinctively observed (Fig. 50). The reasons for this have not been determined.

Figure 50. Porcine TM cultures grown in the presence of SFF-SLN coculture conditioned media and immunohistochemically stained using a chicken anti-human SLN polyclonal peptide antibody. Pictured is a field of densely confluent porcine TM cells which show a cluster of at least four cells which are positively stained for SLN and may have arisen from the same precursor cell. SLN-negative cells in the field are not visible.



IV. DISCUSSION

A. The Need for an Human Stromelysin Expression System

The goal of this project was to develop a system for the expression of the proteolytic enzyme, SLN. Although human skin fibroblast SLN mRNA had been cloned and sequenced (55), the protein product made from this cDNA had not been expressed. Therefore, before the SLN made from this cDNA could be used for desired studies in glaucoma, it had to be characterized to show it had appropriate properties and enzymatic activity.

Human SLN had previously been purified from media conditioned by stimulated rheumatoid synovial fibroblasts (61). The drawback to this method is that this transient induction of SLN also results in the induction of interstitial collagenase and the 92 kD form of Type IV collagenase (43, 61). TIMP-1 is also induced under conditions which induce the MMPs (91). Studies done with SLN first required its purification away from other secreted proteins, particularly, the other MMP's and TIMP-1. This has been a tedious process, since there is considerable sequence homology between the MMP's, thus columns frequently bind and coelute all MMPs (61, 9).

SLN purification is done most efficiently with a precipitating antibody, but

sequences for making antibodies and probes must be carefully selected or they will identify all MMP's. Peptide antibodies, such as those used in this project, are seldom optimum for immunoprecipitation. This was found to be true with our rabbit anti-SLN antibody. The chicken anti-SLN antibody which was also used is an IgY rather than an IgG immunoglobulin making the immunoprecipitation protocol more complicated.

The rat SLN homolog, transin, had been moderately well characterized (69, 51, 123, 67, 52, 68, 135) by Matrisian et al. "Transin" was first described as an oncogene and EGF-inducible mRNA; when it was subsequently sequenced (67) it was found to be a SLN homolog. A COS cell expression system using a transin cDNA has been used to express and study the protein product of the transin cDNA (51, 52).

During the course of this project, Whitman et al. (24, 131) cloned a human gingival fibroblast SLN cDNA and set up an expression system using the SV-40 promoter and COS cells. This COS cell system and their vector, while giving a high level of inducible expression, is a transient expression and the cell lines are not permanent (131).

B. Results of Stromelysin Expression Using Ping-Pong Amplification

The use of the Ping-pong amplification retroviral expression system has several advantages (114, 115). The protein product will undergo eukaryotic processing, it will be constitutively expressed at relatively high levels using the retroviral promoters, it will create permanent cell lines expressing the protein of interest, and the virions produced will be capable of infecting other cell lines of interest. The data from the SFF-GH PCR experiment also shows that the host cell is capable of splicing a retroviral RNA correctly to remove even intervening sequences from a complete genetic coding sequence subcloned into the retroviral vector (Fig. 21, 22).

1. Preprostromelysin processing and post-translational modification

The SLN cDNA cloned into pSFF contained the "prepro" sequence as shown in the sequencing data (Fig. 14), therefore, the nascent peptide should be correctly routed in the golgi/RER organelles. The immunohistochemistry carried out with and without detergent support this expectation (Fig. 30, 31).

It had previously been reported that SLN, which was produced by phorbol-ester stimulated human fetal lung fibroblasts, underwent post-translational modification in the golgi (55). On SDS-PAGE gels stained with Coomassie blue, the major protein product in the conditioned media appears to be SLN, present in both a minor glycosylated and major nonglycosylated form. The Western blot

verified this doublet was immunoreactive, using both a rabbit and chicken peptide antibody (Fig. 33). Endoglycosidase D digestion showed a shift of the higher molecular weight, minor band to the lower nonglycosylated form (Fig. 35). The digestion, however, did not go to completion and may be due to the presence of hybrid oligosaccharides, which Endoglycosidase D does not efficiently remove. Digestion with N-glycosidase F may give better results because it cuts high mannose polysaccharides and is not inhibited by sialic acid and other such moieties.

2. Prostromelysin secretion

Secretion of SLN from cells is assumed to be by way of the constitutive pathway (70). TPA induction gives an initial increase in SLN mRNA. This is followed by a rise in proSLN found extracellularly starting at 6 hours post-stimulation and peaking at approximately 36 hours (70).

The SFF-SLN clonal cell lines also show greatly increased levels of SLN mRNA (Fig. 19) compared to mock transfected control cells and SFF-GH clones (Fig. 47). The major identifiable band on Western blots of SFF-SLN conditioned media immunostained with anti-human SLN peptide antibodies is the latent propeptide form of SLN (Fig. 33). If the active form of SLN is present in the conditioned media, no band has been visually detected at the expected 47kD size

on Western blots or in the zymograms (Fig. 34). While the in vivo mechanism for activation of proSLN is unknown (61, 136), this data suggests it is a specific, well controlled event.

C. Functional Activity of Stromelysin

1. Reduction of cys disulfide does not inhibit enzymatic activity

When conditioned media from SFF-SLN clonal cell lines was first reduced with DTT and then electrophoresed on a 10% SDS-PAGE gel, the immunoreactive proSLN doublet was found to shift from 57/60 kD to 60/62 kD (Fig. 33). There is one cysteine pair (cys²⁹⁰ and cys⁴⁷⁷) which forms a disulfide bond (55) and would be capable of undergoing reduction in proSLN to produce this molecular weight shift. After electrophoresis on a zymogram (Fig. 34) and enzyme activation, the reduced proSLN appears to retain its enzymatic activity, although it has not been shown the cysteine disulfide bond has not reformed during the incubation stage. Enzymatic activity was abolished in the presence of 1,10-phenanthroline (Fig. 34), a chelator which removes the zinc atom from the enzyme's active site (25).

2. Activation of latent stromelysin

Western blots and zymograms showed SLN to be present in the clonal conditioned media in the latent propeptide form (Fig. 33, 34). It was necessary

to show that the latent retrovirally-expressed, recombinant proSLN could undergo processing to its enzymatically active form. The two methods chosen for this, trypsin activation and APMA activation, had been described for both purified human proSLN from rheumatoid synovial fibroblast conditioned media (61, 63, 136) and rat transin (51, 52).

a. Trypsin activation

Trypsin activation was conducted at an estimated molar ratio of 140 nM trypsin to 11 nM SLN, at 37° C and over an 18 hour time course. Western blots (Fig. 39) and zymograms (Fig. 40) show that the latent proSLN undergoes an initial tryptic digestion to yield an intermediate form at an estimated 54/57 kD. It is further cleaved to its mature, active 47/50 kD form very rapidly (within 30 min.), followed by an equally rapid degradation to smaller molecular weight forms. Smaller SLN fragments at 28 and 21 kD (51, 61) were undetectable on Western blots (Fig. 39). The C-terminus domain, which is cleaved to yield these forms, is also the region recognized by the antibodies (127). On zymograms, there was a region of clearing (Fig. 40), which may be the 28 kD SLN (51, 61). There was also a band of enzymatic activity found at a lower molecular weight (estimated at approximately 15 kD) (51, 61) which increases in intensity over the time course of the experiment. Trypsin activation of the retrovirally expressed

proSLN was consistent with activation data that has been published for interstitial procollagenase (25), purified human rheumatoid synovial fibroblast proSLN (61, 63, 136) and recombinant protransin (51, 52).

b. APMA activation

Organomercurial activation was carried out with 5 mM APMA and an estimated 11 nM SLN. Organomercurials activate MMPs by an unknown mechanism, but the process of activation can be inhibited by mercaptans (25). The first step in activation is suggested to be the dissociation of the propeptide's cysteine sulfhydryl from the zinc active site (63, 136). Interstitial procollagenase, which is activated by a similar mechanism to proSLN (25, 136), has been shown by Stricklin et al. (25) to have enzymatic activity when it is in this form. Ionic detergents, such as SDS, initiate the activation process by conformational perturbation, as well (25).

In the second step of APMA activation, an intramolecular cleavage within the propeptide sequence occurs between Glu⁶⁸ and Val⁶⁹ (25, 63) by an unknown mechanism. This form of SLN electrophoresed at approximately 47 kD (52, 136) and is present on Western blots (Fig. 41) and zymograms (Fig. 42) of retrovirally expressed proSLN treated with APMA (estimated molecular weight is 49-50 kD in Figs. 41 and 42). Next, the intermediate activated state reportedly undergoes

an intermolecular cleavage, which produces the 45 kD fully active form of SLN (51, 52, 63). APMA-treated proSLN, expressed by the SFF-SLN clonal cell lines also produced this molecular weight form (Fig. 41, 42).

The zymogram of APMA activated conditioned media (Fig. 42) shows a strong band of enzymatic activity at 49 kD. This may be due to a differential level of activity between the intermediate activated forms of proSLN generated by trypsin and APMA (52), or it may be the minor glycosylated form of active SLN has electrophoresed as a more diffuse band overlaying the 49 kD intermediate.

The activation by APMA occurs more slowly than it does with trypsin. The time course with APMA activation shows that the molecular weight shift from proSLN (60 kD) to the active form (45 kD) is still progressing at 2 hours, whereas trypsin activation is completed in approximately 30 minutes.

D. SFF-SLN Clonal Cell Lines

1. Northern blot shows increased level of expression of retroviral RNA

The use of the Ping-pong amplification system also allowed the establishment of permanent, high-producing murine fibroblast clonal cell lines. On a Northern blot (Fig. 24), a SLN-cDNA probe hybridized to two RNA bands

containing SLN message. These messages were the predicted sizes for RNA made from the SFF-SLN provirus. The larger (6.0 Kb) message is the full genomic RNA; the smaller (3.3 Kb) is the subgenomic message made from the larger RNA following a splicing event (Fig. 25). Control RNA (from SFF-GH cells) did not contain any detectable SLN bands. If murine fibroblast SLN were being induced by the retrovirus, it would be seen at approximately 1.9 Kb (67). Zymograms also showed that the 72 kD and 92 kD Type IV collagenase as well as interstitial collagenase were present in the media only in low, barely detectable levels, consistent with unstimulated basal secretion (70).

2. PCR analysis shows stromelysin mRNA is present in SFF-SLN clonal cell lines

Screening of SFF-SLN clonal cell lines using PCR showed SLN mRNA to be present only in SFF-SLN cell lines (Fig. 19) and not in SFF-GH or mock transfected controls (Fig. 47). Bovine trabecular meshwork cells were able to produce SLN mRNA in response to TPA stimulation (Fig. 47), however, the amount of mRNA produced was never as high as that produced from murine SFF-SLN clonal cell lines. The levels of SLN mRNA found in SFF-SLN clonal cell lines also correlated with Western blots of conditioned media from the same clones (Fig. 33), i.e. clones with high levels of SLN mRNA also had high levels of

proSLN (data not shown).

3. Estimation of prostromelysin concentration

Coomassie blue stained SDS-PAGE gels and Western blots showed proSLN was the major protein present in SFF-SLN clonal conditioned media. Scanning densitometry gave an absorbance for proSLN, which when analyzed based on a standard curve of BSA protein concentration versus absorbance, allowed an estimation of proSLN concentration. This was estimated to be 6 $\mu\text{g/ml}$, or 30 μg of proSLN per 10^6 cells per 24 hours (i.e. one T25 flask with 5 mls conditioned media). This synthesis and secretion surpasses the amount of proSLN produced through TPA stimulation of rabbit capillary endothelial cells (15 μg proSLN per 10^6 cells per 48 hours) (70). The SFF-SLN expression system, therefore, represents a greatly improved method for producing relatively large amounts of processed SLN.

4. Clonal cell lines are unstable with high stromelysin production

MMPs have been shown to be vectorially secreted upon the formation of tight junctions (132). The major form of SLN found in the media using Western blots and zymograms was the propeptide (Fig. 33, 34), however, with vectorial secretion, a small amount of SLN being activated may be sufficient to sever matrix-cellular connections, making these cultures more prone to detach from the

surface of the culture flask. The in vivo mechanism for activation of proSLN is not known, however, recent work has suggested the activator for the 72 kD Type IV collagenase is membrane associated (137).

E. Cell-Matrix Destabilization -- A Possible Feedback Loop?

A coordinated regulation has been described for MMPs that shows their production is down-regulated as the cell becomes confluent (8). Indeed, a lack of such down-regulation is a property of metastatic tumor cells. This has suggested to several investigators that the cell may have some mechanism for detecting whether or not it has reached homeostasis (8, 138, 139, 140). Werb et al. (139) and Ingber and Folkman (138), have suggested that fibronectin and integrins may play a role in stabilizing the cell's cytoskeleton, which is in turn "read" by the nucleus as a signal to move into a differentiation gene program.

Since the clones containing the SFF-SLN provirus are constitutively expressing proSLN, we reasoned that they could not reach homeostasis as they became confluent. This seemed to be an ideal system, therefore, to examine whether the inhibitors for MMPs, TIMP-1 and TIMP-2, could be induced in response to this lack of extracellular stability. PCR was conducted with RNA extracted from clonal cell lines as they became densely confluent (Fig. 43, 44).

The data showed these fibroblasts normally synthesize an appreciable amount of TIMP-2 in a constitutive fashion. Stetler-Stevenson et al. (92), have suggested this role for TIMP-2, because the gene does not have a TPA responsive-element (TRE) as does TIMP-1 in its upstream promoter region. TIMP-1, which has both a TRE and a serum responsive-element (91) seemed the most likely candidate to be upregulated if the nucleus were able to detect cytoskeletal destabilization. TIMP-1, however, did not appear to change its level of synthesis as a function of confluency of the clonal cell lines under the conditions of the PCR assay as described. The PCR assay was not quantitative, however, without an RNA standard curve to demonstrate the PCR products were within a linear range.

F. Establishment of Cell Lines Infected with SFF-SLN

The amphotropic viruses produced by the PA-12 packaging cell line during the course of the ping-pong amplification process are capable of infecting cells of any mammalian species. They were used, therefore, to establish cultures of bovine and porcine trabecular meshwork cells, which were capable of producing SLN in a constitutive manner. These cultures were shown to have both SLN mRNA present, by PCR (Fig. 46) and an immunoreactive SLN protein, by immunohistochemistry (Fig. 48, 49, 50).

The cultures were estimated to contain 32% infected cells, based on the immunohistochemical staining. This rate of infection of TM cells is not nearly as great as the level achieved using the murine coculture amplification system. The lower rate of infection is consistent with either a low viral titer in the coculture conditioned media, which was used to produce the infected TM cultures, or a low rate of infectivity of TM cells by these amphotropic viruses. The amount of infection could be increased in the future, by raising the concentration of virus that the cultures are exposed to, thereby increasing the number of cells infected. It is also possible that the SFF promoter is not an efficient promoter in TM cells, which are of neuroectoderm origin, thereby giving a lower level of SLN mRNA expression than in the murine fibroblasts.

G. Implications for the Study of Glaucoma

Trabecular meshwork cultures which constitutively produce SLN lend themselves to the development of the first in vitro system designed for the study of glaucoma and its progression. No animal models currently exist for the study of flow dynamics through the trabecular meshwork. Glaucoma is a slow, chronic, nonfatal disease, so available human glaucomatous tissue has generally been subjected to years of drug and laser treatment. Cultures grown on a flow filter or

explants cultured in a perfusion chamber can be used to study flow dynamics and changes that occur when the ECM undergoes a more rapid remodeling.

Construction of a pSFF-TIMP expression vector would allow specific manipulation of fluid dynamics with TM cultured cells expressing either SLN or TIMP or both.

V. SUMMARY

Using the Ping-pong amplification system for the expression of a previously sequenced but unexpressed SLN cDNA allowed the establishment of permanent clonal cell lines, which produced high levels of proSLN. This proSLN was antigenically reactive with two SLN peptide antibodies, could be localized intracellularly using immunohistochemistry and underwent post-translational modifications, which appear to be consistent with endogenous SLN synthesis. Secreted proSLN exhibited similar electrophoretic mobilities and underwent enzymatic activation in a manner as described for SLN in the literature. This enzymatic activity was inhibited by 1,10-phenanthroline, a zinc chelator.

Establishment of permanent clonal cell lines producing high levels of SLN provides a system for the study of cell homeostasis, extracellular matrix turnover, and regulation of expression of MMPs, their inhibitors and ECM components. Initial studies suggest an absence of direct feedback from SLN over-production on levels of TIMP-1 and TIMP-2 mRNA levels.

Amphotropic virions produced by the murine fibroblast cocultures have been shown to infect trabecular meshwork cultures and become stably expressed. This provides a means of producing an *in vitro* model for studying the maintenance and

turnover of extracellular matrix in the trabecular meshwork and the role it may play in the etiology and treatment of glaucoma.

VI. REFERENCES

1. Saksela, O., D. Moscatelli, A. Sommer and D. Rifkin. Endothelial cell-derived heparan sulfate binds basic FGF and protects it from proteolytic degradation. *Journal of Cell Biology*, 107:743-751, 1988.
2. Weinreb, R. and M. Ryder. In situ localization of cytoskeletal elements in the human trabecular meshwork and cornea. *Investigative Ophthalmology and Visual Science*, 31:1839-1847, 1990.
3. Heinegard, D. and M. Paulsson. Structure and metabolism of proteoglycans. In: *Extracellular Matrix Biochemistry*, edited by Piez, K. and Reddi, A. New York: Elsevier, 1984, p. 277-328.
4. Ruoslahti, E., E. Hayman and M. Pierschbacher. Extracellular matrices and cell adhesion. *Arteriosclerosis*, 5:581-594, 1985.
5. Brown, E. The role of extracellular matrix proteins in the control of phagocytosis. *Journal of Leukocyte Biology*, 39:579-591, 1986.
6. Takigawa, M., Y. Nishida, F. Suzuki, J. Kishi, K. Yamashita and T. Hayakawa. Induction of angiogenesis in chick yolk-sac membrane by polyamines and its inhibition by tissue inhibitors of metalloproteinases (TIMP and TIMP-2). *Biochemical and Biophysical Research Communications*, 171:1264-1271, 1990.
7. Hunt, T. Prospective: A retrospective perspective on the nature of wounds. In: *Growth Factors and Other Aspects of Wound Healing: Biological and Clinical Implications*, edited by : Alan R. Liss, Inc., 1988, p. 13-20.
8. Liotta, L., P. Steeg and W. Stetler-Stevenson. Cancer metastasis and angiogenesis: An imbalance of positive and negative regulation. *Cell*, 64:327-336, 1991.
9. Okada, Y., H. Nagase and E. Harris. A metalloproteinase from human rheumatoid synovial fibroblasts that digests connective tissue matrix components. *Journal of Biological Chemistry*, 261:14245-14255, 1986.

10. Sanes, J., E. Engvall, R. Butkowski and D. Hunter. Molecular heterogeneity of basal laminae: Isoforms of laminin and collagen IV at the neuromuscular junction and elsewhere. *Journal of Cell Biology*, 111:1685-1699, 1990.
11. Yue, B., E. Higginbotham and I. Chang. Ascorbic acid modulates the production of fibronectin and laminin by cells from an eye tissue - trabecular meshwork. *Experimental Cell Research*, 187:65-68, 1990.
12. Yamashita, T. and D. Rosen. The elastic tissue of primate trabecular meshwork. *Investigative Ophthalmology and Visual Science*, 3:85-95, 1964.
13. Iwamoto, T. Light and electron microscopy of the presumed elastic components on the trabecular and scleral spur of the human eye. *Investigative Ophthalmology and Visual Science*, 3:144-156, 1964.
14. Lutjen-Drecoll, E., T. Shimizu, M. Rohrbach and J. Rohen. Quantitative analysis of 'plaque material' in the inner- and outer wall of Schlemm's canal in normal and glaucomatous eyes. *Experimental Eye Research*, 42:443-445, 1986.
15. Alvarado, J., I. Wood and J. Polansky. Human trabecular cells. II. Growth pattern and ultrastructural characteristics. *Investigative Ophthalmology and Visual Science*, 23:464-478, 1982.
16. Lark, M., J. Laterra and L. Culp. Close and focal contact adhesions of fibroblasts to a fibronectin-containing matrix. *Federation Proceedings*, 44:394-403, 1985.
17. Worthen, D. and P. Cleveland. Fibronectin production by cultured human trabecular meshwork cells. *Investigative Ophthalmology and Visual Science*, 23:265-269, 1982.
18. Yurchenco, P. and J. Schnitty. Molecular architecture of basement membranes. *The FASEB Journal*, 4:1577-1590, 1990.
19. Rodrigues, M., S. Katz, J. Foidart and G. Spaeth. Collagen, factor VIII antigen and immunoglobulins in the human aqueous drainage channels. *Annals of the Academy of Ophthalmology*, 87:337-344, 1980.

20. Hirano, K., M. Kobayashi, K. Kobayashi, T. Hoshino and S. Aways. Experimental formation of 100 nm periodic fibrils in the mouse corneal stroma and trabecular meshwork. *Investigative Ophthalmology and Visual Science*, 30:869-874, 1989.
21. Lutjen-Drecoll, E., M. Bittig, J. Rauterberg, R. Jander and J. Mollenhauer. Immunomicroscopical study of type IV collagen in the trabecular meshwork of normal and glaucomatous eyes. *Experimental Eye Research*, 48:139-147, 1989.
22. Ethier, C., R. Kamm, B. Palaszewski, M. Johnson and T. Richardson. Calculations of flow resistance in the juxtacanalicular meshwork. *Investigative Ophthalmology and Visual Science*, 27:1741-1750, 1986.
23. Emonard, H. and J. Grimaud. Matrix metalloproteinases. A review. *Cellular and Molecular Biology*, 36:131-153, 1990.
24. Whitham, S.E., G. Murphy, P. Angel, H. Rahmsdorf, B. Smith, A. Lyons, T. Harris, J. Reynolds, P. Herrlich, and A. Docherty. Comparison of human stromelysin and collagenase by cloning and sequence analysis. *Biochemistry Journal* 240: 913-916, 1986.
25. Stricklin, G., J. Jeffrey, W. Roswit and A. Eisen. Human skin fibroblast procollagenase: Mechanism of activation by organomercurials. *Biochemistry*, 22:61-68, 1983.
26. Shuman, M., J. Polansky, C. Merkel and J. Alvarado. Tissue plasminogen activator in cultured human trabecular meshwork cells. *Investigative Ophthalmology and Visual Science*, 29:401-405, 1988.
27. Park, J., R. Tripathi, B. Tripathi and G. Barlow. Tissue plasminogen activator in the trabecular endothelium. *Investigative Ophthalmology and Visual Science*, 28:1341-1345, 1987.
28. Dano, K., P. Andreasen, J. Grondahl-Hansen, P. Kristensen, L. Nielsen and L. Skriver. Plasminogen activators, tissue degradation and cancer. *Advances in Cancer Research*, 44:139-266, 1985.
29. Reynolds, J.J., R.A.D. Bunning, T.E. Cawston, and G. Murphy. Tissue

metallo-proteinase inhibitors and their role in matrix catabolism. In: Cellular Interactions, edited by Dingle and Garber, Eds., 1981, p. 205-213.

30. Alexander, J., J. Samples, E. Van Buskirk and T. Acott. Expression of matrix metalloproteinases and inhibitor by human trabecular meshwork, *Investigative Ophthalmology and Visual Science*, 32:172-180, 1991.

31. Van Buskirk, E., V. Pond, R. Rosenquist and T. Acott. Argon laser trabeculoplasty: Studies of mechanism of action. *Ophthalmology*, 91:1005, 1984.

32. Parshley, D., J. Alexander, J. Bradley, E. Van Buskirk, J. Samples and T. Acott. Trabecular meshwork secretion of matrix metalloproteinases is affected by several growth factors. *Investigative Ophthalmology and Visual Science Suppl.*, 31:339, 1990.

33. Ruddat, M., J. Alexander, J. Samples, E. Van Buskirk and T. Acott. Early changes in trabecular metalloproteinase mRNA levels in response to laser trabeculoplasty are induced by a media-borne factor. *Investigative Ophthalmology and Visual Science Suppl.*, 30:280, 1989.

34. Hadaegh, A., J. Bradley, S. Gibson, A. Fisk, J. Samples, E. Van Buskirk and T. Acott. Analysis of changes in trabecular stromelysin immunolocalization in response to laser trabeculoplasty. *Investigative Ophthalmology and Visual Science Suppl.*, 32:875, 1991.

35. Fields, G., H. Van Wart and H. Birkedal-Hansen. Sequence specificity of human skin fibroblast collagenase. Evidence for the role of collagen structure in determining the collagenase cleavage site. *Journal of Biological Chemistry* 262:6221-6226, 1987.

36. Miller, E., E. Harris, E. Chung, J. Finch, P. McCroskery and W. Butler. Cleavage of type II and III collagens with mammalian collagenase: Site of cleavage and primary structure at the amino-terminal portion of the smaller fragment released from both collagens. *Biochemistry*, 15:787-792, 1976.

37. Weingarten, H. and J. Feder. Cleavage site specificity of vertebrate collagenases. *Biochem. Biophys. Res. Commun.*, 139:1184-1187, 1986.

38. Seltzer, J., S. Adams, G. Grant and A. Eisen. Purification and properties of a gelatin-specific neutral protease from human skin. *Journal of Biological Chemistry*, 256:4662-4668, 1981.
39. Murphy, G., C. McAlpine, C. Poll and J. Reynolds. Purification and characterization of a bone metalloproteinase that degrades gelatin and types IV and V collagen. *Biochemica et Biophysica Acta*, 831:49-58, 1985.
40. Murphy, G., J. Reynolds, U. Bretz and M. Baggiolini. Partial purification of collagenase and gelatinase from polymorphonuclear leucocytes. *Biochemical Journal*, 203:209-221, 1982.
41. Seltzer, J., A. Eisen, E. Bauer, N. Morris, R. Glanville and R. Burgeson. Cleavage of type VII collagen by interstitial collagenase and type IV collagenase (gelatinase) derived from human skin. *Journal of Biological Chemistry*, 264:3822-3826, 1989.
42. Murphy, G., T. Cawston, W. Galloway, M. Barnes, R. Bunning, E. Mercer, J. Reynolds and R. Burgeson. Metalloproteinases from rabbit bone culture medium degrade types IV and V collagens, laminin and fibronectin. *Biochemistry Journal*, 199:807-811, 1981.
43. Chin, J.R., G. Murphy and Z. Werb. Stromelysin, a Connective Tissue-degrading Metalloendopeptidase Secreted by Stimulated Rabbit Synovial Fibroblasts in Parallel with Collagenase. *Journal of Biological Chemistry*, 260:12367-12376, 1985.
44. Fini, E., I. Plucinska, A. Mayer, R. Gross and C. Brinckerhoff. A gene for rabbit synovial cell collagenase: Member of a family of metalloproteinases that degrade the connective tissue matrix. *Biochemistry*, 26:6156-6165, 1987.
45. Van Wart, H. and H. Birkedal-Hansen. The cysteine switch: A principle of regulation of metalloproteinase activity with potential applicability to the entire matrix metalloproteinase gene family. *PNAS*, 87:5578-5582, 1990.
46. Woessner, J. Matrix metalloproteinases and their inhibitors in connective tissue remodeling. *The FASEB Journal*, 5:2145-2154, 1991.

47. Muller, D., B. Quantin, M. Gesnel, R. Millon-Collard, J. Abecassis and R. Breathnach. The collagenase gene family in humans consists of at least four members. *Biochemistry Journal*, 253:187-192, 1988.
48. Quantin, B., G. Murphy and R. Breathnach. Pump-1 cDNA codes for a protein with characteristics similar to those of classical collagenase family members. *Biochemistry*, 28:5327-5334, 1989.
49. Woessner, J. and C. Taplin. Purification and properties of a small latent matrix metalloproteinase of the rat uterus. *Journal of Biological Chemistry*, 263:16918-16925, 1988.
50. Collier, I., J. Smith, J. Kronberger, E. Bauer, S. Wilhelm, A. Eisen and G. Goldberg. The structure of the human skin fibroblast collagenase gene. *Journal of Biological Chemistry*, 263:10711-10713, 1988.
51. Park, A.J., L.M. Matrisian, A.F. Kells, R. Pearson, Z. Yuan and M. Navre. Mutational analysis of the transin (stromelysin) autoinhibitor region demonstrates a role for residues surrounding the "cysteine switch". *Journal of Biological Chemistry*, 266:1584-1590, 1991.
52. Sanchez-Lopez, R., R. Nicholson, M. Gesnel, L. Matrisian and R. Breathnach. Structure-function relationships in the collagenase family member transin. *Journal of Biological Chemistry*, 263:11892-11899, 1988.
53. Wilhelm, S., I. Collier, B. Marmer, A. Eisen, G. Grant and G. Goldberg. SV40-transformed human lung fibroblasts secrete a 92-KDa type IV collagenase which is identical to that secreted by normal human macrophages. *Journal of Biological Chemistry*, 264:17213-17221, 1989.
54. Collier, I., S. Wilhelm, A. Eisen, B. Marmer, G. Grant, J. Seltzer, A. Kronberger, C. He, E. Bauer and G. Goldberg. H-ras oncogene-transformed human bronchial epithelial cells (TBE-1) secrete a single metalloprotease capable of degrading basement membrane collagen. *Journal of Biological Chemistry*, 263:6579-6587, 1988.
55. Goldberg, G. Human 72 kDa type IV collagenase forms a complex with tissue inhibitor of metalloproteases designated TIMP-2. *PNAS*, 84:6725, 1989.

56. Galloway, W., G. Murphy, J. Sandy, J. Gavrilovic, T. Cawston and J. Reynolds. Purification and characterization of a rabbit bone metalloproteinase that degrades proteoglycan and other connective-tissue components. *Biochem. J.*, 209:741, 1983.
57. Murphy, G. and J. Reynolds. The origin of matrix metalloproteinases and their familial relationships. *FEBS*, 289:4-7, 1991.
58. Vallee, B. and D. Auld. Zinc coordination, function, and structure of zinc enzymes and other proteins. *Biochemistry*, 29:5647-5659, 1990.
59. Birkedal-Hansen, H. and R. Taylor. Detergent activation of latent collagenase and resolution of its component molecules. *Biochem. Biophys. Res. Commun.*, 107:1173-1178, 1982.
60. Lazarus, G., J. Daniels, J. Lian and M. Burleigh. *American Journal of Pathology*, 68:565-578, 1972.
61. Okada, Y., E. Harris and H. Nagase. The precursor of a metalloendopeptidase from human rheumatoid synovial fibroblasts. *Biochemistry Journal*, 254:731-741, 1988.
62. Bauer, E., G. Stricklin, J. Jeffery and A. Eisen. Collagenase production by human skin fibroblasts. *Biochem. Biophys. Res. Commun.*, 64:232-240, 1975.
63. Nagase, H., J. Enghild, K. Suzuki and G. Salvesen. Stepwise activation mechanism of the precursor of matrix metalloproteinase 3 (stromelysin) by proteinases and (4-aminophenyl)mercuric acetate. *Biochemistry*, 29:5783-5789, 1990.
64. Jung, J., S. Warter and Y. Rumpler. Localization of stromelysin 2 gene to the q22.3-23 region of chromosome 11 by in situ hybridization. *Annals of Genetics*, 33:21-23, 1990.
65. Matrisian, L., N. Glaichenhaus, M. Gesnel and R. Breathnach. Epidermal growth factor and oncogenes induce transcription of the same cellular mRNA in rat fibroblasts. *EMBO Journal*, 4:1435-1440, 1985.

66. Machida, C., K. Rodland, L. Matrisian, B. Magun and G. Ciment. NGF induction of the gene encoding the protease transin accompanies neuronal differentiation in PC12 cells. *Neuron*, 2:1587-1596, 1989.
67. Matrisian, L.M., L. Pierre, C. Ruhlmann, M. Gesnel and R. Breathnach. Isolation of the Oncogene and Epidermal Growth Factor-induced transin gene: Complex control in rat fibroblasts. *Molecular and Cellular Biology*, 6:1679-1686, 1986.
68. McDonnell, S., L. Kerr and L. Matrisian. Epidermal growth factor stimulation of stromelysin mRNA in rat fibroblasts requires induction of proto-oncogenes c-fos and c-jun and activation of protein kinase C. *Molecular and Cellular Biology*, 10:4284-4293, 1990.
69. Nicholson, R.C., S. Mader, S. Nagpal, M. Leid, C. Rochette-Egly and P. Chambon. Negative regulation of the rat stromelysin gene promoter by retinoic acid is mediated by an AP1 binding site. *EMBO Journal*, 9:4443-4454, 1990.
70. Herron, G.S., Z. Werb, K. Dwyer and M. Banda. Secretion of metalloproteinases by stimulated capillary endothelial cells. *Journal of Biological Chemistry*, 261:2810-2813, 1986.
71. Herron, G.S., M.J. Banda, E.J. Clark, J. Gavrilovic and Z. Werb. Secretion of metalloproteinases by stimulated capillary endothelial cells. II. Expression of collagenase and stromelysin activities is regulated by endogenous inhibitors. *Journal of Biological Chemistry*, 261:2814-2818, 1986.
72. Carmichael, D.F., A. Sommer, R.C. Thompson, D.C. Anderson, C.G. Smith, H.G. Welgus and G.P. Stricklin. Primary structure and cDNA cloning of human fibroblast collagenase inhibitor. *PNAS*, 83:2407-2411, 1986.
73. Stetler-Stevenson, W., H. Kruttsch and L. Liotta. Tissue Inhibitor of Metalloproteinase (TIMP-2). *Journal of Biological Chemistry*, 264:17374-17378, 1989.
74. Goldberg, G.I., B.L. Marmer, G.A. Grant, A. Eisen, S. Wilhelm and H. Chengshi. Human 72-kilodalton type IV collagenase forms a complex with a tissue inhibitor of metalloproteinases designated TIMP-2. *PNAS*, 86:8207-8211, 1989.

75. Murphy, G., P. Koklitis and A.F. Carne. Dissociation of tissue inhibitor of metalloproteinases (TIMP) from enzyme complexes yields fully active inhibitor. *Biochemical Journal*, 261:1031-1034, 1989.
76. Ward, R., R. Hembry, J. Reynolds and G. Murphy. The purification of tissue inhibitor of metalloproteinases-2 from its 72 kDa progelatinase complex. *Biochemical Journal*, 278:179-187, 1991.
77. Nomura, S., B. Hogan, A. Wills, J. Heath and D. Edwards. Developmental expression of tissue inhibitor of metalloproteinase (TIMP) RNA. *Development*, 105:575-583, 1989.
78. Flenniken, A.M. and B.R.G. Williams. Developmental expression of the endogenous TIMP gene and a TIMP-lacZ fusion gene in transgenic mice. *Genes & Development*, 4:1094-1106, 1990.
79. Khokha, R., P. Waterhouse, S. Yagel, P. Lala, C. Overall, G. Norton and D. Denhardt. Antisense RNA-induced reduction in murine TIMP levels confers oncogenicity on Swiss 3T3 cells. *Science*, 243:947-950, 1989.
80. Edwards, D., C. Parfett and D. Denhardt. Transcriptional regulation of two serum-induced RNAs in mouse fibroblasts. *Molecular and Cellular Biology*, 5:3280-3288, 1985.
81. Edwards, D., G. Murphy, J. Reynolds, S. Whitham, A. Docherty, P. Angel and J. Heath. Transforming growth factor beta modulates the expression of collagenase and metalloproteinase inhibitor. *EMBO Journal*, 6:1899-1904, 1987.
82. Chua, C., D. Geiman, G. Keller and R. Ladda. Induction of collagenase secretion in human fibroblast cultures by growth promoting factors. *Journal of Biological Chemistry*, 260:5213-5216, 1985.
83. Bauer, E., T. Cooper, J. Huang, J. Altman and T. Dueul. Stimulation of in vitro human skin collagenase expression by platelet-derived growth factor. *PNAS*, 82:4132-4136, 1985.
84. Murphy, G., J. Reynolds and Z. Werb. Biosynthesis of Tissue Inhibitor of Metalloproteinases by human fibroblasts in culture. *Journal of Biological*

Chemistry, 260:3079-3083, 1985.

85. Clark, S., S. Wilhelm, G. Stricklin and H. Welgus. Coregulation of collagenase and collagenase inhibitor production by phorbol myristate acetate in human skin fibroblasts. *Archives of Biochemistry and Biophysics*, 241:36-44, 1985.

86. Brinkerhoff, C., I. Plucinska, L. Sheldon and G. O'Connor. Half life of synovial cell collagenase mRNA is modulated by phorbol myristate acetate but not by all-trans-retinoic acid or dexamethasone. *Biochemistry*, 25:6378-6384, 1986.

87. Edwards, D., P. Waterhouse, M. Holman and D. Denhardt. A growth-responsive gene (16C8) in normal mouse fibroblasts homologous to a human collagenase inhibitor with erythroid-potentiating activity: evidence for constitutive and inducible transcripts. *Nucleic Acids Research*, 14:8863-8878, 1986.

88. Herrlich, P., P. Angel, H. Rahmsdorf, U. Mallick, A. Poting, L. Hieber, C. Lucke-Huhle and M. Schorpp. The mammalian genetic stress response. *Advances in Enzyme Regulation*, 25:485-504, 1986.

89. Sakyo, K., A. Ito, C. Ogawa and Y. Mori. Hormonal control of collagenase inhibitor production in rabbit uterine cervical fibroblast-like cells. *Biochimica et Biophysica Acta*, 883:517-522, 1986.

90. Clark, S., D. Kobayashi and H. Welgus. Regulation of the expression of tissue inhibitor of metalloproteinases and collagenase by retinoids and glucocorticoids in human fibroblasts. *Journal of Clinical Investigation*, 80:1280-1288, 1987.

91. Campbell, C., A.M. Flenniken, D. Skup and B.R.G. Williams. Identification of a serum- and phorbol ester-responsive element in the murine tissue inhibitor of metalloproteinase gene. *Journal of Biological Chemistry*, 266:7199-7206, 1991.

92. W.G., P.D. Brown, M. Onisto, A. Levy and L. Liotta. Tissue Inhibitor of Metalloproteinases-2 (TIMP-2) mRNA expression in tumor cell lines and human tumor tissues. *Journal of Biological Chemistry*, 265:13933-13938, 1990.

93. Varmus, H. Retroviruses. *Science*, 240:1427-1435, 1988.
94. Coffin, J.M. Retroviridae and their replication. In: *Virology*, edited by Fields, B.N. and Knipe, D.M. New York: Raven Press, Ltd., 1990, p. 1437-1500.
95. Li, J., R. Bestwick, C. Spiro and D. Kabat. The membrane glycoprotein of Friend spleen focus-forming virus: evidence that the cell surface component is required for pathogenesis and that it binds to a receptor. *Journal of Virology*, 61:2782-2792, 1987.
96. Wang, H., M. Kavanaugh, R.A. North and D. Kabat. Cell-surface receptor for ecotropic murine retroviruses is a basic amino-acid transporter. *Nature*, 352:729-731, 1991.
97. Kim, J.W., E. Closs, L. Albritton and J. Cunningham. Transport of cationic amino acids by the mouse ecotropic retrovirus receptor. *Nature*, 352:725-728, 1991.
98. Panganiban, A.T. and D. Fiore. Ordered interstrand and intrastrand DNA transfer during reverse transcription. *Science*, 241:1064-1069, 1988.
99. Steffen, D. and R.A. Weinberg. The integrated genome of murine leukemia virus. *Cell*, 15:1003-1010, 1978.
100. Hughes, S.H., P. Shank, D. Spector, H. Kung, M.J. Bishop and H.E. Varmus. Proviruses of avian sarcoma virus are terminally redundant, co-extensive with unintegrated linear DNA and integrated at many sites. *Cell*, 15:1397-1410, 1978.
101. Ringold, G.M., P.R. Shank, H.E. Varmus, J. Ring and K.R. Yamamoto. Integration and transcription of mouse mammary tumor virus DNA in rat hepatoma cells. *PNAS*, 76:665-669, 1979.
102. Varmus, H.E. Form and function of retroviral proviruses. *Science*, 216:812-820, 1982.
103. Springett, G.M., R.C. Moen, S. Anderson, M. Blaese and W.F. Anderson.

Infection efficiency of T lymphocytes with amphotropic retroviral vectors is cell cycle dependent. *Journal of Virology*, 63:3865-3869, 1989.

104. Miller, D.G., M. Adam and A.D. Miller. Gene transfer by retrovirus vectors occurs only in cells that are actively replicating at the time of infection. *Molecular and Cellular Biology*, 10:4239-4242, 1990.

105. Chen, I.S. and H.M. Temin. Establishment of infection by spleen necrosis virus: inhibition in stationary cells and role of secondary infection. *Journal of Virology*, 41:183-190, 1982.

106. Harel, J., E. Rassart and P. Jolicoeur. Cell cycle dependence of synthesis of unintegrated viral DNA in mouse cells newly infected with murine leukemia virus. *Virology*, 110:202-207, 1981.

107. Kabat, D. Molecular biology of Friend viral erythroleukemia. In: *Current Topics in Microbiology and Immunology*, edited by Vogt, P.K. Berlin-Heidelberg: Springer-Verlag, 1989, p. 1-42.

108. Goebel, M.G. The PU.1 transcription factor is the product of the putative oncogene Spi-1. *Cell*, 61:1165, 1990.

109. Moreau-Gachelin, F., A. Tavitian and P. Tambourin. Spi-1 is a putative oncogene in virally induced murine erythroleukaemias. *Nature*, 331:277-280, 1988.

110. Paul, R., S. Schuetze, S. Kozak, C.A. Kozak and D. Kabat. The Spi-1 proviral integration site of Friend erythroleukemia encodes the ets-related transcription factor Pu.1. *Journal of Virology*, 65:464-467, 1991.

111. Paul, R., S. Schuetze, S. Kozak and D. Kabat. A common site for immortalizing proviral integrations in Friend erythroleukemia: Molecular cloning and characterization. *Journal of Virology*, 63:4958-4961, 1989.

112. Spiro, C., J. Li, R. Bestwick and D. Kabat. An enhancer sequence instability that diversifies the cell repertoire for expression of a murine leukemia virus. *Virology*, 164:350-361, 1988.

113. Linemeyer, D., S. Ruscetti, J. Menke and E. Scolnick. Recovery of biologically active spleen focus-forming virus from molecularly cloned spleen focus-forming virus pBR322 circular DNA by cotransfection with infectious type-C retroviral DNA. *Journal of Virology*, 35:710-721, 1980.
114. Bestwick, R., S. Kozak and D. Kabat. Overcoming interference to retroviral superinfection results in amplified expression and transmission of cloned genes. *PNAS*, 85:5404-5408, 1988.
115. Kozak, S. and D. Kabat. Ping-pong amplification of a retroviral vector achieves high-level gene expression: human growth hormone production. *Journal of Virology*, 64:3500-3508, 1990.
116. Mann, R., R. Mulligan and D. Baltimore. Construction of a retroviral packaging mutant and its use to produce helper-free defective retrovirions. *Cell*, 33:153-159, 1983.
117. Metsikko, K. and H. Garoff. Role of heterologous and homologous glycoproteins in phenotypic mixing between Sendai virus and vesicular stomatitis virus. *Journal of Virology*, 63:5111-5118, 1989.
118. Polansky, J., R. Weinreb, J. Baxter and J. Alvarado. Human trabecular cells. I. Establishemnt in tissue culture and growth characteristics. *Investigative Ophthalmology and Visual Science*, 18:1043-1049, 1979.
119. Sambrook, J., E. Fritsch, and T. Maniatis. *Molecular cloning: A laboratory manual*. Cold Spring Harbor Laboratory Press, Second edition, 1989.
120. Ausubel, F., Brent, R., Kingston, R., et al. *Current protocols in molecular biology*. Greene Publishing Association and Wiley-Interscience, New York, 1987.
121. Heery, D., F. Gannon and R. Powell. A simple method for subcloning DNA fragments from gel slices. *Trends in Genetics* 6:173, 1990.
122. Coulombe, B. and D. Skup. In vitro synthesis of the active tissue inhibitor of metalloproteinases encoded by a complementary DNA from virus-infected murine fibroblasts. *Journal of Biological Chemistry*, 263:1439-1443, 1988.

123. Kerr, L.D., D.B. Miller and L.M. Matrisian. TGF-beta 1 inhibition of transin/stromelysin gene expression is mediated through a fos binding sequence. *Cell*, 61:267-278, 1990.
124. Wasylyk, C., A. Gutman, R. Nicholson and B. Wasylyk. The c-Ets oncoprotein activates the stromelysin promoter through the same elements as several non-nuclear oncoproteins. *EMBO Journal*, 10:1127-1134, 1991.
125. Wilkinson, M. A rapid and convenient method for isolation of nuclear, cytoplasmic and total cellular RNA. *Nucleic Acids Research*, 16:10934, 1988.
126. Qian, L. and M. Wilkinson. DNA fragment purification: removal of agarose ten minutes after electrophoresis. *Biotechniques*, (in press) 1991.
127. Alexander, J., J. Bradley, J. Gabourel and T. Acott. Expression of matrix metalloproteinases and inhibitor by retinal pigment epithelium. *Investigative Ophthalmology and Visual Science*, 31:2520, 1990.
128. Alexander, J., J. Samples, E Van Buskirk and T. Acott. Expression of matrix metalloproteinases and inhibitor by human trabecular meshwork. *Investigative Ophthalmology and Visual Science*, 32:172, 1991.
129. Laemmli, U. Cleavage of structural proteins during the assembly of the head of bacteriophage T4. *Nature*, 227:680-685, 1970.
130. Heussen, C. and E. Dowdle. Electrophoretic analysis of plasminogen activators in polyacrylamide gels containing sodium dodecyl sulfate and copolymerized substrates. *Annals of Biochemistry*, 102:196, 1980.
131. Docherty, A.J.P. and G. Murphy. The tissue metalloproteinase family and the inhibitor TIMP: a study using cDNAs and recombinant proteins. *Annals of Rheum. Dis.*, 49:469-479, 1990.
132. Unemori, E., K. Bouhana and Z. Werb. Vectorial secretion of extracellular matrix proteins, matrix-degrading proteinases, and tissue inhibitor of metalloproteinases by endothelial cells. *Journal of Biological Chemistry*, 265:445-451, 1990.

133. Gewert, D.R., B. Coulombe, M. Castelino, D. Skup and B.R.G. Williams. Characterization and expression of a murine gene homologous to human EPA/TIMP: a virus-induced gene in the mouse. *EMBO Journal*, 6:651-657, 1987.
134. DeNoto, F.M., D.D. Moore and H.M. Goodman. Human growth hormone DNA sequence and mRNA structure: possible alternate splicing. *Nucleic Acids Research*, 9:3719-3730, 1981.
135. Matrisian, L., T. Bowden, P. Krieg, G. Furstenberger, J. Briand, P. Leroy and R. Breathnach. The mRNA coding for the secreted protease transin is expressed more abundantly in malignant than in benign tumors. *PNAS*, 83:9413-9417, 1986.
136. Nagase, H., Y. Ogata, K. Suzuki, J. Enghild and G. Salvesen. Substrate specificities and activation mechanisms of matrix metalloproteinases. *Biochemical Society Transactions*, 19:715-718, 1991.
137. Ward, R., S. Atkinson, P. Slocombe, A. Docherty, J. Reynolds and G. Murphy. Tissue inhibitor of metalloproteinases-2 inhibits the activation of 72 kDa progelatinase by fibroblast membranes. *Biochimica et Biophysica Acta*, 1079:242-246, 1991.
138. Ingber, D. and J. Folkman. How does extracellular matrix control capillary morphogenesis? *Cell*, 58:803-805, 1989.
139. Werb, Z., P. Tremble, O. Behrendtsen, E. Crowley and C. Damsky. Signal transduction through the fibronectin receptor induces collagenase and stromelysin gene expression. *Journal of Cell Biology*, 109:877-889, 1989.
140. Sang, Q., E. Thompson, D. Grant, W. Stetler-Stevenson and S. Byers. Soluble laminin and arginine-glycine-aspartic acid containing peptides differentially regulate Type IV collagenase messenger RNA, activation, and localization in testicular cell culture. *Biology of Reproduction*, 45:386, 1991.
141. Huhtala, P., A. Tuuttil, L. Chow, J. Lohi, J. Lohi, J. Keski-Oja, and K. Tryggvason. Complete structure of the human gene for 92 kDa type IV collagenase. *Journal of Biological Chemistry*, 266: 16485-16490, 1991.

142. Wilhelm, S., I. Collier, A. Kronberger, A. Eisen, B. Marmer, G. Grant, E. Bauer, and G. Goldberg. Human skin fibroblast stromelysin: Structure glycosylation, substrate specificity and differential expression in normal and tumorigenic cells. PNAS, 84: 6725-6729, 1987.

143. Creighton, T. E. In Proteins: Structures and molecular principles. Published by W. H. Freeman and Co., 1984.